ROCK MAGNETISM and PALEOGEOPHYSICS

volume 3
1975

Published by the

ROCK MAGNETISM AND PALEOGEOPHYSICS RESEARCH GROUP IN JAPAN

まえがき

本書は、GDP II-1-(2)「古地磁気学的方法」の研究グループの報告書として刊行されるものである。岩石磁気学・古地球物理学グループでは、Annual Reportの形で、以前から英文の報文集を刊行してきた。(Annual Progress Report of the Rock Magnetism Research Group in Japan, 1963, 1964, 1965; Annual Progress Report of the Paleogeophysics Research in Japan, 1967, 1968).

これらのAnnual Reportは、諸外国の研究者の間でかなり広く利用されており、これまでの実績を継続するためにも、GDPの研究報告書ではあるが英文で刊行される。日本国内の研究者の方々にいく分御面倒をおかけすることになるが、このような事情なので御了承いただきたい。

報文の配列の仕方は便宜的なものであるが、一応大まかに、(1) 岩石や鉱物の磁性・物性、(2) 古地磁気および地殻変動、(3) アイソトープ地学および絶対年代決定、(4) 地球磁場および磁場と他の地学現象の関連 という分類がしてある。

"Rock Magnetism and Paleogeophysics" は発刊当初から(vol. 1, 1973年12月; vol. 2, 1974年12月), Extended Abstract集を目指してきた。本巻についてもこの考えは変らない。ここにおさめられた報文は、progress report的なものを除いて、いずれ完全なかたちの論文として、さまざまな学術誌に投稿・発表される予定である。

なお本巻には、"National Report of the Geodynamics Project of Japan" (1975年8月) から「古地磁気学的方法」研究グループの報告を転載した。

1975年12月

古地磁気学・古地球物理学研究グループ

PREFACE

This volume is the annual progress report of the Rock Magnetism and Paleogeophysics Research Group in Japan for the year 1975. As the previous volumes were so, this volume is a collection of summaries or extended abstracts of various research works carried out in our group. Many of the reports contain substances which may be changed or revised as the research work continues. In this respect, this volume contains many tentative results.

Except for the ones written as pure progress reports, the papers in this volume will be published in academic journals in full detail and length. This volume may be referenced, but if a paper is published in such an academic journal, readers are requested to quote the paper from that journal. We hope that this volume is a useful source of advance information of recent works on rock magnetism and paleogeophysics in Japan.

This volume also constitutes a scientific report of the Rock Magnetism and Paleogeophysics Research Group in the Geodynamics Project of Japan. The summary of the activities of our group is reprinted from "National Report of the Geodynamics Project of Japan" presented to the Inter-Union Commission on Geodynamics in August 1975.

We would like to acknowledge the partial financial support for this publication and for the investigations included in this volume from the Ministry of Education as a part of the Geodynamics Project.

December 1975

Masaru Kono
Editor

ROCK MAGNETISM AND PALEOGEOPHYSICS SYMPOSIUM

The seventh Rock Magnetism and Paleogeophysics Symposium was held on 23rd and 24th November, 1975 at Shimane University. Titles of papers presented at this symposium is as follows.

23 November

Y. Tanaka (Kyoto Univ.) Polar wandering and plate tectonics.

H. Aoki (Nagoya Univ.) The down-going plate under the Japanese islands.

N. Kawai (Osaka Univ.) Geomagnetism and the climate change.

S. Nishimura (Kyoto Univ.) Age determination by fission track method.

T. Ui (Yamagata Univ.) The relation between K_2O content of volcanic rocks and the plate structure — Quaternary volcanoes on the Japanese islands.

H. Muneoka and H. Domen (Yamaguchi Univ.) Natural remanent magnetization of Neogene andesite from southeastern part of Yamaguchi Prefecture.

J. Nishida and S. Ishida (Kyoto Univ.) Paleomagnetism of marine and fresh water clays of Osaka Group — Matuyama-Brunhes boundary.

H. Watanabe (Tokyo Univ.) Simulation of geomagnetic reversals by an α-ω dynamo.

24 November

T. Furuta and J. Segawa (Tokyo Univ.) Geomagnetic anomalies in Northeast Japan and Hokkaido and the basement rocks responsible for the anomalies.

K. Hirooka, T. Kondo and S. Miura (Fukui Univ.) Paleomagnetism of Kyo-ga-take in Okuetsu district of Fukui Prefecture.

K. Maenaka (Hanazono Univ.) A reappraisal of paleomagnetic stratigraphy of Plio-Pleistocene in Kinki district.

T. Sato, T. Sueishi and N. Kawai (Osaka Univ.) Geomagnetic variations from deep sea sediments.

M. Kono (Tokyo Univ.) The sampling trip to Madagascar.

CONTENTS

IMPURE TITANOMAGNETITES CHARACTERISTIC TO SOME ALKALINE BASALTS IN SOUTHWEST JAPAN

Sadao SASAJIMA, Junichi NISHIDA

Dept. Geology and Mineralogy
Kyoto University, Kyoto 606

Takashi KATSURA

Tokyo Institute of Technology
Ookayama, Meguro, Tokyo 152

Introduction

During the course of a paleomagnetic investigation of Plio-Pleistocene alkaline basalts in Southwest Japan, Nishida and Sasajima(1974) have found that most of titanomagnetite separates possess P-type magnetization with an exception of Kozuike basalt which shows N-type magnetization. In the paper we noticed that the chemical composition of N-type titanomagnetites in Kozuike basalt might be similar to that reported by Schult(1968, 1971); i.e. described as titanomaghemites in a strict sense. And basing on the assumption of pure titanomagnetite composition ($FeO-Fe_2O_3-TiO_2$ system) oxidation parameter(z) of the N-type titanomagnetites has been estimated to be about 0.45.

On the other hand, an extensive study on petrogenesis of these basalts was made by Takamura(1973). According to Takamura(1973), those basalts are characterized by noticeable amount of inclusion of basic nodules, and inferred to have been derived from some kind of essential magma, therefore, it may be rather natural to suppose that titanomagnetites of such rocks contain considerable amount of Al^{3+} and/or Mg^{2+} ions in place of Fe^{3+} and/or Fe^{2+} ions respectively. In view of this we have carried out a precise wet chemical analysis of the titanomagnetites in order to confirm exactly the existence of such cation impurities and to make clear of their relevance to rock- and paleo-magnetism.

Result of Chemical analysis

Chemical analyses of 12 titanomagnetites specimens were conducted with a high precision by one of present authors (T.K.). The result obtained is listed in Table 1. In addition, Curie points and lattice parameters of the spinel structure of those specimens are also noted. As seen in table 1 seven out of twelve specimens were selected for further detailed analyses; the remained ones were thought useless because of their heavy contamination of silicates. The final result of analysis has validated our expectation mentioned above, but unfortunately that of Kozuike basalt was failed to succeed.

It is clear from the data obtained that in all specimens concerned the mole percent of both Al_2O_3 and MgO is too large to be neglected. And if one plots the data(in mole fraction)

Tabel 1. Chemical Composition of Titanomagnetites

	(1)	(2)	(3)	(4)	(5)	(6)	(7)
FeO	40.51%wt	39.44	37.95	40.25	41.35	30.69	41.46
Fe_2O_3	19.06	30.66	26.74	22.69	25.08	29.33	17.51
TiO_2	19.46	21.17	19.97	21.50	19.23	15.12	21.31
Al_2O_3	10.61	5.60	6.56	6.10	7.01	7.48	9.61
MgO	4.65	1.56	4.69	5.23	3.18	8.92	3.96
Cr_2O_3	1.56	-	-	-	-	-	-
MnO	0.70	0.58	0.70	0.66	0.61	0.57	0.66
CaO	1.25	tr	1.55	0.75	0.83	2.05	1.47
SiO_2	2.92	1.31	1.91	2.99	3.55	5.96	4.86
Total	100.72	100.32	100.07	100.17	100.84	100.12	100.84
	Mole %						
R O	59.3	53.4	57.2	59.4	58.4	59.2	58.9
R_2O_3	19.5	22.5	20.6	17.4	20.1	23.5	17.8
TiO_2	21.2	24.1	22.2	23.2	21.5	17.3	23.3
Tc(°C)	150	250	105	95	245	85	10
a(Å)	8.466	8.451	8.465	8.467	8.462	8.447	8.485

	(8)	(9)	(10)	(11)	(12)
FeO	24.72%wt	30.99	28.27	36.32	24.19
Fe_2O_3	17.37	17.89	27.20	20.44	23.26
TiO_2	12.35	13.94	12.67	16.04	9.02
Total	54.44	62.82	68.14	72.80	56.47
	Mole %				
FeO	56.64	60.08	54.47	60.59	56.57
Fe_2O_3	17.91	15.60	23.57	15.34	24.46
TiO_2	25.45	24.31	21.95	24.07	18.97
Tc(°C)	190	150	420	110	320
a(Å)	8.463	8.445	8.441	8.468	8.447

Tc: Curie point a(Å): lattice parameter

(1): Ôguso-yama, Shimane Pref. (2): Taiza, Kyoto Pref. (3): Iwagase, Hiroshima Pref. (4): Takashima, Saga Pref. (5): Yakuno, Kyoto Pref. (6): Saigo, Shimane Pref. (7): Une, Hiroshima Pref. (8): Kôzuike, Hiroshima Pref. (9): Myojin-yama, Okayama Pref. (10): Takashima, Saga Pref. (11): Kannabe, Hyogo Pref. (12): Miyaka Island, Tokyo City (Tholeiite)

onto such a ternary system as $RO-R_2O_3-TiO_2$, a diagram shown in Fig. 1 can be obtained, where RO and R_2O_3 means $(Fe^{2+}+Mg^{2+})O$ and $(Fe^{3+}+Al^{3+})_2O_3$ respectively.

Discussion and conclusions

The equilibrium in the $FeO-Fe_2O_3-TiO_2$ system containing about 0.2 mole fraction of $MgAl_2O_4$ in the stoichiometric $Fe_2TiO_4-Fe_3O_4$ solid solution has been established by Katsura et al(1975), and the result is discussed in comparison with what having no $MgAl_2O_4$ component. It is concluded from the study that titanomagnetites with high TiO_2 contents crystallized from basaltic magma might not be so affected thermochemically by the presence of appreciable amount of spinel ($MgAl_2O_4$). In Fig. 1 a broadly parallel broken line along $Fe_2TiO_4-Fe_3O_4$ tie line indicates the outer boundary of stable single phase of ulvospinel-magnetite solid solution containing 0.2 mole $MgAl_2O_4$. Almost all specimens dealt in this paper seem to be plotted inside the stable range of single spinel phase bounded by the two extreme lines. From the fact one may recognize that all the specimens except for specimen No. 2 are proved to be stoichiometry or scantly oxidized; No. 2 being separated from Taiza basalt, of which occurrence is an intrusive sheet of Miocene age, and therefore such a progress in oxidation state can be reasonably accepted by us. Anyway result thus obtained is quite defferent from our previous presumption, that is, cation deficient titanomagnetites which have been resulted from a hypothetical assumption of pure titanomagnetites.

Recently Prevot and Mergoil(1973) have made clear of three generations of homogeneous impure titanomagnetites in an alkaline basalt by means of electron microprobe analysis; especially of a systematic changes of Al, Mg and Cr contents in three kinds of titanomagnetites crystals with different generation 1-3. They have also pointed out that highly substituted titanomagnetites with Al, Mg and Cr cations are important as a positive reflection of their intratelluric origin.

On the other hand, Creer and Ibbetson(1970) have presented a method to estimate the degree of oxidation(z) of cation deficient titanomagnetites combining electron microprobe analysis and Curie

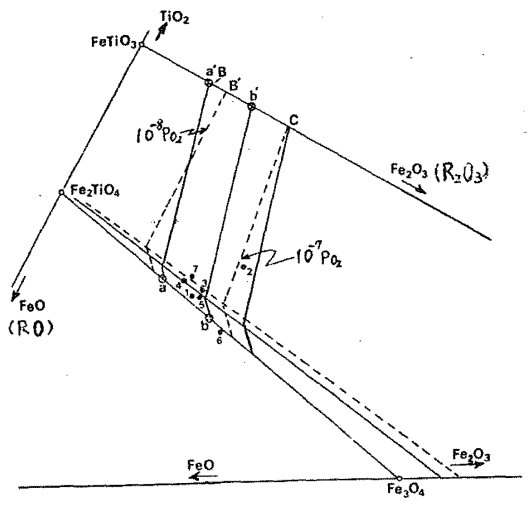

Fig.1. Equilibria diagram showing both ranges of single phased ulvospinel-magnetite solid solution and that containing about 0.2 mole $MgAl_2O_4$ (dotted boundary); data points 1-7 correspond to respective specimen shown in Table 1.

point-composition triangle diagram (Readman and O'Reilly, 1972). Recently Richards et al(1973) have advanced the work and modified the method in order to cancel the effect due to Al^{3+} and Mg^{2+} impurities involved in titanomagnetites. According to their result a large number of basalts in the world possess unexpectedly higher oxidation parameters (0.7-1.0), and therefore are assumed to have much possibility of the self-reversal of their natural remanent magnetizations. This is very important in association with the common interpretation of ocean floor magnetic anomalies.

Our result of chemical compositons and Curie point data were put into the, calculation of their oxidation parameter(z) to check the reliability of Richards et al's method. The obtained oxidation parameter(z) of these specimens are as follows:

Sp. No. 3, z=0.5; No. 1, No. 5 and No. 7, z=0.6; No. 4, z=0.7; No. 2, z=0.8.

There happened amazingly different results by two methods; these specimens, of course, must be nearly stoichiometry excepting specimen No. 2 as already mentioned above. We can not explain decisively the reason of such a discrepancy resulted from the two methods, but it may be pointed out that the estimated Curie point of the substituted stoichiometric titanomagnetite, Tc(est.) would not be correctly led solely from on algebraic subtraction of each contribution due to the Al and Mg contents.

In conclusion, it is mentioned that the alkaline basalts dealt in this study are believed to have been derived from some essential magma and those titanomagnetite are characterized by high concentration of MgO and Al_2O_3. From this fact those impure titanomagnetites could be safely correlated with the 'generation 1' defined by Prévot and Mergoil. Considering from the present state of progress of EPMA technique it is emphasized that for the purpose of oxidation problem of titanomagnetite precise wet chemical analyses of ferric and ferrous irons are still necessary. Substitutions of Mg and Al into titanomagnetites should be further studied in close association with the self-reversal of NRM.

References

Creer, K. M. and J. D. Ibbetson(1970) Geophys, J. R. astr. Soc. 21, 485.

Katsura, T., R. Aoyagi and S. Sasajima(1975) J. Volcanology, Japan, (in Japanese) in press.

Nishida, J. and S. Sasajima(1974) Geophys, J. R. astr. Soc. 37, 453.

Prévot, M. and J. Mergoil(1973) Mineral. Mag. 39, 474.

Richards, J. C. W., J. B. O'Donovan, Z. Hauptman, W. O'Reilly and K. M. Creer(1973) Phys. Earth Planet. Interior 7, 437.

Readman, P. W. and W. O'Reilly(1972) J. Geomag. Geoelectr. 24, 69.

Schult, A.(1968) Earth Planet. Sci. Lett. 4, 57.

————(1971) Zeit. Geophys. 37, 357.

Takamura, H. (1973) Geological Report of the Hiroshima Univ., 18, 1.

"Status" (To be published in Mem. Fac. Sci. Kyoto Univ. 43).

TITANOMAGNETITE AND TITANOMAGHEMITE CONTAINING ALUMINIUM

Masato JOSHIMA

Geological Survey of Japan, 135
Hisamoto-cho, Takatu-ku, Kawasaki-shi
, Kanagawa Prefecture

1. Introduction

Study on magnetization of marine basalts is necessary for understanding marine magnetic anomalies. The mineral that bears the magnetization of marine basalts is mainly titanomaghemite which is oxidized from titanomagnetite (Ozima and Larson 1970). Synthesis of titanomaghemite was done by several scientists, but there seems to be some discrepancies, especially in lattice parameters, among their results.
I have studied some titanomaghemite separated from marine basalts and measured oxidization level, chemical composition, Curie temperature, lattice parameter and saturation magnetization of those minerals (Joshima 1973). A tentative conclusion in that paper was that lattice parameters are too small to be explained solely by contamination in them, particularly Al and Mg. So Ihave studied the effect of Al contamination in titanomagnetite and titanomaghemite. The effect of Al contamination in titanomagnetite was also studied by Richards et al. (1973).

2. Method

To synthesize samples of titanomagnetite and titanomagnetite containing Al, the method of vacuum sealing in silica tube was utilized. Fe, Fe O , TiO and Al were calculated by the following formulas;

$$x + 2y + z + u = 3$$
$$3y + 2z = 4$$
$$\text{ulvospinel ratio} = 3z / (x + 2y + z + u)$$
$$\text{molecular ratio of Al O} = (u / 2) / (x + y + z + u / 2)$$

where x, y, z, u are molecular ratios of Fe, Fe O , TiO and Al, respectively, of the samples. They were mixed in mortar, and made into tablets 2mm in thickness and 1cm in diameter by pressing at 100 kg / cm . After that, the samples were sealed in silica glass at 10 torr, and kept at a temperature of 1150°C for one day. Then, the samples were ground in water by ballmlling for 150 hours, and after dried, they were oxidized at 160, 190, 210, 250, 270 and 320°C for one day. Curie temperatures and lattice parameters of these samples were measured.

3. Results

The change of particle size due to grinding is indicated by the form of peaks in x-ray diffractograms. In Fig.1, peaks at 2O of 45° and 80° (Fe target) are shown for the samples after they were ground in mortar, ballmilled for 150 hours, and after oxidized for one day.

Saturation magnetization - temperature curves are shown in Fig.2.

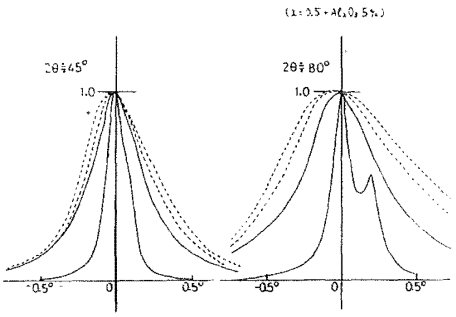

Fig.1 All peaks are normalized. Horizontal axis is 2θ (unit is degree).
From inside to outside;
1. ground in mortar 2. ground in ballmill for 150 hours 3. oxidized at 160°C 4. oxidized at 210°C

In case of oxidized samples of 0.6 to 0.8 ulvospinel ratios, their Js-T curves show maxima at about 150°C. This phenomenon is interpreted to be caused by their unsaturated magnetization.

Fig.3 is Js-T curve of sample of 0.8 ulvospinel ratio ballmilled for one day and oxidized at 200°C. Magnetic field is 7 kOe, 4 kOe, 2 kOe, respectively.

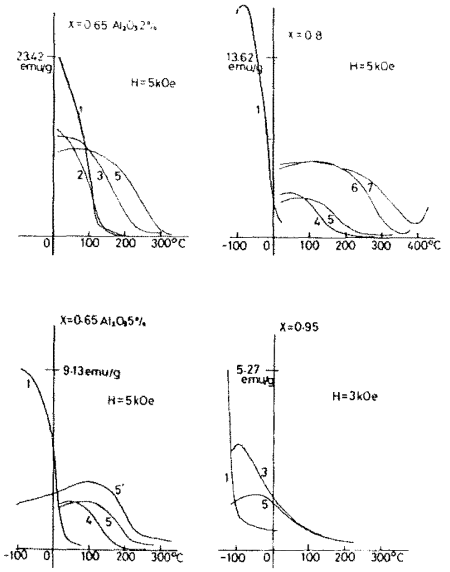

Fig.2 Js-T curves of samples 1. synthesized titanomagnetite 2. after ballmilling for 150 hours 3. oxidized at 160°C 4. the same at 190°C 5.the same at 210°C 6. the same at 250°C 7. the same at 270°C 5'. after ballmilled in acetone for 40 hours, oxidized at 200°C

Fig.3

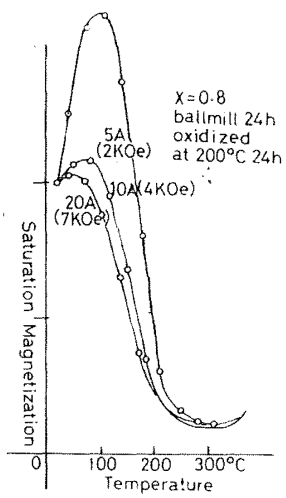

Results are summarized in Table 1. Table 2 is for oxidized titanomagnetite containing Al.

In Fig.4 to Fig.7, horizontal axis is Curie temperature and vertical axis is lattice parameter, therefore, samples are plotted according to their Curie temperatures and lattice parameters. Temperature at which they were oxidized or oxidization level is written near the point. For example, I compiled the data of Ozima and Sakamoto (1971) and Readman and O'Reilly (1972), and showed in Fig.4. Parameter z is oxidization level. The slope of open circles is steeper than that of open circles. Fig.7 shows the results of 0.65 and 0.8 ulvospinel ratio, and

their slopes resemble to that of Readman and O'Reilly. The slopes of oxidized titanomagnetite containing Al seem to be steeper than that of titanomaghemite, and the more containing Al, the more seems to be steeper. This means that lattice parameter decreases faster than usually with oxidization.

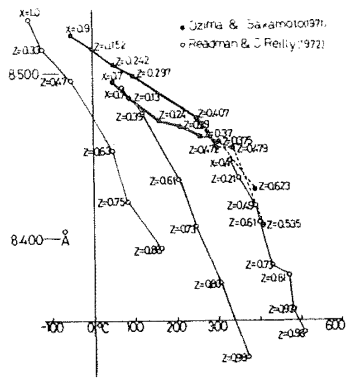

Fig.4 Horizontal axis--Curie temperature Vertical axis --lattice parameter

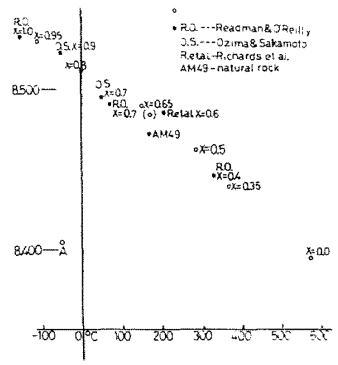

Fig.5 Synthesized samples shown in the same way to Fig.4 open circle is mine and closed is others

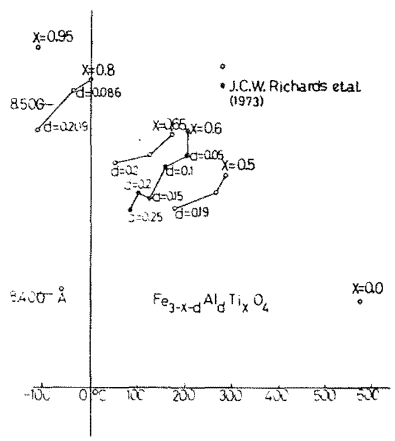

Fig.6 Titanomagnetite containing Al

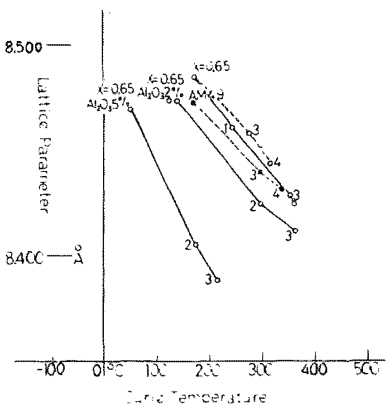

Fig.7 Titanomaghemite and titanomaghemite containing Al. Ulvospinel ratio x = 0.65 and 0.8. 1; oxidized at 160°C 2; at 190°C 3; at 210°C 4; at 250°C Dashed lines are other experiments which are AM49, separated mineral from natural rocks, and oxidized sample of shorter ballmilling time, ten hours.

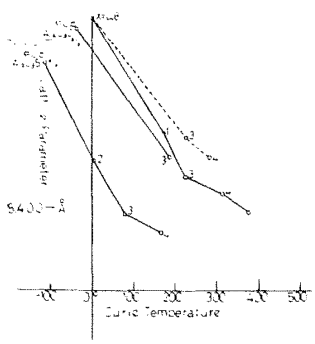

Table 1 synthesised titanomaghemite

Ulvo. ratio		Synthesis	after ball milling	Oxidized at 160°C	Oxidized at 210°C	Oxidized at 250°C	Oxidi 270°C
0.35	l	8.440A		8.419A	8.396A		
	c	368°C	387°C				
0.65	l		8.484A	8.460	8.424		
	c		172	243°C	362°C		
	s	59emu/g (at -50°C)			17 emu/g (maxima)		
0.8	l	8.513		8.444	8.418	8.408A	8.379A
	c	0		173	224	314	388±12
	s	16 (at -100°C)		3.4	3.0	5.7	5.7
0.95	l		8.530	8.493	8.446		
	c	-109°C		21	130		
	s	5.27 (at -127°C)	2.5 (at -100°C)	1.5 (at -50°C)			
AM49	l	8.472			8.440	8.431	
	c	170			297	338	
	s	8.8 (at room temp.)			16	17	

l; lattice parameter c; Curie temperature s; saturation magnetization Saturation magnetization of oxidized sample is the value of maxima.

Table 2 Synthesized titanomaghemite containing Al

Sample name		Synthesis	after ballmill	Oxidized at 160°C	Oxidized at 190°C	Oxidized at 210°C	Oxidiz 250°C
0.5+Al O 2%	l	8.454A		8.416A		8.319A	
	c	265°C					
0.5+Al O 5%	l	8.445		8.414		8.386	8.370A
	c	178		256°C		318°C	362°C
	s	18emu/g (at 20°C)		24emu/g		22emu/g	25emu/g
0.65+ Al O 2%	l	8.473	8.473			8.424	8.411
	c	124	137°C	223		298	363
	s	14 (at 20°C)				11.3	
0.65+ Al O 5%	l	8.469			8.405A	8.388	
	c	51			174°C	218	
	s	2.3 (at 20°C)			2.4emu/g	(at 20°C)	
0.8+Al O 2%	l	8.507				8.430	
	c	-36				187	
	s	15 (at -100°C)					
0.8+Al O 5%	l	8.486			8.428	8.396	8.385
	c	-111			6	80	167
	s	2.21 (at -118°C)			2.5 (at -50°C)	2.4 (at -50°C)	1.2 (at 20°C)

Sample name shows ulvospinel ratio and the value how much the sample contains Al (in molecular percent of Al O).

4. Discussion

Because the oxidization level cannot be determined exactly , only the pattern how Curie temperature and lattice parameter vary with increasing oxidization level can be recognized. The pattern of the present results is similar to that of Readman and O'Reilly up to 250°C. But over 250°C my samples began to contain hematite. In the case of samples containing Al, the decrease of lattice parameter is more rapid than that of pure titanomaghemite. So we may explain the too low

value of the lattice parameter of marine basalts by oxidization of titanomagnetite containing Al.

For oxidizing titanomagnetite at low temperature we have the method of wet grinding, and inthis method water is expected to play a important role. So I ground titanomagnetite in other liquid, in this case acetone. 5', Js-T curve in Fig.2 and x-ray diffraction analysis showed that oxidization was occured remaining the sample in one phase. So the role of water seems to me to keep fine particles airy and enable oxygen to be apt to go to the particles.

Reference

Joshima, M. (1973) Rock mag. and paleogeophys. 1, 9.
Ozima, M. and E.E.Larson (1970) J. Geophys. Res. 75, 1003.
Ozima, M. and N.Sakamoto (1971) J. Geophys. Res. 76, 7035.
Readman, P.W. and W.O'Reilly (1972) J. Geomag. Geoelectlr. 24, 69.
Richards, J.C.W., J.B.O'Donovan, Z.Hauptman, W.O'Reilly and K.M.Creer (1973) Phys. Earth Planet. Inter. 7, 437.

INFLUENCE OF PARTIAL PRESSURE OF OXYGEN ON THERMOREMANENT MAGNETIZATION OF BASALTS

Masaru KONO and Hidefumi TANAKA

Geophysical Institute, University of Tokyo, Bunkyo-ku, Tokyo 113

1. Introduction

Volcanic rocks such as basalts are the most frequently used materials in paleomagnetism. The natural remanent magnetization (NRM) in these rocks are often quite stable as it is most certainly of thermoremanent magnetization (TRM) origin. In the case of paleointensity determinations, they are the ideal materials because they carry TRM, which is almost the only stable magnetization of rocks that can be satisfactorily reproduced in a laboratory. Therefore, most paleointensity investigations have been performed with basalts or other volcanic rocks as samples. In such studies (e.g., Thellier and Thellier, 1959; Wilson, 1961; van Zijl et al., 1962), it is customary to measure the magnitudes of NRM and TRM (or partial components of them) in a same sample and to determine the paleointensity using the linearity of TRM with weak magnetic field, i.e.,

$$\frac{NRM}{TRM} = \frac{J_N}{J_T} = \frac{F}{F_{LAB}}$$

where F is the magnitude of the magnetic field in which the rock acquired the NRM.

However, it has been frequently observed that, in contrast to baked earths and other archeomagnetic objects which are usually stable to heat treatments, volcanic rocks often show irreversible changes in magnetic properties when they are heated, and consequently the TRM produced in a laboratory may not have the same characteristics as the NRM (e.g., Kono, 1968, 1974; Coe and Grommé, 1973). The use of the above relation for such samples will lead to an erroneous estimate of paleointensity. This is mainly because basalts and other volcanic rocks are formed in a oxygen-poor enviromment (Sato and Wright, 1966), while heating experiments are usually carried out in oxidizing conditions (e.g., air, vacuum).

It is the aim of the present paper to investigate changes in the properties of TRM in basalts by varying the oxygen fugacities of the furnace in heating experiments. A new electric furnace was built for this purpose (Tanaka and Kono, 1974). Oxygen fugacity is varied by flowing mixtures of H_2 and CO_2 in different volume ratios. All the measurements of remanences were carried out at room temperature by a Schonstedt spinner magnetometer. As characteristics of TRM, the magnitude and the alternating field (AF) demagnetization spectra were measured in most cases and were compared with those of the NRM. The present experiments are only preliminary and the results cannot be explained in a simple, systematic way. We hope, however, that such data will be of use in understanding the nature of TRM in igneous rocks as well as in obtaining paleointensities of good quality. Samples were taken from the present or recent basalt lavas of Oshima, Japan and Kilauea, Hawaii. The NRMs of these

rocks are very stable to AF demagnetization and only very small amount of secondary components are present. The magnitudes of the ambient geomagnetic field when these rocks were cooled are fairly well known (Table 1), so that the comparison of NRM and TRM intensities gives a measure of changeability of TRM capacity of a sample. Magnetic properties of the samples are listed in Table 1.

Table 1. Magnetic Properties of the Samples

Lava	Sample No.	Year	F, Oe	J_N, emu/cc	T_c, °C	a, Å
OS50	OS5061	1950	0.46±.04	9.6 x 10^{-3}	330, 515	8.436±.016
HA 1	HA 1-4	1972	0.36±.02	2.2	580	
HA 2	HA 2-4	1750	"	18	485	
HA 3	HA 3-4	1955	"	2.1	535	
HA 4	HA 4-2	1840	"	7.0	470	8.431±.003
HA 5	HA 5-4	1868	"	14	295	

F, Intensity of the ambient geomagnetic field; J_N, Intensity of the NRM; T_c, Curie Temperature; a, lattice parameter of cubic phase of ferromagnetic minerals.

2. Experiments and Results

The following experiments were performed.

Experiment 1

To see roughly the effect of atmosphere in the furnace on the TRM, Hawaiian samples were heated in four different gas or gas mixtures. The atmospheres used were (1) air, (2) CO_2, (3) a mixture of H_2 and air with unknown voloume ratio, and (4) H_2, with oxygen fugacities changing from high to low in the above order. Samples were heated to and kept at 600°C in the specified atmosphere for one hour before they were cooled to the room temperature in a magnetic field of 0.4 Oe.

Fig. 1 shows the TRM/NRM ratios obtained by heating samples in these atmospheres. The thick dash-dot line and the thin solid lines indicate the TRM/NRM ratios needed to give a right estimate of F_{LAB}/F and the 10 percent error ranges. There is a clear correlation between P_{O_2} and TRM capacity, the latter being increased (decreased) for oxidizing (reducing) conditions. Also to be noted is that extreme values of NRM/TRM ratios may be obtained for some samples. For example, HA 3 samples attain TRMs 20-30 times greater than NRMs when heated in air or CO_2, while in neutral (H_2 + air) or reducing (H_2) atmospheres the TRM/NRM ratios are between 0.8 and 2. Another interesting thing is that the changeability of the TRM/NRM ratios differ considerably among different lava flows. For instance, the ratio

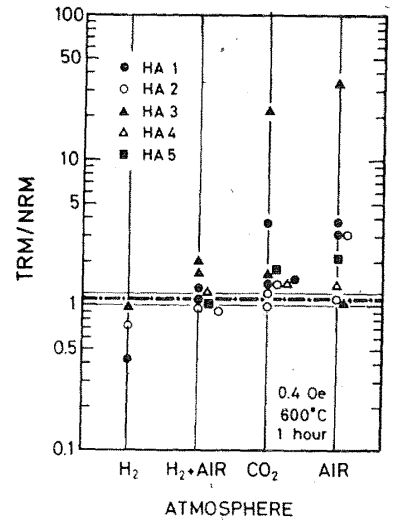

Fig. 1. TRM/NRM ratios.

of maximum to minimum values of TRM/NRM is about 40 for HA 3, about 10 for HA 1, but only about 4 for HA 2. For HA 4 and HA 5 heating in H_2 was not carried out, but it appears that the variability of the TRM/NRM ratios may be even smaller.

The coercivity spectra of NRM and TRM are compared in Fig. 2 where the points correspond to demagnetization steps of 0, 50, 100, 200, 300, and 400 peak Oe. The comparison of NRM and TRM at various AF demagnetization stages is the basis of paleointensity determination by van Zijl's method (van Zijl et al., 1962). More recent method modified from van Zijl's method (e.g., Schwarz and Symons, 1973) use the proportionality of NRM and TRM at many stages as an additional criterion of reliability of a datum. Such proportionality was observed in some of the present samples heated in H_2, but the "inferred paleointensities" F are about 0.5 and 1 Oe, considerably different from the expected field intensity of 0.36 Oe. It should be remarked that, while the present experiments are not intended to evaluate the reliability of paleointensity methods, the internal consistency criteria commonly employed in such methods may not be sufficient for really distinguishing good paleointensity data from bad ones.

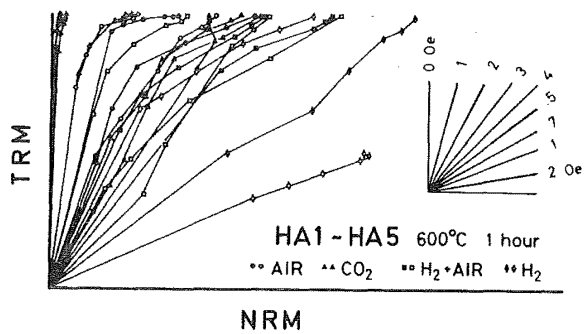

Fig. 2. AF demagnetization diagram of the Hawaiian samples of Fig. 1. Inset shows the field intensities expected from the gradient of the demagnetization diagram.

Another important feature of Fig. 2 is that almost all curves are concave down, showing that TRM is usually magnetically harder than NRM, i.e., smaller portion of TRM is demagnetized at low AF fields compared to NRM. This seems to be a common feature of artificially produced TRM except those produced in extremely reducing conditions.

Experiment 2

The former experiment was repeated with Oshima samples. This time, the samples were heated to 800°C for one hour and the oxygen fugacities in the furnace was monitored by an yttria-doped zirconia probe (Sato,1971). The results are shown in Fig. 3. For the Oshima sample OS5061, the trend that TRM/NRM ratio is larger for higher fO_2 and smaller for lower fO_2 is similar to the Hawaiian samples, but the range of TRM/NRM values is much smaller than those for the Hawaiian rocks. However, the manner of change is not monotonic with the change of oxygen fugacity. A local minimum exists near $fO_2 = 10^{-7}$ atm. The TRM/NRM ratios after AF demagnetization of 200 Oe show this more clearly; TRM/NRM ratios are nearly constant and close to the expected value (0.87, shown by the thick dash-dot line) between the range of fO_2 of 10^{-5} to 10^{-20} atm., except for the minimum at 10^{-7} atm. The significance of the local minimum was not further studied in the present study.

The demagnetization diagram for the Oshima samples (not

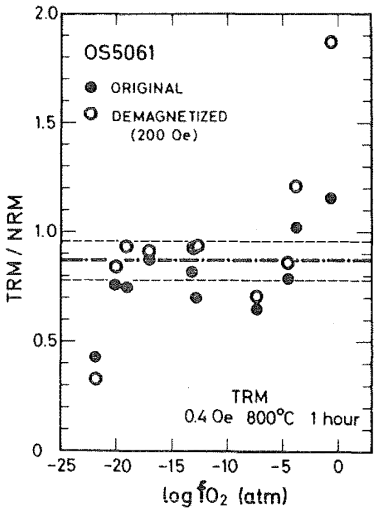

Fig. 3. TRM/NRM ratios of the Oshima samples. Solid and open circles represent ratios at AF demagnetization stages of 0 and 200 Oe, respectively.

shown) also show that TRMs have more high-coercivity components than NRMs and the diagrams are concave-down. The exception is the TRM obtained in the H_2 atmosphere which is more easily demagnetized than the NRM up to the field of 300 Oe. Samples heated in 10^{-17} and 10^{-19} oxygen partial pressures show sublinear curves in NRM-TRM diagram. The "paleointensity" indicated from such relations is about 0.5 Oe, in close agreement with the observed field intensity of 0.46 $\pm$ 0.04 Oe.

Experiment 3

The former experiment was performed on different samples from a same lava flow. The foregoing results may therfore be due, at least in part, to the difference among different samples. In order to eliminate such effects, the same sample was heated in this experiment in various atmospheres. The results are shown in Fig. 4. For one sample (triangle in Fig. 4), the heating was started in air and proceeded to less oxidizing conditions reaching finally to H_2. The other sample (circle) was treated in the reverse order. Apparently, the TRM/NRM ratio is not uniquely determined by the oxygen fugacity in the furnace; rather, it is a function, at least, of fO_2 and the former heat treatments. Such phenomenon is quite natural if one considers that true equilibrium is not expected to prevail at moderate temperatures such as 800 °C in the experimental time. That TRM/NRM values for two samples are close to each other at the extreme fugacities (air and H_2) may indicate that nearly the same states were attained at these conditions in spite of the difference in the previous treatments.

The results of this experiment is inconclusive as to the TRM-oxygen fugacity relation, but the following remarks may be appropriate. The TRM/NRM ratio is larger (smaller) for more (less) oxidizing atmospheres. It is also apparent from the figure that TRMs produced in oxidizing con-

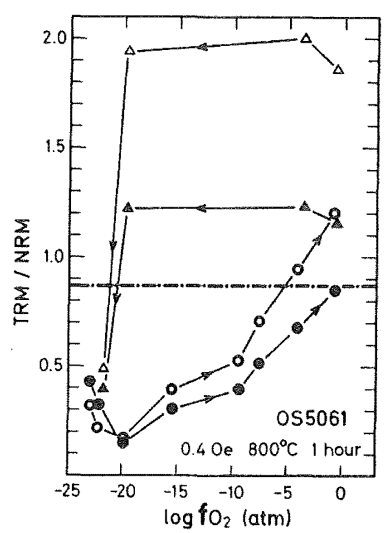

Fig. 4. Change of TRM/NRM ratio observed by heating the same samples in successively different conditions. Solid and open symbols are for AF demagnetization stages of 0 and 200 Oe, respectively.

ditions are usually magnetically harder than the NRM.

3. Change of Ferromagnetic Minerals due to Heating

It is probable that most, if not all, of the variations in TRM properties are caused by chemical changes of ferromagnetic minerals such as oxidation, reduction, unmixing, or homogenization. The most sensitive method to observe such changes is to compare the thermomagnetic curves of the samples before and after the heat treatment. Accordingly, thermomagnetic analyses were carried out after Experiment 2 of Section 2. The results are shown in Fig. 5. In this figure the intensity of magnetization is normalized by the room temperature values of individual samples. The comparison of magnitudes are therefore impossible, but in most cases changes in the absolute magnitudes were not greater than 50 percent.

The original sample contain two magnetic phases with Curie temperatures at 330°C and 510°C, respectively. As shown by Akimoto (1955), the Oshima lava of 1950-1951 contains titanomagnetite solid solution with 42 percent ulvospinel as the main ferromagnetic constituent, so that the lower Curie point can be identified with this phase. The higher Curie point must represent a spinel phase with less Ti content (less than 20 percent), which is a product of high temperature oxidation of the former.

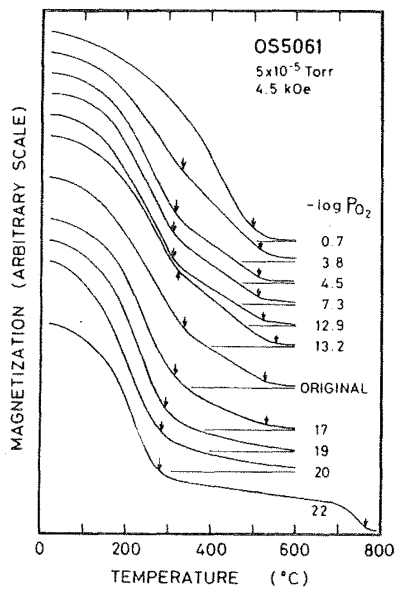

Fig. 5. Thermomagnetic curves of Oshima samples after they were heated in various atmospheres at 800°C for one hour (Fig. 3). The intensity is normalized by the room temperature values.

It is clearly seen from this figure that the amount of high Curie point phase increased when the sample was previously heated in oxidizing atmospheres and decreased when heated in reducing atmospheres. The sample heated in air to 800°C for one hour shows almost no trace of low Curie point component, suggesting a complete unmixing to magnetite solid solution and ilmenite solid solution (Ozima and Larson, 1970). For the range of oxygen fugacities between 10^{-17} and 10^{-20} atm., the relative amount of the high Curie point phase in the total magnetization decreases successively, indicating the prevalence of the reverse reaction (homogenization).

At extremely reducing condition (H_2), the Curie point of iron (770°C) appears in the thermomagnetic curve. The overall scheme of oxidation-reduction is quite consistent with the present data, and so it may be concluded that a major part of the changes in the TRM characteristics revealed in the present study is due to the chemical changes of ferromagnetic minerals caused by heating. However, an examination of phase diagrams of titanomagnetites (Buddington and Lindsley, 1964) show that

equilibrium was not realized in our experiments. For instance, heating in air or in H_2 shoud result in complete oxidation or reduction of iron at 600°C or 800°C. Actually, however, spinel phase containing both Fe^{2+} and Fe^{3+} still exist in samples heated in air or in H_2. Such non-equilibrium condition must be quite common in paleomagnetic experiments where heatings are usually restricted to short intervals sufficient for attaining a homogeneous temperature distribution in the sample, and to temperatures which are high enough for equilibrium to prevail. An important point to note is that chemical changes may take place in such low temperatures within experimental time.

Qualitatively, the changes in TRM capacity and in coercivity spectra may be explained in terms of reduction or oxidation of samples; the oxidized spinel phase contain less titanium and the saturation magnetization increases with the decrease of Ti in the spinel phase (Akimoto, 1955), while the coercivity increases proportionally with the magnitude of TRM (Nagata, 1961). However, such phenomenological interpretation should be made with caution, since it is certain that the reactions in the present experiments are not taking place in equilibrium. Factors other than oxygen fugacity should be taken into account for the complete understanding of the TRM changes.

4. Implications for Paleointensity Determinations

There are some important implications for paleointensity experiments. First of all, the TRM/NRM ratios cannot be taken as a reliable measure of paleointensities. It was demonstrated that for some lavas ratios almost two orders of magnitude different from each other can be obtained by simply heating in different conditions.

Secondly, TRM is usually largest when a sample is heated in air, which means that paleointensities smaller than the true values will be obtained if TRM/NRM ratios of samples heated in air are used in estimation. The possibility of such bias in the existing paleointensity data have already been pointed out by Kono (1974). The proportionality between some portions of coercivity or blocking temperature spectra of NRM and TRM, the reliability criteria often employed in van Zijl's or Wilson's methods, may not be good enough condition for rejecting bad paleointensity data.

Thirdly, the difficulty of producing a TRM which has the same properties as the NRM is to be noted. Though we compared only the magnitudes and coercivity spectra of NRM and TRM, there was hardly any TRM which was the same as the NRM in these respects. If we take other properties such as blocking temperature spectra, the difficulty may be more pronounced. This must reflect the fact that it is not possible to reproduce in a laboratory the actual physical conditions of the cooling of a lava in nature.

With considerations to the above points, we think that we should consider reliable only paleointensity data which have positive proofs of the absence of changes in TRM characteristics by the laboratory heatings. Reults from the Thelliers' method are reliable in this respect since it is, in other words, an experiment to detect the occurrence of changes in the blocking temperature spectrum. Kono (1971, 1974) therefore used only data obtained by the Thelliers' method in his compilation. For some samples, reliable data may be obtained by other method

(e.g., McElhinny and Evans, 1968). However, it is very difficult to satisfy the criterion suggested above, and usually this point is neglected in other methods. It may therefore be a reasonable idea to use only the results of the Thelliers' method until a better criterion is established.

References

Akimoto, S.(1955) Jap. J. Geophys. 1, 1.

Buddington, A.F. and D.H. Lindsley (1964) J. Petrol. 5, 310.

Coe, R.S. and C.S. Grommé (1973) J. Geomag. Geoelectr. 25, 415.

Kono, M. (1968) J. Geomag. Geoelectr. 20, 353.

Kono, M. (1971) Earth Planet. Sci. Lett. 11, 10.

Kono, M. (1974) J. Geophys. Res. 79, 1135.

McElhinny, M.W. and M.E. Evans (1968) Phys. Earth Planet. Inter. 1, 485.

Nagata, T. (1961) Rock Magnetism, Revised Edition, 350pp., Maruzen, Tokyo.

Ozima, M. and E.E. Larson (1970) J. Geophys. Res. 75, 1003.

Sato, M. (1971) in Research Techniques for High Pressure and High Temperature, edited by G.C. Ulmer, p.43, Springer, New York.

Sato, M. and T.L. Wright (1966) Science 153, 1103

Schwarz, E.J. and D.T.A. Symons (1970) J. Geophys. Res. 75, 6631.

Thellier, E. and O. Thellier (1959) Ann. Géophys. 15, 285.

Van Zijl, J.S.V., K.W.T. Graham and A.L. Hales (1962) Geophys. J. Roy. Astron. Soc. 7, 23.

Wilson, R.L. (1961) Geophys. J. Roy. Astron. Soc. 5, 45.

(Presented at IAGA Symposiun held at 16th General Meeting of the IUGG in Grenoble; submitted to Phys. Earth Planet. Interiors)

NATIVE IRON DISCOVERED IN THE LAVA FLOW OF NISHINOSHIMA-SHINTO, JAPAN

Kan-ichi MOMOSE

Department of Geology, Shinshu University
Asahi 3-1-1, Matsumoto 390, Japan

As previously reported by Momose(1974), through the thermomagnetic measurement the occurrence of native iron has been ascertained in the lava of a new-born volcanic island "Nishinoshima-shinto". However, at that time, the grains in question were not detected by the reflection microscope.

Recently, a few grains(approximately 30μ across) of native iron were recognized microscopically in the hand specimens. The electronprobe microanalysis made on these samples also confirmed the grains being native iron(Momose, 1975).

The grain occurs as an enclosure within a silicate mineral grain which coexists with grains of titanomagnetite in the groundmass : hence it is very difficult to explain the generation of the native iron.

This report concerns the fact that native iron was discovered in lava.

References

Momose,K,(1974) Rock Magnetism and Paleogeophysics, Vol.2,1.
Momose,K,(1975) Kagaku,Vol.45,637. (in japanese)

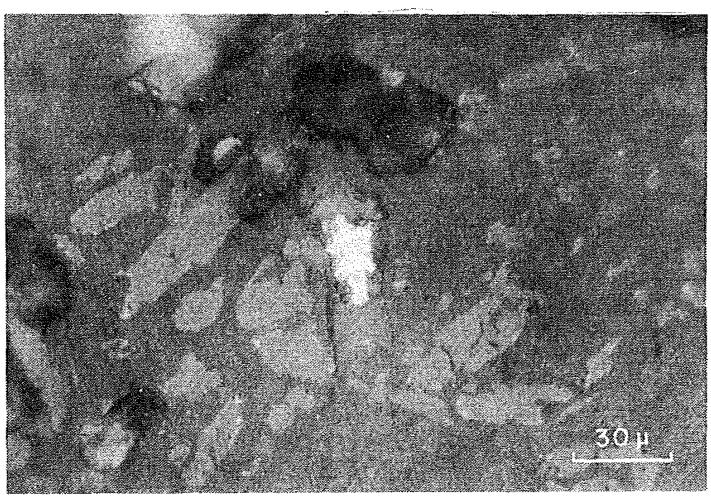

Reflecton microscopic photograph of polished surface of native iron grain (white point) contained in rock.

GROWTH OF NICKEL OLIVINE SINGLE CRYSTALS BY THE FLUX METHOD

Mituko OZIMA

Institute for Solid State Physics, University of Tokyo
Minato-ku, Tokyo 106, Japan

Introduction

Nickel orthosilicate, Ni_2SiO_4 is one of the olivine group minerals and is named liebenbergite (de Waal and Calk(1973)) in mineralogy. In contrast to other olivines such as Mg_2SiO_4, Co_2SiO_4, and Mn_2SiO_4 which melt congruently, Ni_2SiO_4 melts incongruently to NiO plus melt at about 1650°C (Phillips, Hutta and Warshaw(1963)). This resulted in the difficulty of growing single crystals of Ni_2SiO_4 olivine. Although this mineral occurs seldom in nature, crystal chemical properties of Ni_2SiO_4 olivine have attracted much attention in the field of earth science (Matsui and Syono(1968), Ringwood(1962), Akimoto, Fujisawa and Katsura (1965), Ma(1974)) because of its substitution of forsterite in natural olivines.

Several attempts have been made to obtain single crystals of Ni_2SiO_4, but no success in growing single crystals have been reported yet and almost all experimental work have been done using polycrystals. Flux growth is one of the promising method to grow incongruent-melting crystals. This report describes flux-growth of transparent single crystals of Ni_2SiO_4 olivine together with some physical properties.

Experimentals

Li_2O-MoO_3 system was adopted as a flux, because this is soluble in water, vaporizes little at high temperatures, and was known to be useful for growing forsterite Mg_2SiO_4 (Vu Tien, Grandin de Leprevier, Gabis and Anthony(1972)). Mixture of Li_2CO_3, MoO_3, SiO_2, and NiO were put in platinum crucible of 10 or 50 cm^3 in volume, heated at about 1400°C for about 20 hours in a muffle furnace, and slow-cooled to about 800°C. The rate of cooling was 3.8 °C/h. The weight of flux charged was 10 to 80 gramms and the nutrient was 2 to 30 weight percent of the flux. The crucibles were put out of the furnace at about 800°C to quench in the air. Thus quenched crucibles were washed in hot water so that crystals were easily separated from the solidified lithium-molybdenum oxide flux. Olivine crystals were found to grow at the bottom and/or rim of the crucible as shown in Figure 1.

X-ray microprobe-analysis was carried out on these crystals with an X-ray microanalyser (Japan Electron Optics Laboratory Co., Ltd., Model JXA-5 with 40 take-off angle). Synthetic NiO and SiO_2 crystals were used as standard materials and corrections were made by the method reported by Bence and Albee(1968) (Nakamura and Kushiro(1970)). Specific gravity of these crystals were measured using a Berman balance.

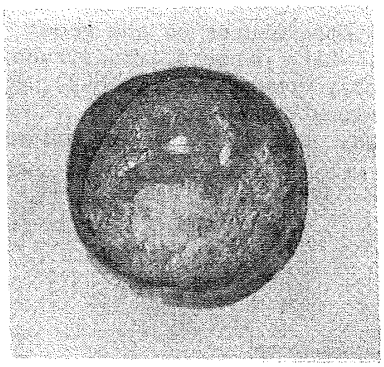

Fig. 1 Top view of the crucible before dissolution of the flux.

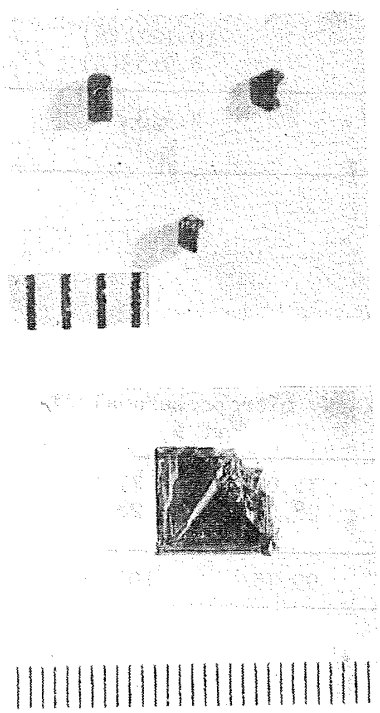

Fig. 2 As-grown Ni_2SiO_4 olivine crystals.
Upper: Small euhedral
Lower: The largest
One division of the scale shows 1 mm.

Results and Discussion

Production of olivine crystals is much sensitive to the composition of the flux. The flux $Li_2Mo_2O_7$ (Li_2O-$2MoO_3$) and $Li_2Mo_{1.5}O_{5.5}$ (Li_2O-$1.5MoO_3$) did not produce olivine at all and reacted with the nutrient so that a new material of NiO-Li_2O-MoO_3 system (determined as $Li_2Mo_3Ni_2O_{12}$ by chemical analysis (Ozima and Zoltai(1976)) and SiO_2 were produced. The flux Li_2MoO_4 (Li_2O-MoO_3) worked most effectively. Even in this case, processes seem to be much complicated and NiO and/or lithium-silicate phases besides olivine crystals were grown. Detailed report on the phase relations are now in preparation. Single crystal of Ni_2SiO_4 olivine is transparent and has a color of dark green like an emerald.

The crystal habit of the olivine seems to be controlled by the composition of the nutrient. Both in the case of the excess NiO or excess SiO_2, comparatively large rectangular plate-shaped olivines grew as well as numerous small euhedral ones. On the other hand, only euhedral crystals were grown in the case of the stoichiometric nutrient (NiO/SiO_2 = 2.0).

Figure 2 shows some as-grown Nickel olivine crystals by this method. Euhedral crystals are characterized by the (010), (021), and (001) faces and this is identical with the habit of natural olivines. Plate has always (010) face. These were confirmed by Laue-photograph and measuring d-spacings of these planes by an X-ray diffractometer.

Lattice parameters were determined precisely by an X-ray diffractometer using 38 reflections and are given in Table 1. In the table, lattice parameters by other authors are also listed. X-ray density was calculated using these lattice parameters and this is compared with the measured specific density. The origin of this discrepancy should be attributed to impurities or inclusions which are inevitable in the flux method.

Chemical analysis was carried out for these crystals. Unfortunately, Ni_2SiO_4 olivine is very hard of dissolving and we failed to have a result for NiO and SiO_2 contents by the wet-

chemical analysis. Instead, the composition of the crystals were determined with an X-ray microprobe analyser. The result is compared with the ideal value as shown in Table 2.

Magnetic properties were measured at low-temperatures on the grown Ni_2SiO_4 olivine crystals using a torque-meter. Like other olivines such as Fe_2SiO_4 and Co_2SiO_4 (Kondo and Miyahara(1963), Nomura et al(1964)), Ni_2SiO_4 was found to show antiferromagnetic properties below 30 K. The easy axis of the spin is parallel to b-axis. Details will be published elsewhere.

Table 1

Lattice parameter and X-ray density of Ni_2SiO_4 olivine at room temperature

Lattice Parameter (A)	This work L-1	ASTM-card No.15-388	Matsui and Syono Ni8
a	4.7285(2)	4.725	4.7287(3)
b	10.1179(7)	10.118	10.1214(6)
c	5.9132(4)	5.908	5.9153(3)
X-ray density	4.917(1)	4.925	4.913
Specific gravity	4.93		

Table 2

Chemical composition of Ni_2SiO_4 olivine crystals

Chemical Composition	Stoichiometric wt %	X-ray microprobe analysis wt %	
NiO	71.32	71.07	71.44
SiO_2	28.68	28.68	28.72
total	100.00	99.75	100.16

References

Akimoto, S., H. Fujisawa and T. Katsura (1965) J. Geophys. Res., 70, 1969.
Bence, A. E. and A. L. Albee (1968) J. Geology, 76, 382.
de Waal, S. A. and L. C. Calk (1973) American Mineralogist, 58, 733.
Kondo, H. and S. Miyahara (1963) J. Phys. Soc. Japan, 18, 305.
Ma, C. (1974) Contr. Mineral. Petrol., 45, 257.

Matsui, Y. and Y. Syono (1968) Geochemical J., 2, 51.
Nakamura, Y. and I. Kushiro (1970) Contr. Mineral. Petrol., 26, 265.
Nomura, S., R. Santoro, J. Fang and R. Newnham (1964) J. Phys. Chem. Solids, 25, 901.
Ozima, M. and T. Zoltai (1976) in press.
Phillips, B., J. J. Hutta and I. Warshaw (1963) J. Am. Ceram. Soc., 46, 580.
Ringwood, A. E. (1962) Geochim. Cosmochim. Acta, 26, 457.
Vu Tien, L., A. Grandin de Leprevier, V. Gabis and A. M. Anthony (1972) J. Crystal Growth, 13/14, 601.

(Submitted to J. Crystal Growth)

EXPERIMENTAL DATA ON THE ARCHEO-MAGNETIC FIELD INTENSITY DETERMINED BY THE STEPWISE DE- & RE-MAGNETIZATION IN THE PRESENT GEOMAGNETIC FIELD

Haruo DOMEN

Institute of Physical Sciences, Faculty of Education,
Yamaguchi University, 753 Japan

The method presented in this report is such that a couple of test specimens was partially demagnetized and remagnetized successively by the stepwise thermal treatment *in the present geomagnetic field*. The remanent magnetization of the thermally treated specimen was measured before and after every stepwise successive thermal treatment. And the ratio of the ancient geomagnetic field intensity to the present one was decided.

The natural remanent magnetization (NRM) of the sample, whose NRM should be given by thermal origin ; say thermo remanent magnetization (TRM), was measured by means of an ordinal astatic magnetometer at first as well as general paleomagnetic investigations. Several pillars of the specimen (rod like long shaped, square pillar specimens) were cut out along the original NRM direction and/or meridian from the old roof tiles or rocks. A couple of test specimens thus prepared were put in the non-inductively wound electric furnace such a way that one of them should be placed its NRM direction in parallel to the present geomagnetic field and another specimen in anti-parallel. These specimens were heated up to a certain temperature, T, then, cooled down to the room temperature. The NRM of the test specimen may be destroyed partially and replaced by the partial TRM within the temperature interval between the room temperature and T.

Now, let assume that the partial TRM of specimens is proportional to the week ambient magnetic field of both ancient and present respectively and also to the treating temperature.

Finally, the following equation was obtained;

$$NRM - (Ha/Hp)I_-/2 = I_+/2,$$

where Ha and Hp are the geomagnetic field intensities for the ancient and the present, in which original NRM was given and partial TRM was given respectively. I_- is the subtraction of remanent magnetization of paralleled specimen and anti-paralleled one after thermal treatment up to T and I_+ for addition of these two intensities.

For a pair of specimens cut out from the same sample, having the same dimension, the successive stepwise thermal treatments and remanent magnetic measurements give several sets of I_- and I_+ combinations for each treating temperature. The mean Ha/Hp ratio is decided by the method of least squares as a tangent of the straight line on the I_- *vs* I_+ diagram for the equation mentioned above.

In general, the NRM direction may deviate from the long axis of the roof tile specimen, then the original field intensity Ha* affects to the axis of the prism specimen as Ha*$\cos\theta$,

where Θ is the angle between NRM direction and the long axis of the specimen. The present geomagnetic field Hp* makes an angle *I* which is the geomagnetic field inclination, and the thermal treatment mentioned here is generally performed along the long axis of specimen keeping in the horizontal north. Then Hp in the preceding equation should be read as Hp*$\cos I$.

Table 1 shows some numerical examples of the paleo/archeo magnetic field intensity thus decided.

Table 1

Specimen	Ha*/Hp*	Ha*
Tiles		
NT; Present	0.81	0.38 Oe
TT; 40 yBP	1.10	0.53
RT; 80 "	3.04(?)	1.44(?)
OT;100 "	1.25	0.60
KT;200 "	1.37	0.65
FT;300 "	1.21	0.58
Rock		
CR;Early Holocene	1.62	0.77

A minute calculation concerned with the present work have been published (Domen 1974). This work with some data was read on the IAGA Meeting at Grenoble, France in 1975 and it will appear as one of papers submitted to the meeting in "Physics of the Earth and Planetary Interiors" as a special issue for the symposium in the near future.

Reference

Domen, H. (1974) Bull. Fac. Educ., Yamaguchi Univ. **24**, 7.

PALAEOMAGNETISM OF LAKE BIWA SEDIMENT

Naoto KAWAI, Tadashi NAKAJIMA, Katsumi YASKAWA*, Masayuki TORII and Nobuyoshi NATSUHARA

Department of Physics, Faculty of Engineering Science, Osaka University, Toyonaka, Japan

1) Introduction

When Horie succeeded in drawing out a long boring core from Lake Biwa (1971), he asked one of the present authors(N.K.) to make use of it for the paleomagnetism. Several small blocks were first tested with a sensitive magnetometer installed in Osaka University (early in Jan., the next year).

Despite the weak magnetic susceptibility, each had a stable permanent magnetism sufficiently determinable. A preliminary survey, therefore, was started subsequently. Three small specimens vertically adjointing were cut off at 40 points of the entire core at every 5 m interval. When all the pieces were measured within a short period of two months, the first report (Kawai et al.,1972) appeared in the Proceedings of the Japan Academy.

Meanwhile, reports on the geochemical (Koyama 1972, Handa 1972, Nakai 1972), pollen (Fuji and Horie 1972) sedimentational (Horie 1972 and 1974) analyses followed, using the same specimens. Summing up the data, Kawai (1972) published a paper entitled "The magnetic control on the climate in the geologic time".

Next, the entire core was split up into a vertical sequence of cubic samples so that unavoidable gap between one sample and another might be made as thin as possible. The measurement of the cube near the core-top had no sooner started than a measurement plan was laid in detail.

The work proceeded slowly at first but progressively quickly, so that it soon became a routine. The measured part of the core is now fathomed as 60 m from the core-top. The measured samples have increased in number up to 3,000 pieces by now. The results summed up are shown in this paper.

The informations gathered from the upper 30 m of the same core were reported in some journals (Yaskawa et al. 1973, Nakajima et al. 1973, Nakajima and Kawai 1974, Yaskawa 1974). Two papers (Nakajima and Kawai 1974, Yaskawa 1974) have appeared on the basis of the same results with different interpretations.

2) Age-depth relation in the core

Prior to the study, a representation of the geomagnetic field in the historical time, using baked clays, had been undertaken by the same group of Osaka University. The data

---

*Present Address; Faculty of Science, Kobe University, Nada, Kobe, Japan

amassed in the laboratory were compiled by Hirooka into his thesis (1971).

Lake Biwa is located in proximity to the places from which the historical secular change has been disclosed. If the remanent vector in each cube can be considered as frozen geomagnetism which existed while the layer thickened up to 2 cm (for about 80 years), the NRM of one cube and that from the baked clays must agree within the experimantal error in case the two have the same age. The geomagnetic three elements found from the core and those from the baked clays vary with time quite concordantly. The depth at any point in the upper core is determinable, when the obtained two curves are assumed to possess common respective maxima and minima as approximately as possible (Nakajima and Kawai 1974). Big questions still remain as to how fast the remanent vector is to be frozen, and how quickly the consolidation of the oozy upper layer of sediments is to be completed.

In regard to the pre-historic period we have no such means by which to data the core. But the core involves specimens which reflects the latest geomagnetic stage called the Blake event. It is assumed to exist between 108,000 and 114,000 yrBP by Smith and Foster(1969). In Lake Biwa it corresponds to the sediment layers ranging from 49 to 56 m in depth. The correlation was reported in detail in the previous papers (Kawai et al. 1972, Nakajima et al. 1973, Yaskawa et al.1973). Besides, three volcanic ash layers were perceived at places 38, 63 and 100 m downward from the core-top. They all were dated by the fission track method as 80,000, 110,000 and 180,000 yrBP, respectively, by Nishimura and Yokoyama (1973). It is quite likely that we have acquired an almost continuous geomagnetic record in a long geologic time since 110,000 yrBP.

3) Measurement and the results

Prior to the measurement of natural remanent magnetism (NRM), each cubic sample is cleaned up with AC decreasing field from 100 to zero Oe smoothly in a non-magnetic space made up of three μ metal layers. The viscus component of magnetism is assumed to have completely been removed.

On the other hand, in order to obtain the isothermal saturation magnetism (ISRM), each cube is placed under a steady field of 7,000 Oe and the remanent vectors are similary measured, using the same instrument.

The ratio, NRM/ISRM is then calculated and the change of the ratio with depth (or time) is shown in the upper part of Fig. 1, while in the lower part of it that of NRM alone with time is indicated.

The inclination change is also shown as a function of depth in the core.

The mean is calculated out of 5 vertically adjoining specimens in both cases of intensity and inclination as shown in Fig. 2. A vertical line drawn at each point indicates the standard deviation.

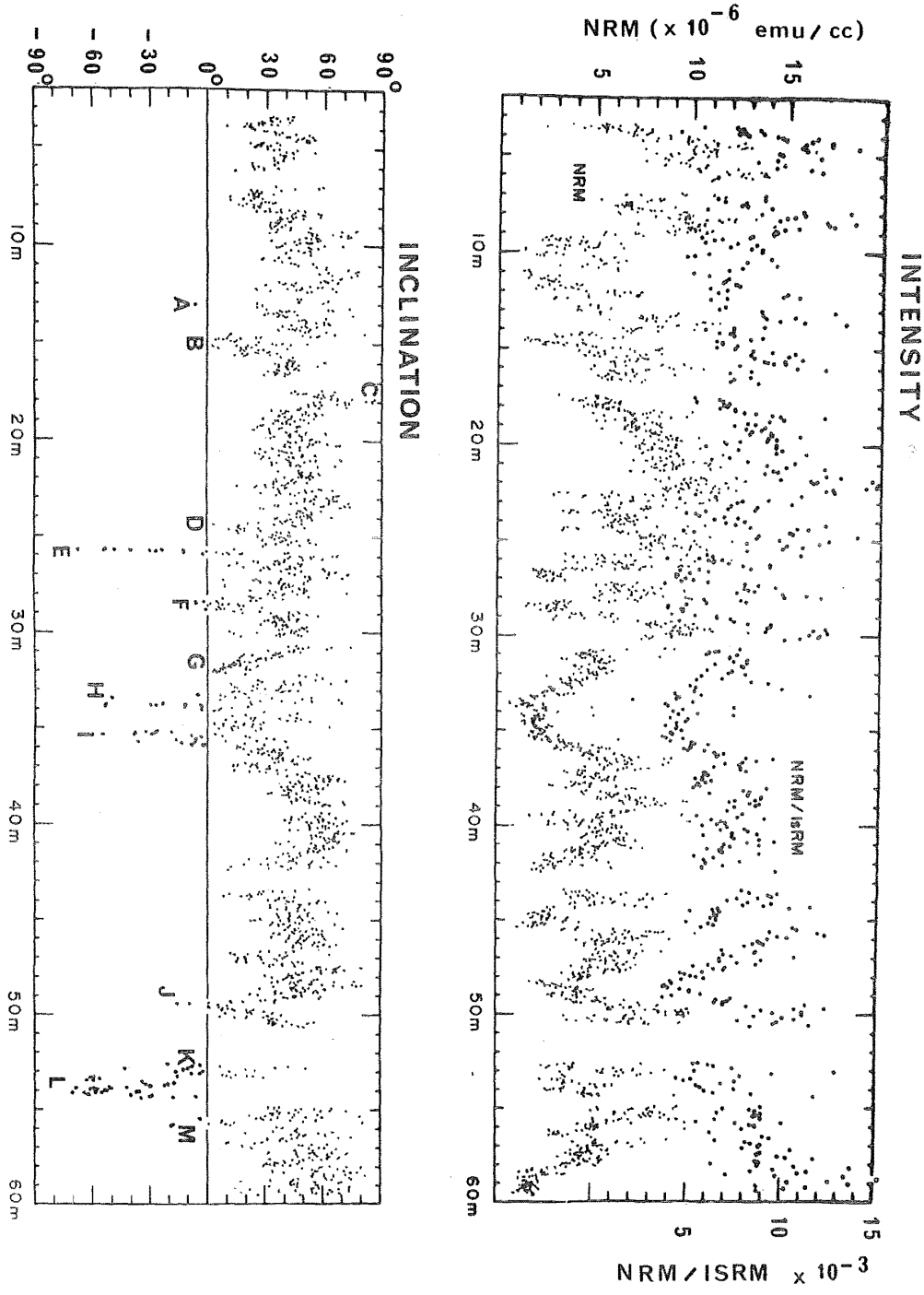

Fig. 1 Data of measurements.
Small dot shows the value of NRM, and large dot the ratio (NRM/ISRM).

4) Change in inclination

The core of Lake Biwa sediments obtained is exactly 197.2 m long. Unfortunately, it is broken up into a large number of vertical columns. We have tried to unite two adjoining columns, magnetically assuming that the specimens near the joint possibly have the same magnetization. Too large an experimental error is unavoidable in this method of displaying the secular declination in one diagram.

In contrast, the inclination in each cubic specimen can be shown because the axis of the core is nearly parallel to the plumb line of the boring spot and perpendicular to the strata in the lake sediments. Thus, we can now disclose the inclination all along from the core-top down to the depth of 60 m.

As shown in Fig. 1 dip angle fluctuates unexpectedly greatly as well as they do so frequently with the increasing depth. Except for the abnormal points described later, dip angle moves from point to point so continuously that it may easily be possible to draw a curve by tracing the mean value of every 5 inclinations as shown in Fig. 2. The fluctuation demonstrates as if such a field as the archaeosecular variation had existed throughout the entire period.

A sudden flip of dip angle appears at A, B, C, D, E, F, G, H, I, J, K, L and M, each occurring in a short interval of time of the order 10^2 - 10^3 years. Almost horizontal or even negative inclination is seen at each point except at C, where it reaches almost + 90°. Of these points only A and E were regarded as the times when excursions of the pole position occurred (Nakajima et al. 1973, Yaskawa et al. 1973). K is separated from L by an interval shorter than 1,000 years. G, H and I appear successively likewise within a short interval. A weak field intensity is associated with each particular interval. The interval between K and M is considered to be that of the Blake event, as it is represented by a long persistence of negative inclination.

Next, a fact reciprocal to the above relation is to be emphasized. So long as the high intensity is retained, the dip angle keeps a mean value of about 50 degrees, however greatly it may fluctuate in amplitude. 50 degrees is very close to the present dip angle now observable around the lake.

5) Change in intensity

Irving and Major(1964) made an experimental test to confirm the time when NRM could be acquired during sedimentation. They concluded that the NRM is born not when falling magnetic particles in water reach and set in the upper layer of sediments but evidently after that time, and called it post-depositional remanent magnetism or PDRM. Kent (1973) refined the experiment later and found that the remanent vector of sediment is almost proportional to the applied geomagnetic vector. We also have found that the ratio NRM/ISRM is the best scale to measure the the palaeomagnetic intensity, since it is independent of the quantity of magnetic particles contained in the sediments. Yaskawa (1974) tried to estimate the time when the particles become fixed in the nonmagnetic matrix in case no leakage but

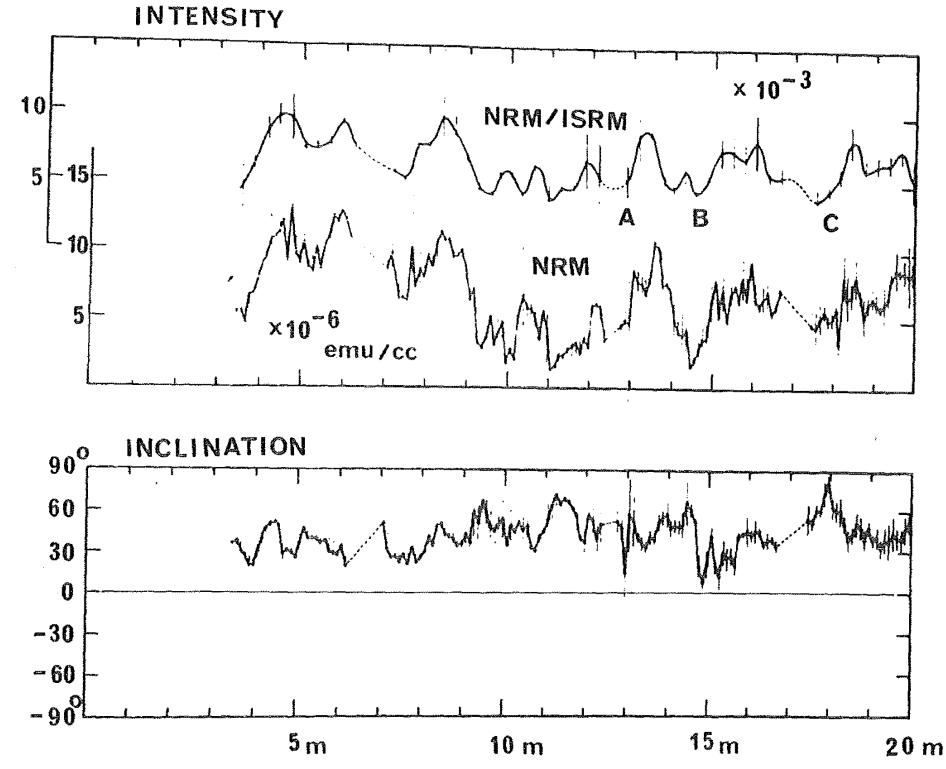
INTENSITY
10
5
15
10
5
x 10⁻³
NRM/ISRM
A
B
C
NRM
x10⁻⁶
emu/cc
INCLINATION
90°
60
30
0
-30
-60
-90°
5 m
10 m
15 m
20 m

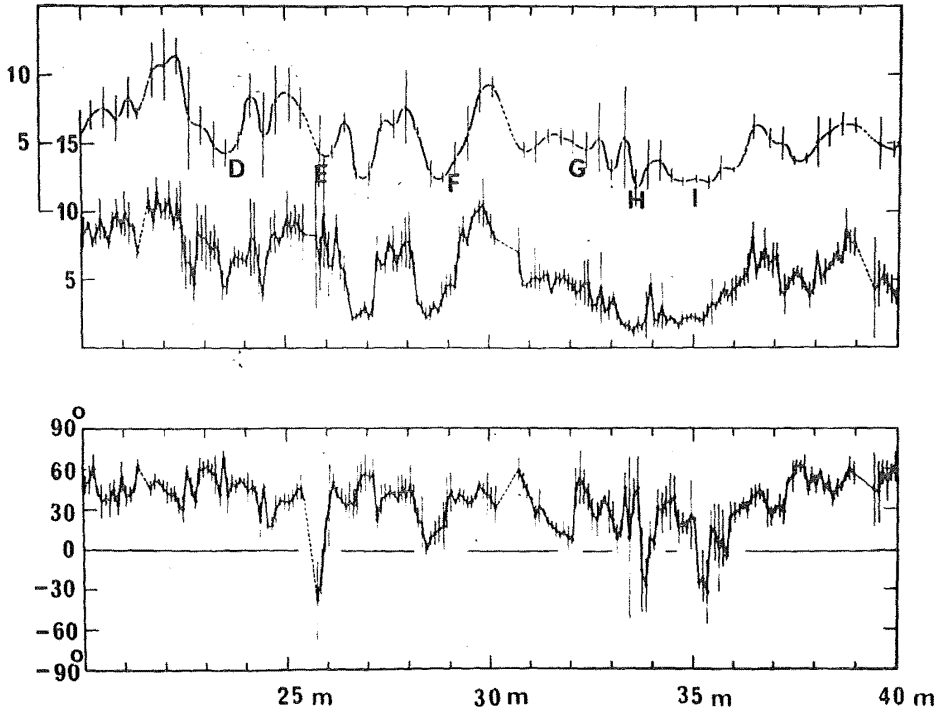
10
5
15
10
5
D
E
F
G
H
I
90°
60
30
0
-30
-60
-90°
25 m
30 m
35 m
40 m

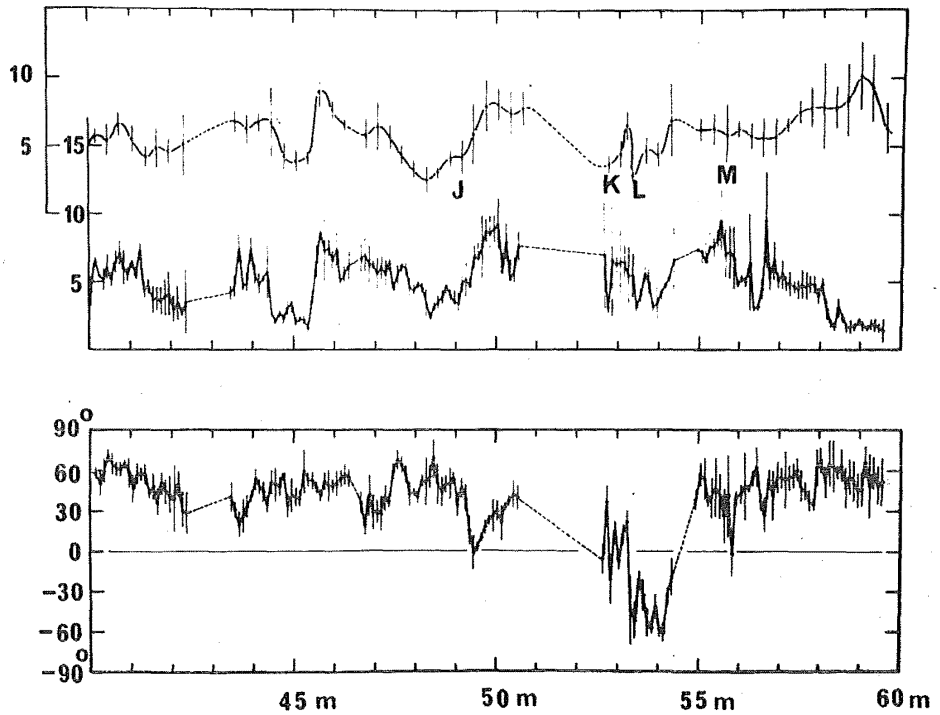

Fig. 2 Change of the mean taken out of every 5 specimens.
A vertical line drawn at each point indicates the standard deviation.

the upward replacement of water occurs to make the oozy sedimets more consolidated.

The change of the NRM/ISRM ratio we have obtained from the present core is also shown in Fig. 1, together with the change of NRM itself.

Although the ratio NRM/ISRM and the NRM move concordantly on the time span, the above relation is broken up at several points. The NRM/ISRM goes up, while NRM gose down in a region around 57 m. This region is considered to correspond to the time when the Blake event sets in and begins.

We first should be aware of that the non-magnetic matrix of the sediment decreases rapidly, making bigger magnetic particles/cc and NRM and secondly that the geomagnetic intensity drops, as the NRM/ISRM ratio decreases in the early stage or even prior to it. The non-magnetic matrix is made up of clay particles and organic substances derived from the past living matters, as discovered by Handa (1972).

Kawai (1972) predicted (1) that such a rapid decrease of organic substances is the consequence of very low photo-synthetic activity in and around the lake, (2) that the field prior to each Brunhes event is quite high but suddenly drops, as soon as the event starts and (3) that a climatic depression soon follows the magnetic decline.

In addition to the above, one of the present authors (N.K.) is conscious of a fact that the ferromagnetic particles themselves increase in the early stage of the event. When the field declines, the magnetosphere must shrink three dimensionally. Not only the high energy particles but also the charged ferromagnetic dusts trapped by external line of force are all gathered and carried towards the earth, although many of them are scattered into space by solar wind. But some can trespass on the atmosphere through magnetic windows up above the north and south poles. They are soon uniformly distributed in the atmospheric convection cells till all fall directly on the earth or as the nuclei of icy or water particles. If so, a very small ratio of NRM/ISRM is due to this reason.

Such a case has been comfirmed at the time of the geomagnetic extinction in the stage transitional from the Matuyama and the Brunhes epoch (Kawai et al. 1975, Kawai and Nakajima 1975). Besides, it is quite likely that the green house effects around the earth become much reduced too in the event of the geomagnetic weakening as suggested by Kamiyama and Yamamoto (private communication).

References

Fuji, N. and S.Horie (1972) Proc. Japan Acad. 48, 500.
Handa, N. (1972) Proc. Japan Acad. 48, 510.
Hirooka, K. (1971) Mem. Fac. Sci. Kyoto Univ., Sel. Geol. Mineral. 38, 167.
Horie, S. (ed. 1972) Paleolimnology of Lake Biwa and the Japanese Pleistocene (First Issue), 93pp.
Horie, S. (ed. 1974) Paleolimnology of Lake Biwa and the Japanese Pleistocene (Second Issue), 288pp.
Irving, E. and A. Major (1964) Sedimentology 3, 135.
Kawai, N., K. Yaskawa, T. Nakajima, M. Torii and S. Horie (1972) Proc. Japan Acad. 48, 186.
Kawai, N. (1972) Proc. Japan Acad. 48, 687.
Kawai, N., Y. Otofuji, T. Nakajima and K. Kobayashi (1975) Proc. Japan Acad. 51, 634.
Kawai, N. and T. Nakajima (1975) Proc.Japan Acad. 51, 640.
Kent, D.V. (1973) Nature 246, 32.
Koyama, T. (1972) Proc. Japan Acad. 48, 505.
Nakai, N. (1972) Proc Japan Acad. 48, 516.
Nakajima, T., K. Yaskawa, N. Natsuhara, N. Kawai and S. Horie (1973) Nature Phys. Sci. 244, 8.
Nakajima, T. and N. Kawai (1974) Paleolimnology of Lake Biwa and the Japanese Pleistocene (Second Issue), 65.
Nishimura, S. and T. Yokoyama (1973) Proc. Japan Acad. 49, 615.
Smith, D. and J.H. Foster (1969) Science 163, 565.
Yaskawa, K., T. Nakajima, N. Kawai, M. Torii, N. Natsuhara and S. Horie (1973) J. Geomag. Geoelectr. 25, 447.
Yaskawa, K. (1974) Rock Magnetism and Paleogeophysics 2, 15.
Yaskawa, K. (1974) Paleolimnology of Lake Biwa and the Japanese Pleistocene (Second Issue), 77.

PALEOMAGNETIC STUDY OF OSAKA GROUP USING MARINE AND NONMARINE CLAYS NEAR KOMYOIKE, OSAKA PREFECTURE

Junichi NISHIDA & Shiro ISHIDA
Department of Geology and Mineralogy, Faculty of Science, Kyoto University, Kyoto Japan

Introduction

Osaka Group represents the typical Plio-Pleistocene strata in Southwest Japan(Ishida S. 1970). Ishida et.al.(1968) and Torii et.al.(1974) reported paleomagnetic results of volcanic ashes in Osaka Group. Ishida et.al. assumed Matuyama-Brunhes boundary between Azuki tuff in Ma 3 and Fukakusa tuff in fresh water clay, upper than Ma 4. Torii et.al. reported Matuyama-Brunhes boundary as near Sayama volcanic ashes intercalated in nonmarine clay just below Ma 3.

Nishimura and Sasajima(1970) reported 0.87± 0.07 m.y. for the age of Azuki tuff by fission track method. It can be safely assumed that the stratigraphic sequence of Matuyama-Brunhes boundary lies near Sayama volcanic tuff between Azuki tuff and Fukakusa tuff. In these previous works, the measurement of NRMs of marine and nonmarine clays are not achieved since the intensity of NRMs of these clays are too weak to measure in those days. So, the precise stratigraphic sequence of Matuyama-Brunhes boundary is not determined up to date.

Our prime purpose of this study is to decide the stratigraphic sequence of Matuyama-Brunhes boundary. We considered that successive measurement of marine and nonmarine clays can afford the information not only of the stratigraphic sequence of Matuyama-Brunhes boundary but also of the detailed feature of the change of paleomagnetic field since the sedimentation rate of Osaka Group is far greater than that of deep sea sediments.

Samples

We collected clays and Azuki tuff from nonmarine clays below Ma 3 to Ma 4 succesively. The locality is situated at the western clif of road of southwest of Komyoike, Izumi City, Osaka Prefecture. As Komyoike is considered to be the margine of subsiding basin of Osaka Bay, the rate of sedimentation is not so

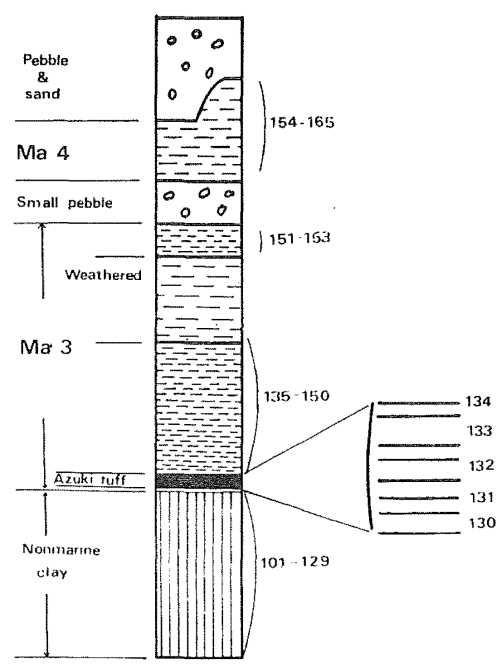

Fig. 1 Stratigraphic column of Osaka Group near Komyoike.

large as that in Lake Biwa. The stratigraphic succession of the samples is shown in column (Fig. 1). The lowermost horizon of the exposure is nonmarine clay below Ma 3. The uppermost horizon of the exposure is Ma 4. Sixty-five samples are collected from the bottom to the top of this road cutting.

Experimental procedure

Thirty samples are chosen for the present study from the collected samples. About 10 specimens are prepared from each sample. Measurement was carried out by spinner magnetometer. The NRMs of the specimens are measured before and after the magnetic cleaning. Ideally, a progressive demagnetization curve should be obtained for each individual sample. In view of the large number of specimens involved in the present study, this would have been impractical. For the present study, all the specimens were demagnetized in a peak field of 100 Oe alternating field using three axis tumbler.

In Fig. 2, the example of the result for alternating field demagnetization is shown. As shown in this figure, the NRMs deviate to the present north pole along large circle before demagnetization. After demagnetization, they gathered together on southern upper hemisphere. In Fig.3 is also shown another example. As shown in this figure, the NRMs are distributed in lower hemisphere before magnetic cleaning. After magnetic cleaning, the directions of NRMs appeared in southern upper hemisphere. Normal NRMs are also affected by secondary soft component, and the directions of NRMs move significantly after magnetic cleaning. Fig.4 and Fig.5 are the results of magnetic cleaning for normal NRMs. It may be noted that in these two cases, the mean direction of NRM moves towards the

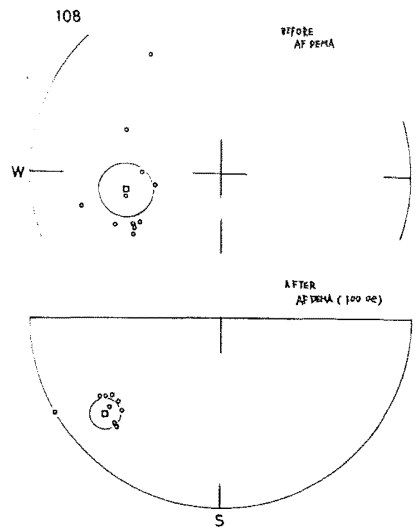

Fig. 2 Example of the result for AF demagnetization of reversed sample. Open circles are on the upper hemisphere. Square represents mean direction.

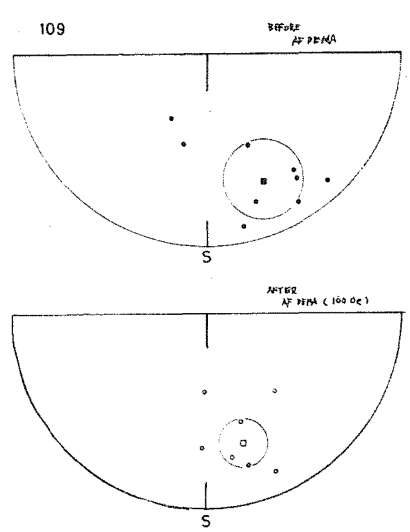

Fig. 3 Example of the result for AF demagnetization for reversed sample. Open circles are on the upper hemisphere. Closed circles are on the lower hemisphere. Sqare represents mean direction.

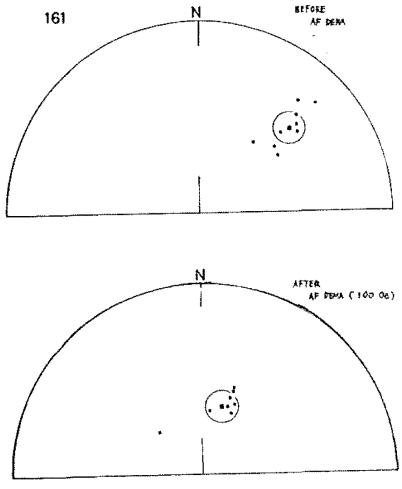

Fig. 4 Example of AF demagnetization for normal sample. Symbols are equivalent with those in Fig.3.

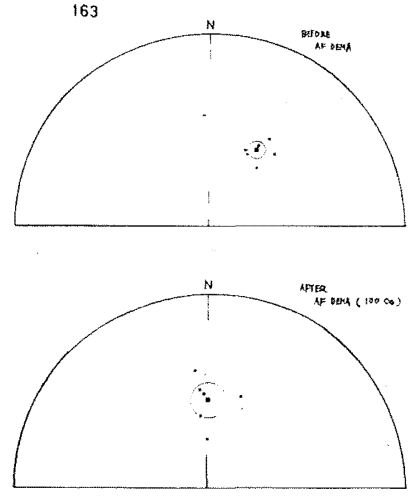

Fig. 5 Example of AF demagnetization for normal sample. Symbols are equivalent with those in Fig. 3.

direction of axial geocentric dipole. We cannot explain the cause of soft component in these samples hitherto.

It may be noted here that the direction of NRMs after magnetic cleaning of 100 Oe do not exhibit satisfactorily the direction of original remanent magnetization. Further demagnetization is considered to be needed.

In Fig.6, declination and inclination of each samples are plotted against the stratigraphic sequences of sampling sites.

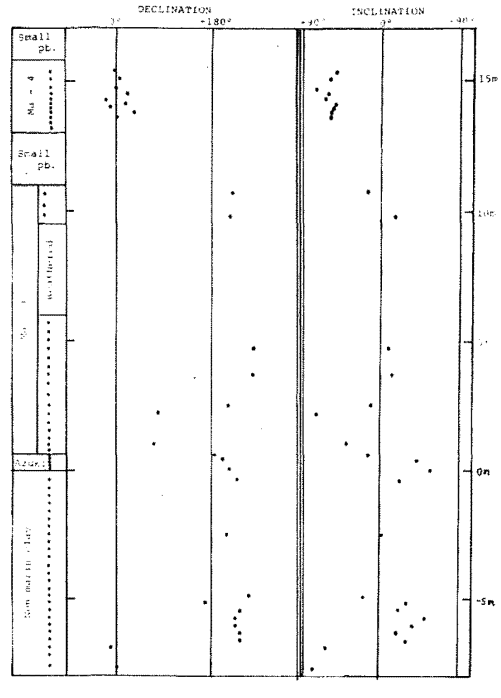

Fig. 6 Summary of paleomagnetic results after magnetic cleaning. Points in the column corresponds to the specimen number in Fig. 1.

Discussion

As shown in Fig.6,only normal polarities are observed in Ma 4 except to the lowermost part and reversed polarities in upper part of Ma 3. Another measurement on Ma 4, near Fukakusa in Kyoto Prefecture made by us(unpublished data) suggest the normal to

reversed transition in lower part of Ma 4. It may be assumed that the stratigraphic sequence of Matuyama-Brunhes boundary is the lower part of Ma 4.

Two normal polarities are recognized in our measurement, one on the upper horizon of Azuki tuff, one the bottom of this stratigraphic succession. Watkins(1968) suggested the possibility of short duration normal event at about 0.82 m.y., which is non-dipole activated or global extent. The normal event on the Azuki tuff may be correlated to B-zone of Watkins.

The normal polarities are observed in the bottom of this exposure. Ishida et.al.(1968) correlated the Komyoike tuff, normally magnetized, with Jaramillo event. The horizon of the Komyoike tuff is below Ma 2. Recently, Maenaka et.al.(1975) assumed it as normal polarity not reported yet in Matuyama epoch. They considered Jaramillo event as Kamikatsura tuff between Ma 2 and Ma 3. The normal polarity in the bottom of this exposure also may be correlated to Jaramillo event.

It is also noted from the result shown in Fig.6, that the inclination of reversed polarities are shallow and declination deviate to the west. Similar directions of NRMs are also observed in some volcanic rocks in southwest Japan. Though the alternating peak field of 100 Oe is not enough to remove the secondary viscous component, it may have some unexplained meaning. This problem is now in progress by using volcanic rocks.

References

Ishida, S.(1970), The Quaternary Res.,9,101
Ishida, S., K. Maenaka & T. Yokoyama(1968), Jour. Geol. Soc. Japan, 75,183
Maenaka, K., T. Yokoyama & S. Ishida(1975), E.P.S.L. in press.
Nishimura, S. & S. Sasajima(1970), Chikyu-Kagaku, 24, 222
Torii, M., S. Yoshikawa & M. Itihara(1974) Rock magnetism and Paleogeophysics 2, 34
Watkins, N.D.(1968) E.P.S.L., 4 341

PRELIMINARY REPORT OF MAGNETOSTRATIGRAPHY OF TOKONAME GROUP IN CHITA PENINSULA

Yo-ichiro OTOFUJI, Takeshi MAKINOUCHI
AND
Junichi NISHIDA
Department of Geology and Mineralogy, Faculty of Science,
Kyoto University, Kyoto, Japan

Introduction

In the Pliocene, there existed larger lake in the present Ise Bay and the surrounding areas. This extinct lake is called as " Lake Tokai" (Takehara et. al., 1961, 1964), at present. The sediments accumulated in this Lake are spread around the Ise Bay, namely, the Agĕ Group in the Ise district, the Seto Group in the Nagoya district and the Tokoname Group in the Chita peninsula. The " Tokai Group " is a general term for them (Ishida and Yokoyama, 1969). The Tokoname Group occupies the lower part of the Tokai Group (Makinouchi, 1975).

In order to correlate the Pliocene-Pleistocene strata with global scale, paleomagnetic survey has been made of the Cenozoic strata. Ishida et. al. (1968) established the time table of Cenozoic strata in Kinki and Tokai district of magnetostratigraphy by using volcanic ashes interbedded in sediments. On the other hand, Tokai Group is left behind from their paleomagnetic survey.

It is very interesting to suppose the period of the deposition of Tokoname Group pleomagnetically. Since Tokoname Group is one of the first sediments in Lake Tokai of the Pliocene-Pleistocene basin, the knowledge about the age of beginning of subsidence may be expected to render great information about the historical geology of Setouchi Province.

Another purpose of our study is to estimate the degree of paleosecular variation by using thick ash layer. The hypothesis of correlation between volcanic activity and the geomagnetic reversal proposed by Kennett and Watkins (1970) might be examined.

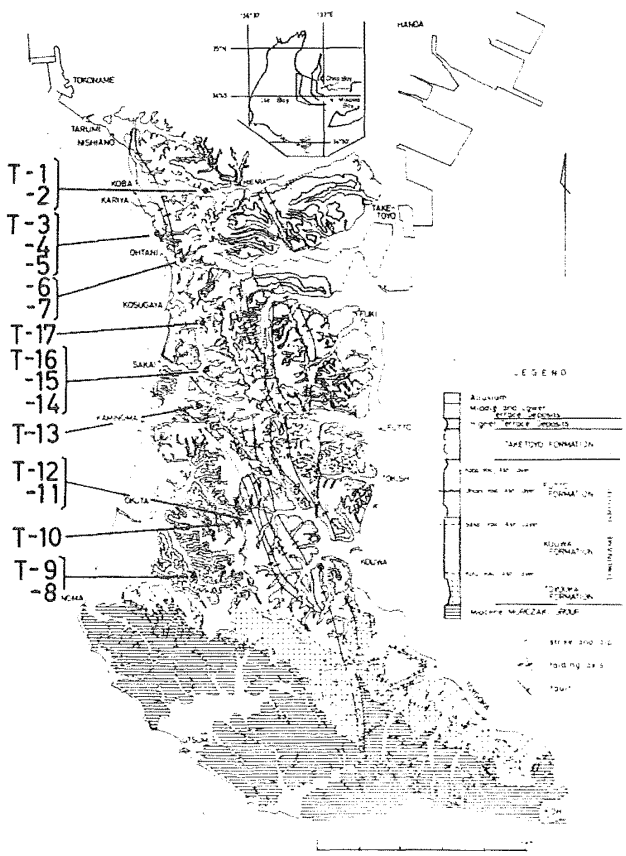

Fig. 1 Geologic map of the Chita Peninsula and sampling sites.

Geological Outline

The Chita Peninsula is composed of the Miocene Morozaki Group, the Pliocene Tokoname Group, the lower Pleistocene Taketoyo Formation and the terrace deposits.

The Morozaki Group is exposed in the southern extremity of the peninsula. The Tokoname Group, which covers the Morozaki Group unconformably, constitutes hills over the whole peninsula, and is partly covered by the Taketoyo Formation and the terrace deposits with unconformity. Lithologically, the Tokoname Group is divided into three formations, the Toyooka, the Kouwa and Futto Formations in ascending order, in the southern part of the peninsula. The Toyooka Formation, 65 to 100 m in thickness, is characterized by gravelly beds with intercalation of mud layers. The Kouwa and Futto Formations, 150 to 180 m and more than 280 m thick respectively, are composed of alternation of sand and mud beds. Slight differences are recognized between these two formations in lithology, supply of sediments and so on (Makinouchi, 1975). The Kouwa and Futto Formation have intercalations of eleven volcanic ash layers. Among them, we sampled eight layers for the paleomagnetic measurement. They are the Kofu, Chita Pink, Shirasawa-no-ike, Kaminoma, Sakai, Kosugaya, Ohtani and Koba Volcanic ash layers in ascending order (Fig. 1 and Fig. 2).

Methods and Results

Oriented samples were collected from each ash layer as blocks 10x10x5 cm. Two or more block samles were obtained from the bottom to the top of ash layers of which thickness was more than 20 cm. Six or more specimens, about 2 cm cube, were cut from each block sample. Natural remanent magtization (NRM) was measured by spinner magnetometer.

One pilot specimen from each sample was demagnetized in alternating field (AF) in steps with peak field value of 50, 100, 150, 200, 300 and 400 Oe. Some of pilots with reversal (T-1, T-5, T-7) revealed the intensity rise at the initial AF demagnetization stage, up to 150 Oe. And, in most samples, the direction of NRM moved toward the direction of northern or southern geocentric dipole after AF demagnetization up to 300 Oe.

The results of measurement, before and after AF demagnetization (peak field 300 Oe), are summarized in Table 1. Since the direction of NRM for T-11 from Shirasawa-no-ike tuff scattered after AF demagnetization, the result was excluded from paleomagnetic consideration. However, T-12 collected from same tuff shows normal polarity with small α_{95}. Therefore it is considered that the Shirasawa-no-ike tuff has a normal polarity.

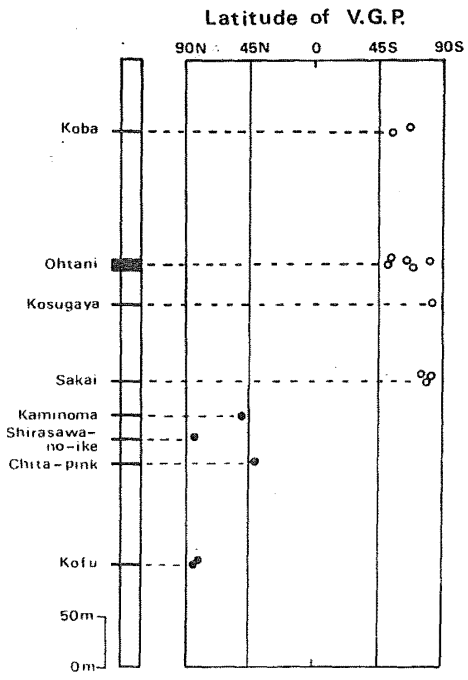

Fig. 2 The latitude of the VGPs. Left column indicates the horizon of the ash layers.

Table 1. Summary of Paleomagnetic Data of the Tokoname Group.

Volcanic ash layer	Site No.	(NRM) D	(NRM) I	(NRM) α_{95}	(NRM) J	(After AF Dema.) D	(After AF Dema.) I	(After AF Dema.) α_{95}	(After AF Dema.) J	(VGP) Lat.	(VGP) Long.
Koba	T - 1	154.0	-53.4	2.7	4.3	152.4	-53.3	3.3	4.0	-67.2	221.5
	T - 2	117.5	-49.3	8.4	2.6	138.0	-65.4	5.3	2.1	-56.4	262.1
Ohtani	T - 3	133.5	-15.1	5.5	1.0	136.4	-55.9	15.4	0.19	-54.8	262.4
	T - 4	139.4	-36.9	2.6	1.7	149.6	-61.0	5.3	0.78	-65.3	252.8
	T - 5	175.8	-49.8	13.6	0.46	-169.2	-55.4	6.0	0.33	-81.2	56.7
	T - 6	-102.0	-40.7	10.3	0.19	-129.6	-50.7	7.8	0.12	-48.1	36.8
	T - 7	-127.5	-60.4	10.0	0.28	-153.8	-54.4	8.4	0.27	-68.5	54.5
Kosugaya	T - 17	-165.2	-55.6	8.5	0.23	-173.1	-52.6	9.4	0.22	-84.0	61.8
Sakai	T - 16	-177.0	-37.9	6.7	3.5	170.0	-41.7	8.1	2.7	-76.1	178.2
	T - 15	-179.3	-53.8	4.3	1.3	173.1	-53.0	2.2	1.0	-84.1	215.4
	T - 14	-179.5	-53.5	2.4	0.93	175.1	-55.5	2.8	0.76	-85.5	210.4
Kaminoma	T - 13	34.2	16.9	27.5	0.09	32.2	10.5	18.0	0.05	48.0	264.3
Shirasawa-no-ike	T - 12	1.4	54.9	7.1	0.83	4.4	52.2	7.4	0.54	85.8	255.1
	T - 11	11.1	11.8	55.8	0.13	----	----	---	----	----	-----
Chita pink	T - 10	24.0	44.1	46.1	0.16	-42.0	9.1	52.5	0.15	40.1	19.5
Kofu	T - 9	-21.4	29.0	2.7	0.48	0.4	48.1	5.0	0.19	80.6	323.2
	T - 8	-15.6	15.9	3.1	55.1	-1.2	43.8	11.0	9.2	84.6	313.6

J = Mean intensity of magnetization in emu $cc^{-1} \times 10^{-6}$
Sites are arranged in descending order from the younger to the older.

From the result shown in Table 1 and Fig. 2, it is evident that the ash layers above the Sakai have reversed polarity and those below the Kaminoma normal. It is considered from this fact that only one polarity change from normal to reverse has occurred in the time when the Tokoname Group has been deposited.

Discussion

1) Magnetostratigraphy

The absence of key ash layers spreading over the Tokoname and Kobiwako Groups has made it difficult to assume the age of the former. However, the existence of N-R polarity pattern in the Tokoname Group would give some hold on this problem.

It must be noted that *carya* pollen is not found in the strata above the Ohtani tuff (Nasu, 1971). The extinction of this flora suggests that this group was formed in upper Pliocene. In the Tokoname Group, the thickness of the strata with normal polarity, from the Kofu to the Kaminoma ash layer is about 140 m and that with reversal, from the Sakai to the Koba is about 280 m. From this fact both of normal and reversal periods may be assumed as significantly long polarity intervals.

Next three boundaries may be considered for the N-R polarity boundary of the Tokoname Group.

1) Gauss-Matuyama boundary; the boundary falls on 2.34 m.y. The maximum polarity intervals are supposed 37×10^4 years for normal and 30×10^4 years for reversal, respectively.
2) Lower boundary of Mammoth event in Gauss epoch; the boundary falls on 3.06 m.y. The maximum intervals are assumed 26×10^4 and 26×10^4 years, respectively. In this case, we presumed that the volcanic ash was not deposited between Kaena and Mammoth events in the Tokoname Group.
3) Upper boundary of Cochiti event in Gilbert epoch; the boundary falls on 3.7 m.y. The maximum intervals are 22×10^4 and 38×10^4 years.

(Ages of the polarity boundaries are based on the geomagnetic polarity epoch time table of McElhinny (1973).)

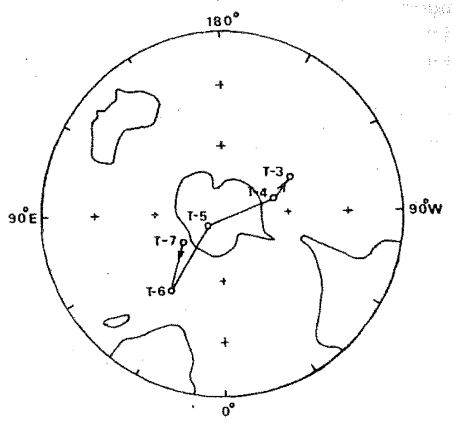

Fig. 3 Change of the VGPs from T-7 to T-3 for the Ohtani ash layer.

We cannot decide which N-R boundary corresponds to this group precisely from the information described above, at present. Fission track age determination is now in preparation by us.

2) Ohtani ash layer

Ohtani ash layer is the thickest one (3-10 m) in the Tokoname Group. We collected five samples at interval of 1.5 m. Inclination of five samples show nearly the same value. However, declination seems to change systematically from east to west more than 90 degrees, from lower to upper horizon. In Fig. 3, the change of the VGPs is shown.

In other tuffs, such as the Koba, the Sakai and the Kofu, directions of NRM for the same ash layer agree well with each other. The directions of these samples locate around geocentric dipole and the values of α_{95} of each sample are small. This suggests that the remanent magnetism in these layers would have been acquired at the time when the ash layer was formed and that the remanences have not been affected by the diagenetic re-magnetization.

In the Ohtani ash layer, if direction changes were caused by the re-magnetization, larger change could be expected for inclination as much as declination, and larger value for α_{95} would be expected. Therefore, we should consider that these changes were caused by the change of ambient magnetic field at the time when ash layer was deposited.

If the sedimentation rate of ash fall is not so fast as has been presumed geologically, it may be considered that the magnetic record in this ash fall merely reflects large paleo-secular variation. In such a case, it may be considered that the fall of this tuff continued for more than a few hundred years.

From the geological view point, volcanic ash layer has been cansidered to be formed for a few decades at most. It is difficult to explain such a rapid change by the movement of the non-dipole component of the geomagnetic field, since westward drift of it moves only 0.2°/ a year and its magnitude is at most 20% of the dipole component (Yukutake and Tachinaka, 1968). So, swing of the direction must be caused by the extraordinarily rapid change of the geomagnetic field.

Kennett and Watkins (1970) suggested that the close correlation existed between volcanic activity and the reversal of the geomagnetic field. This suggestion is attractive for explaining the cause of rapid change of NRMs direction in the Ohtani ash layer, since this layer is so thick compared with other ash layers in Osaka, Kobiwako and Tokoname Group, that a vast volcanic activity might be expected. At this stage, it is not adequate to present such hypothesis easily. We will be, however, able to examine this hypothesis by the use of thick layer.

References

Ishida, S., K. Maenaka and T. Yokoyama (1968) J. Geol. Soc. Japan, 75, 183.
Ishida, S. and T. Yokoyama (1969) Japan Quat. Res., 8, 31.
Kennett, J.P. and N.D. Watkins (1970) Nature, 227, 930.
McElhinny, N.W. (1973) Palaeomagnetism and Plate Tectonics (Cambridge University Press, Cambridge)
Makinouchi, T. (1975) J. Geol. Soc. Japan, 81, 67.
Nasu, T. (1970) Biol. Sci., 24, 1.
Takehara,H., A. Morishita and J. Itoigawa (1961, 1964) Basement of Nagoya bay (Administrating Union of Nagoya harbour)
Yukutake, T. and H. Tachinaka (1968) Bull. Earthquake, Res. Inst., Univ. Tokyo, 46, 1075.

THE POLARITY CHANGE OBTAINED FROM THE WATER-LAID VOLCANIC ASH LAYERS IN PLIO-PLEISTOCENE SEDIMENTS IN KINKI AND TOKAI DISTRICT

Kazuaki MAENAKA

Hanazono College, Hanazono Kitsujikitamachi, Ukyo-ku, Kyoto-shi, Kyoto 616

It was in 1951 when the NRM of the volcanic ash specimens of Osaka Group, representative Quaternary sediments in South-west Japan, was first measured. Kawai (1951) mentioned the reversed magnetization of the Azuki volcanic ash which is one of the best key beds in Osaka Group. Ishida et al. (1969) collected the volcanic ash specimens from each of 156 sites (954 specimens in all) in Kinki and Tokai district, and measured their NRMs. The results were briefly described as follows.

1) The ash specimens from seventy sites out of the 156 sites in all were measurable by means of an astatic magneto-meter, whose limit of dependable measurement is 10^{-7} emu/g. Of these seventy, specimens from forty sites exhibited the normal polarity, while thirty the reversed one. Examination of the twenty-eight layers horizon by horizon disclosed that eighteen layers had the normal, ten layers the reversed polarity.

2) Every one of the five reversed polarity times was found filling an interval between normal polarities. There were at least ten affairs of change in polarity. The paleomagnetic data disposed according to the stratigraphic succession by Ishida and Yokoyama (1969) was correlated with the time scale of polarity change presented by Cox and Dalrymple (1967). Geomagnetic polarity episodes were classified into three epochs; the upper normal polarity epoch. They were correlated respectively with the Brunhes normal epoch, the Matuyama reversed epoch and the Gauss normal epoch. Short period during each epoch were correlated with polarity events.

Recently, Torii et al. (1974) reported the paleomagnetic results on the water-laid volcanic ash layers in the Osaka Group, Sennan and Senpoku hills in Osaka prefecture. They showed that their results agreed well with those of Ishida et al. (1969). On the other hand, some newknowledges have been added to the stratigraphical and geochronological field on Plio-Pleistocene series in Kinki and Tokai district since the paleomagnetic stratigraphy was presented by Ishida et al. (1969). Then the reconstruction of the paleomagnetic stratigraphy was carried out by eliminating the data of the specimens belonged to the indistinct horizon and adopting the data of the fission track age (Maenaka et al. 1976). The results are shown in Figs 1 and 2. Fig. 1 shows the columnar section with the paleomagnetic data and the fission track age's data of the individual areas in Osaka, Kobiwako and Tokai Groups. Fig. 2 shows the summarized paleomagnetic stratigraphy of Plio-Pleistocene series in Kinki and Tokai district. As shown in these figures, it is as before that the geomagnetic polarity episodes are classified into three epochs.

The horizons above the Fukakusa volcanic ash layer in Osaka Group or the Ogoto volcanic ash layer in Kobiwako Group are correlated with the Brunhes normal epoch (0-0.69 M.Y.), the horizons from the Biotite to the Shimakumayama volcanic ash layer in Osaka Group or the Komazuki volcanic ash layer in Kobiwako Group are correlated with the Matuyama reversed epoch (0.69-2.43 M.Y.), and those below the T-2 volcanic ash layer in Osaka Group or the Kaigake B volcanic ash layer in Kobiwako Group are correlated with the Gauss normal epoch (2.43-3.32 M.Y.). Considering from the fission track age and the thickness of the sediments, normal event of

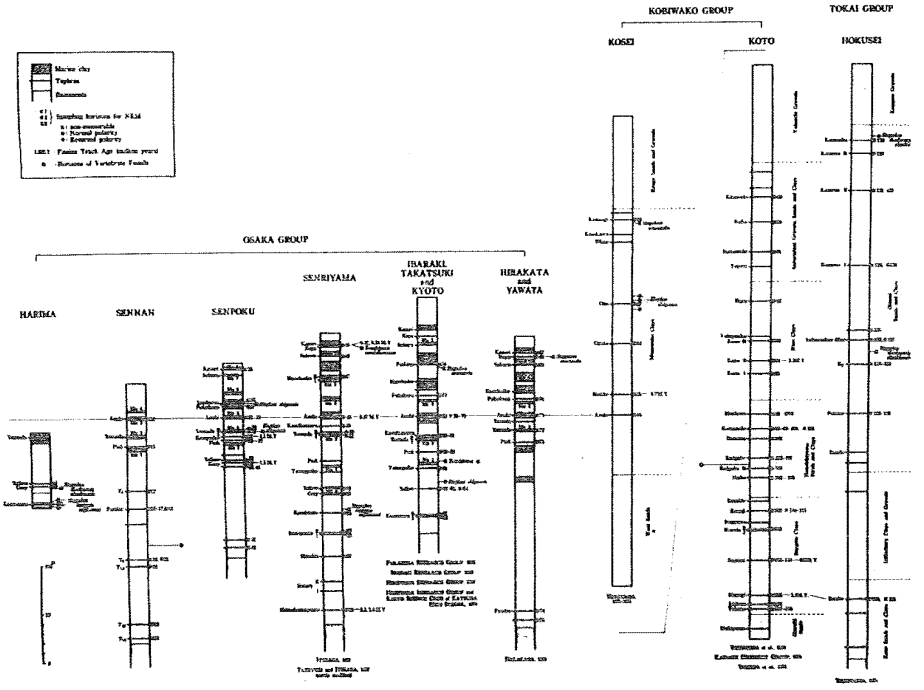

Fig. 1. Columnar sections of the individual areas in Osaka, Kobiwako and Tokai Groups.

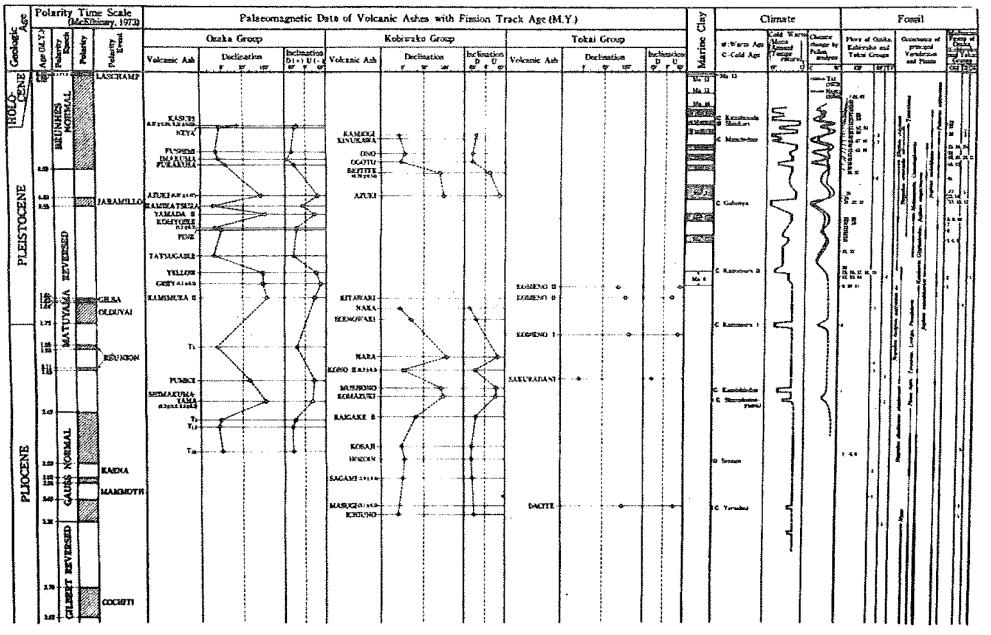

Fig. 2. Correlation of paleomagnetic stratigraphy, biostratigraphy and climatic changes in the Plio-Pleistocene series in Kinki and Tokai district.

Kamikatsura horizon, Naka and Ikenowaki horizons, and Kono II horizon in Matuyama age are respectively correlated to the Jaramillo (0.89-0.95 M.Y.), the Olduvai (1.64-1.79 M.Y.) and the Reunion (1.95-1.98 and 2.11-2.13 M.Y.) normal event. Similarly, the Dacite volcanic ash horizon in the Gauss normal epoch is correlated to the Mammoth reversed event (2.94-3.06 M.Y.). On the contrary, normal polarity of the Komyoike, Pink and Tatsugaike horizons is not rigorously correlated with any known event. The fission track age of Komyoike volcanic ash layer is given as 1.1 M.Y. (Nishimura and Sasajima 1970). This age is considered to be reasonable age judging from the thickness of the sediments between the Azuki (0.89 M.Y. fission track age) and the Grey (1.5 M.Y. fission track age). This means that a new event may be required to be prepared there. If this is true, somewhat symptoms are considered to be appeared in so far reported paleomagnetic data. So this was examined from all angles.

The polarity time scale presented in the left column of Fig. 2 is based upon the paleomagnetic data with K-Ar ages all the world. Fig. 3-A is cited from the report of Cox et al. (1968). In the report, 184 paleomagnetic data with K-Ar ages for the last 15.81 M.Y. (109 data for the Brunhes-Matuyama ages as shown in Fig. 3-A) are listed up. In the report, Cox et al. (1968) themselves pointed out some problems to be remarked. For example, near some of the polarity boundaries, the magnetic polarities and the radiometric ages do not follow in perfect sequence because of errors in the dating. It is difficult to obtain accurate estimates of the duration of events directly from radiometric dating because the dating errors are of the same magnitude as the events. The pattern of the polarity change is still uncertain because of the irregular distribution of K-Ar ages from volcanic rocks. Cox et al. (1968) also suggested that there is growing evidence for at least two, and possibly more, events within the Matuyama reversed epoch.

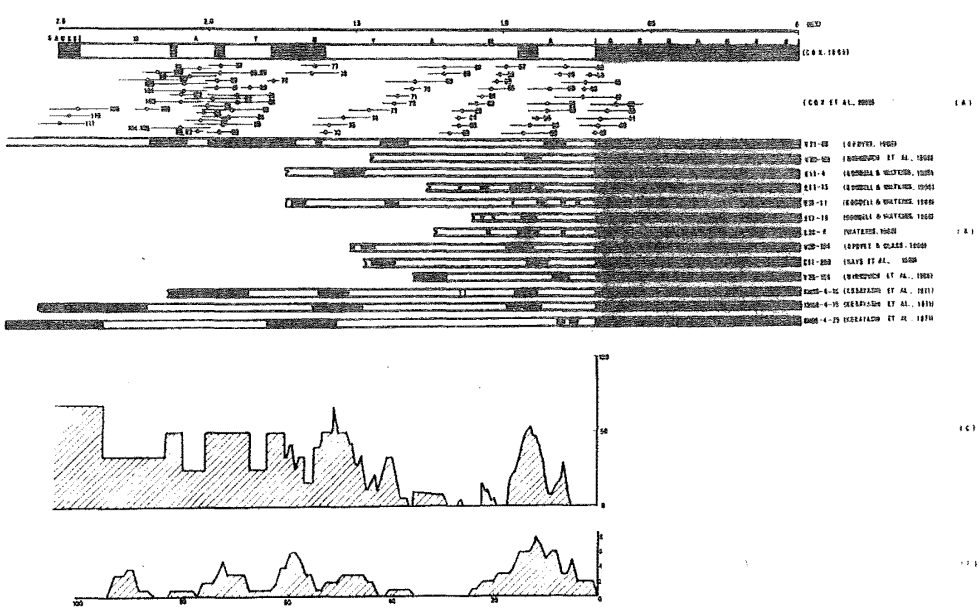

Fig. 3. The record of polarity change in Matuyama age.

Lately, Harrison (1974) analyzed the paleomagnetic data of seventy-one cores which penetrated the Matuyama-Gauss boundary. He expressed the relative positions of the normal events in Matuyama age as a percentage distance from the top of the Matuyama epoch. In the same way, the writer tried to reexamine the residual data which the ratio of the length of the Matuyama age material to the length of the Brunhes age material given in Harrison's report is smaller than two or larger than three is removed. The reason is that they are felt strange considering from the ratio of the duration of the Matuyama epoch (1.74 M.Y.) to that of the Brunhes epoch (0.69 M.Y.) is about 2.5. The extracted data from above-mentioned seventy-one cores is given in Table 1. Fig. 3-D gives the histogram of ages of normal event as a percentage distance (n) from the top of the Matuyama epoch. As a real operation, the number of events between (n-2) and (n+2) is counted by varing the value of n from 0 to 100. As shown in Fig. 3-D, three striking peaks of n=12 (0.9 M.Y.), n=60 (1.7 M.Y.) and n=72 (1.95 M.Y.) are remarked. These are possibly correlated with the Jaramillo, Olduvai and Reunion events respectively. Besides these, it may be recognized that there are five lesser peaks as n=5 (0.75 M.Y.), n=38 (1.35 M.Y.), n=47 (1.5 M.Y.), n=80 (2.1 M.Y.) and n=90 (2.25 M.Y.). Among them, the event which is correlated with the known events is only one.

Core No.	Length of Matuyama age material (cm) (A)	Length of Brunhes age material (cm) (B)	$\frac{A}{B}$	Position of events
E-13-20	310	144	2.15	3 22 38 50 74 91
E13-3	600	222	2.70	3 7 14 55 70
E17-29	420	170	2.47	20 74 91
E17-28	422	144	2.93	10 17 71
E27-2	1040	500	2.08	13 70 88
C11-193	492	180	2.73	12 57 80
C12-63	312	108	2.89	17 60
V20-88	244	106	2.30	10 65
V18-72	340	159	2.13	12 60
V24-62	540	242	2.23	10 45
V20-105	410	158	2.59	7 47
V21-173	750	362	2.07	13 59
E17-10	950	400	2.38	7 50
E15-11	288	100	2.88	45 91
KH68-4-18	581	263	2.21	15 57
KH68-4-25	423	179	2.36	59
V20-65	202	86	2.35	no event

Table 1. The position of events in Matuyama age appeared in the paleomagnetic record of ocean bottom sediments.

Paleomagnetic data of the ocean bottom sediments were also analized from another view point. Of the specimens which penetrated the Brunhes-Matuyama boundary, the specimens that at least one measured data of NRM every ten thousands years is demonstrated in the original paper is selected for avoiding of the omission of the shorter event as brief as five thousands years. Only thirteen data were choosed out from over two hundred fifty data (Ninkovich et al. 1966, Opdyke et al. 1966, Glass et al. 1967, Hays and Opdyke 1967, Watkins and Goodell 1967, Goodell and Watkins 1968, Opdyke 1968, Steuerwald et al. 1968, Hays et al. 1969, Opdyke and Glass 1969, Foster and Opdyke 1970, Kent et al. 1971, Opdyke 1972).

Then the figures as shown in Fig. 3-B were pictured, supposing that the age of the Matuyama-Brunhes boundary is 0.69 M.Y. and that the concerned data have the constant rate of deposition. The frequency of appearance of normal event in the Matuyama age were calculated every ten thousand years from the above mentioned figures. The result is shown in Fig. 3-C. From the figure, it is noted that the frequency curve of appearance of normal event in the Matuyama age have five remarkable peaks and some lesser peaks. It is illustrated that there are a general agreement between Fig. 3-C and Fig. 3-D. It is noticeable that the results obtained from the different ways on the different data agree well with one another.

Summarizing these matters, it may be said that the possibility of the existence of unknown events in the Matuyama age is large. To be regretted, the existence of the event of 1.1 M.Y., from which the discussion was begun, was not supported by any positive proof. The measurement of the remanence of the successive sediments having rapid rate as Osaka Group will be required to solve this problem.

REFERENCES

Cox, A. and G. B. Dalrymple (1967) Earth Planet. Sci. Lett., 3, 173.

Cox, A., R. R. Doell and G. B. Dalrymple (1968) Quart. J. Geol. Soc. London, 124, 53.

Foster, J. H. and N. D. Opdyke (1970) Earth Planet. Sci. Lett., 1, 463.

Glass, B., D. B. Ericson, B. C. Heezen, N. D. Opdyke and J. A. Glass Nature, 216, 437.

Goodell, H. G. and N. D. Watkins (1968) Deep Sea Res., 15, 89.

Harrison, C. G. A. (1974) Earth Science Reviews, 10, 1.

Hays, J. D. and N. D. Opdyke (1967) Science, 158, 1001.

Hays, J. D., T. Saito, N. D. Opdyke and L. H. Burckle (1969) Geol. Soc. Amer. Bull., 80, 1481.

Ishida, S., K. Maenaka and T. Yokoyama (1969) J. Geol. Soc. Japan, 75, 183.

Ishida, S. and T. Yokoyama (1969) Japan Quart. Res., 8, 31.

Kawai, N. (1951) J. Geophys. Res., 56, 73.

Kent, D., N. D. Opdyke and M. Ewing (1971) Geol. Soc. Amer. Bull., 82, 2741.

Kobayashi, K., K. Kitazawa, T. Kanaya and T. Sakai (1971) Deep Sea Res., 18, 1045.

Maenaka, K., T. Yokoyama and S. Ishida (1976) Quart. Res., in press.

Ninkovich, D., N. D. Opdyke, B. C. Heezen and J. H. foster (1966) Earth Planet. Sci. Lett., 1, 476.

Nishimura, S. and S. Sasajima (1970) Earth Science, 24, 222.

Opdyke, N. D. (1968) The history of the earth8s crust (Princeton, USA), p. 61.

Opdyke, N. D. (1972) Rev. Geophys. Space Phys., 10, 213.

Opdyke, N. D. and B. P. Glass (1969) Deep Sea Res., 16, 249.

Opdyke, N. D., B. Glass, J. D. Hays and J. H. Foster (1966) Science, 154, 349.
Steuerwald, B. A., D. L. Clark and J. A. Andrew (1968) Earth Planet. Sci. Lett., 5, 79.
Torii, M., S. Yoshikawa and M. Itihara (1974) Rock Magnetism and Paleogeophysics, 2, 34.
Watkins, N. D. and H. G. Goodell (1967) Earth Planet. Sci. Lett., 2, 123.

CONSISTENCY CHECK OF MAGNETOSTRATIGRAPHIC DATA IN PARALLEL SECTIONS

Ken-ichi MANABE

Department of Earth Science, Faculty of Education, Fukushima University
Fukushima 960, Japan.

Potassium-argon dating and paleomagnetic studies of igneous rocks have led to establishment of the geomagnetic polarity time scale for the past 5 m.y. (Cox, 1969). Cenozoic polarity changes have now been recognized throughout the world in deep-sea sedimentary cores and outcropping late Cenozoic sediments (examples by Opdyke, 1972; Bucha, 1970; Kennett et al., 1971; Kennett and Watkins, 1974).

Similarly, paleomagnetic stratigraphic methods have been applied to late Cenozoic sedimentary sequences in Japan (Nakagawa et al., 1969; Ishida et al., 1969; Manabe et al., 1970; Kawai et al., 1972). In contrast, it has been suggested that a reliable establishment of the polarity stratigraphy is seriously difficult in some cases because of post-depositional normal overprint resulted from the chemical precipitation and aquisition of VRM (Kent, 1973; Kennett and Watkins, 1974; Watkins et al., 1974).

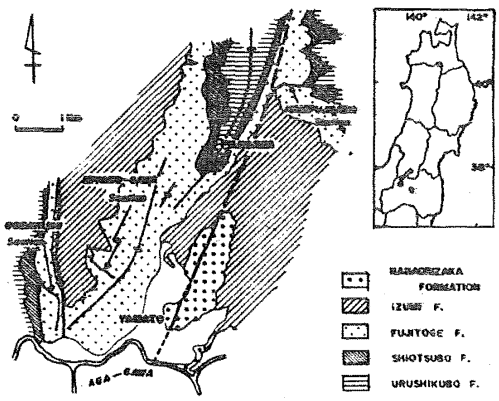

Fig. 1 Geological map of the northwestern portion of the Aizu Basin. The dotted line indicates the location of sections examined in this study.

It is substantial problem whether original depositional polarity has been preserved in sediments or not. But there is no complete experimental technique to remove the post-depositional overprint or to distinguish the original magnetic component from the secondary one. It is considered that, therefore, the most convincing way to demonstrate the validity of paleomagnetic interpretation is to reproduce the results in parallel, separated sections with different lithology and sedimentation rate. Accordingly, multiple sampling of parallel sections and consistency checks of results are necessary.

It is the purpose of this report to describe the outline of the results of paleomagnetic measurements on four separate sections of the Fujitoge Formation.

Geology and sampling

As shown in Fig.1, the sections sampled in this study are in the northwestern portion of the Aizu Basin (139.7°E, 37.7°N). The Fujitoge Formation contains a total thickness of about 300 m of the late Miocene and early Pliocene mostly continental sediments. The Fujitoge subdivided into four parts: the upper, middle, lower and lowermost part on the basis of the lithostratigraphic characteristics.

The upper part consists of poorly-consolidated conglomerate, sandstone and mudstone interbeded with lignite and tuffaceous beds. The middle part consists mainly of conglomerate and numerous distinct strata of volcanic

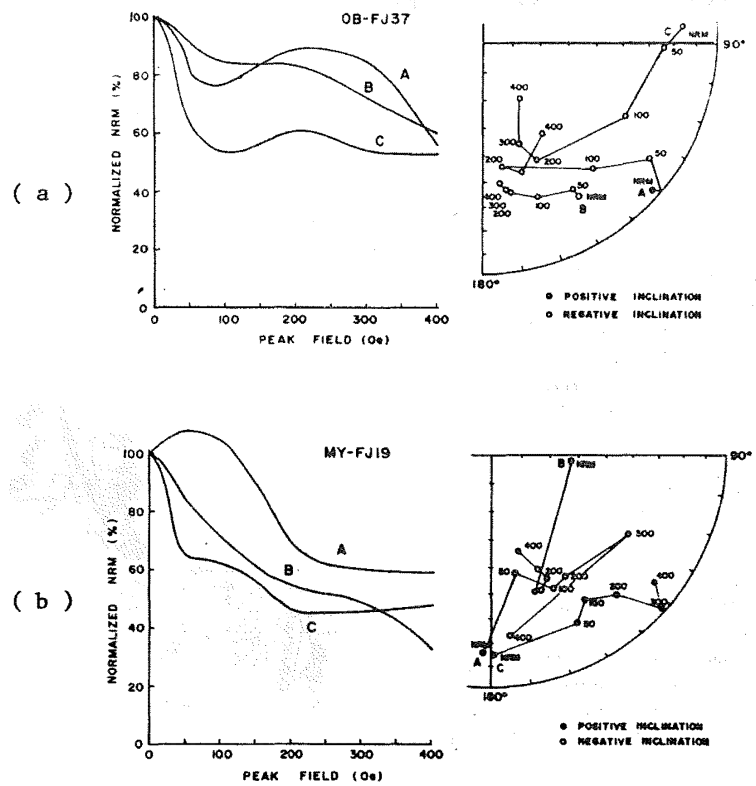

Fig. 2 Changes in relative intensity and direction with progressive alternating field demagnetization of the NRM of specimens from single site in the Oobayashi section (a) and Miyako-gawa section (b). Ambient field up to 300 γ may have been presented.

material. Specially the biotite-bearing tuff marking the top of the middle part is remarkably distinct and can be traced as marker horizon. The lower part is composed of alternated strata of fine-grained sediments. The lowermost part consists of massive white coarse sandstone.

paleomagnetic samples were taken, by using a portable drill, at each of 41 sites in the four separate sections: Kamifujisawa, Miyako-gawa, Oobayashi and Wakarenochaya section. The sampling sites were chosen where possible to maintain a stratigraphic interval of about 10 m, and the outcrops were cleaned off to a depth of 20-30 cm before drilling. In most cases, tuffaceous fine-grained sediments were sampled, and three cores 3.3 cm in diameter and averaging 10 cm in length were taken at each of the sites.

Results and discussion

For the paleomagnetic analysis, a segment of 3.3 cm in length was sliced from each core. NRM was measured with an astatic magnetometer set up within a two-layer mumetal shield.

Unstable component of the remanence was examined by progressive demagnetization in alternating magnetic fields as high as 400 Oe using a 3-axis tumbler. The demagnetization was carefully performed in a field-free space.

Changes in intensity and direction during progressive stepwise AF demagnetization of pilot specimens are shown in Fig.2. These reversely magnetized specimens showed substantial changes in direction. Their intensities increased with increasing demagnetizing fields up to about 200 Oe, then decreased at higher fields while the directions began to stabilize near a reversed field orientation.

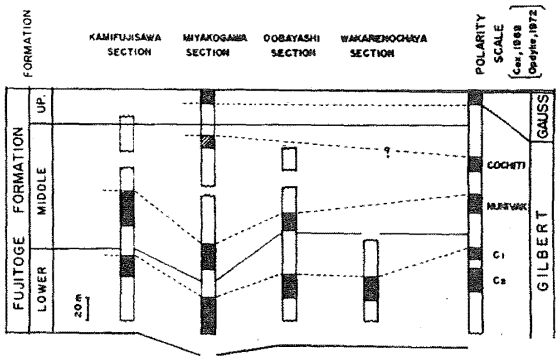

Fig. 3 Compilation of four established magnetozones. Solid line of correlation between sections coincides with stratigraphic subdivision of the Fujitoge Formation. The polarity scale is according to Cox (1969) and Opdyke (1972). Black represents normal, white reversed polarity.

It may be considered that the significantly large normal component has been superposed on a more stable original reversed component.

Therefore, on the basis of the AF demagnetization experiments on pilot specimens, a field of 200 Oe was chosen for magnetic cleaning treatment of all specimens. Typically a peak alternating field of 200 Oe reduced the magnetization to 60 percent of its original value. The scatter of direction within sites generally decreased with the demagnetizing treatment. The unstable component minimized by AF demagnetization is probably VRM created in the past geomagnetic field.

The paleomagnetic stratigraphy established for each section is summarized in Fig.3. For each site, the latitude of the virtual geomagnetic pole (VGP) is adopted as the expression of polarity and is considered in principle to be normal for latitude above 10°N, reversed with latitude higher than 10°S, and intermediate for latitude of less than 10°.

Compilation of four magnetostratigraphic columns based on the stratigraphy is shown in Fig.3, and these four overlapping polarity sequences present a single reversed magnetozone, which is correlated with the Gilbert reversed epoch on the basis of stratigraphic and chronologic evidences.

In the established reversed magnetozone, the Gilbert epoch, three short normal polarity zones were recognized. They are correlated with the Cochiti, Nunivac and Gilbert C event respectively. The lower short normal zone in the Kamifujisawa section is best matched in character by the split Gilbert C event. In contrast, such a split character is uncertain in the other three sections. The Cochiti event is recognized only in the Miyako-gawa section. The event is comparatively short in duration, so that it may be distinguished only where the sedimentation has been rapid.

In the present study of the Fujitoge Formation, the reversed magnetozone believed to represent the Gilbert epoch was confirmed in four parallel sections with different sedimentation rate and lithology. The great similarity of the paleomagnetic data between the sections is convincing support for the validity of the results.

The above-mentioned consistency check and AF demagnetization treatments

suggest, therefore, minimal effects by post-depositional chemical precipitation and sufficient removal of unstable overprint.

References

Bucha, V. (1970) J. Geomag. Geoelec. 22, 253.

Cox, A. (1969) Science 163, 237.

Ishida, S., K. Maenaka and T. Yokoyama (1969) J. Geol. Soc. Japan 75, 183.

Kawai, N., K. Yaskawa, T. Nakajima, M. Torii and S. Horie (1972) Proc. Japan Acad. 48, 186.

Kennett, J.P., N.D. Watkins and P. Vella (1971) Science 171, 276.

Kennett, J.P., and N.D. Watkins (1974) Geol. Soc. Amer. Bull. 85, 1385.

Kent, D.V. (1973) J. Geomag. Geoelec. 25, 87.

Manabe, K., K. Suzuki, R.Yashima, T.Yoshida, S. Ito, H. Nirei, R. Otake, T. Nonaka and K. Baba (1970) Quaternary Research 9, 118.

Nakagawa, H., N. Niitsuma and I. Hayasaka (1969) J. Geol. Soc.Japan 75, 267.

Opdyke, N.D. (1972) Rev. Geophys. Space Phys. 10, 213.

Watkins, N.D., D.R. Kester and J.P. Kennett (1974) Earth Planet. Sci. Lett. 24, 113.

PROGRESS REPORT ON PALEOMAGNETISM OF ANDESITIC ROCKS FROM THE SOUTH-CENTRAL YAMAGUCHI PREFECTURE, WEST JAPAN.

Haruo DOMEN, Hiroshi MUNEOKA and Takashi YOKOYAMA

Institute of Physical Sciences, Faculty of Education,
Yamaguchi University, 753 Japan

More than a hundred oriented samples of hornblende andesite come from seven localities covering the south-central part of Yamaguchi Prefecture, west Japan have been examined their paleomagnetic properties.

The geologic age of these rocks investigated has been reported as the early Pleistocene (Kawano *et al*, 1975).

Obtained samples were cut into about three hundreds of 5cm-cubic specimen, who had been submitted to the NRM measurement. The af demagnetization test for their NRM is being carried on.

Table 1

Locality	N R M		
	Normal	Reversed	Oblique
1. Maru-Yama	17	--	5
2. Ii-no-Yama	12	--	10
3. Shirai-ga-Dake	12	--	3
4. Choja-ga-Hara	--	--	10
5. Mt. Kimpo	20	--	2
6. Shiguma-ga-Dake	12	10	10
7. Dake-San	39	--	27

Numerals show numbers of samples

As shown in table 1, two-third of the directions of NRM of measured samples are showing the normal polarity. The rest shows oblique directions such as that NRM directions have pointed rather north of the declination but having upper inclinations. Few of samples have showed the reversed NRM direction but widely deviated from the present geomagnetic south pole in declination.

Reference

Kawano, M., Y. Okamura, Y. Murakami, T. Mikami, Y. Nishimura and E. Takahashi (1975) Geological Map of Yamaguchi Prefecture (Yamaguchi Prefecture).

THE NATURAL REMANENT MAGNETIZATION OF PLIO-PLEISTOCENE ANDESITES COME FROM THE SOUTHEAST YAMAGUCHI PREFECTURE, WEST JAPAN

Haruo DOMEN, Hiroshi MUNEOKA and Masatsugu KIMURA

Institute of Physical Sciences, Faculty of Education, Yamaguchi University, 753 Japan

Natural remanent magnetization (NRM) of andesites come from both islands of Nagashima (Kaminoseki Town) and Yashiro-shima (Oshima, Tachibana and Towa Towns), southeast Yamaguchi Prefecture, west Japan have been measured. From the geological view point, it seems that these rocks are about one or two million years old and have overlaid Mesozoic granites. More than a hundred oriented samples were collected at eight sites in these districts. The NRM measurement of them had been carried out by means of an astatic magnetometer.

Obtained NRM directions are shown in figure 1. As shown in this figure, the reversed directions are found at the sites; A, B, D, E and F. Samples from site C show the polarity pointing north but having upward dip, and those from site G show normal NRM. Most of all directions of NRM at site H show normal but rather widely scattered. At site E, NRM directions having downward dip are towarding to the east. However the age of samples come from sites, G and H is little older than that of others, A - F, it is hard to be known even relative ages each other.

Some of specimens come from site A are submitted to magnetic stability test by af demagnetizing field. The direction of NRM is not so much affected by the af demagnetizing field up to 400 Oe. The intensity of NRM slowly decreases as increasing intensity of external demagnetizing field. These af demagnetization fashions are shown in figure 2. The specimens come from other sites, B - H are being tested their stability also in af demagnetizing field.

Thermo magnetic analysis about the rock from site A was carried out. The test specimen submitted to the analysis has two different solid solutions within, whose Curie points are about 400 °C and 600 °C respectively. At the first run of the analysis, heating and cooling curves are slightly irreversible, but as second and third runs of the same specimen, those of thermal treatment became gradually reversible. Moreover, curves turned to straight lines in accordance with repeating thermal treatments. This means that two phases of solid solutions have splitted to polyphases.

On the ferromagnetics from the same specimen (from site A), X-ray analysis had been performed. Unit cell parameters of them are classified into two groups at around 8,403 and 8,424 Å respectively. These correspond to the chemical compositions of $(1-0.1)Fe_3O_4-(1-0.9)Fe_2TiO_4$ and $(1-0.25)Fe_3O_4-(1-0.75)Fe_2TiO_4$ respectively. These correlations are shown in figure 3.

The present authors are carrying on further experiments on the specimen from other sites than A as well, and planning the fission truck absolute age determination of these rocks.

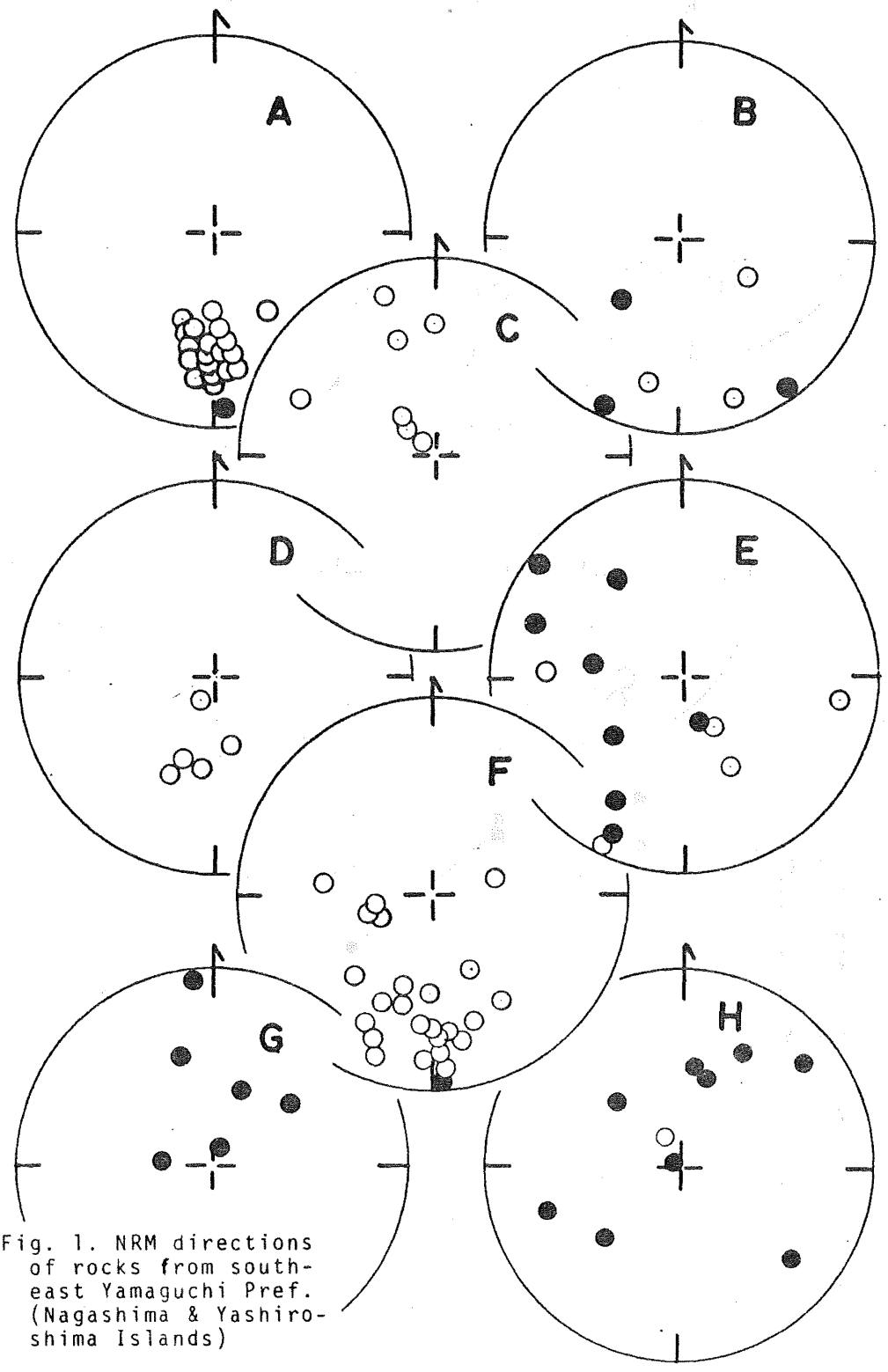

Fig. 1. NRM directions of rocks from south-east Yamaguchi Pref. (Nagashima & Yashiro-shima Islands)

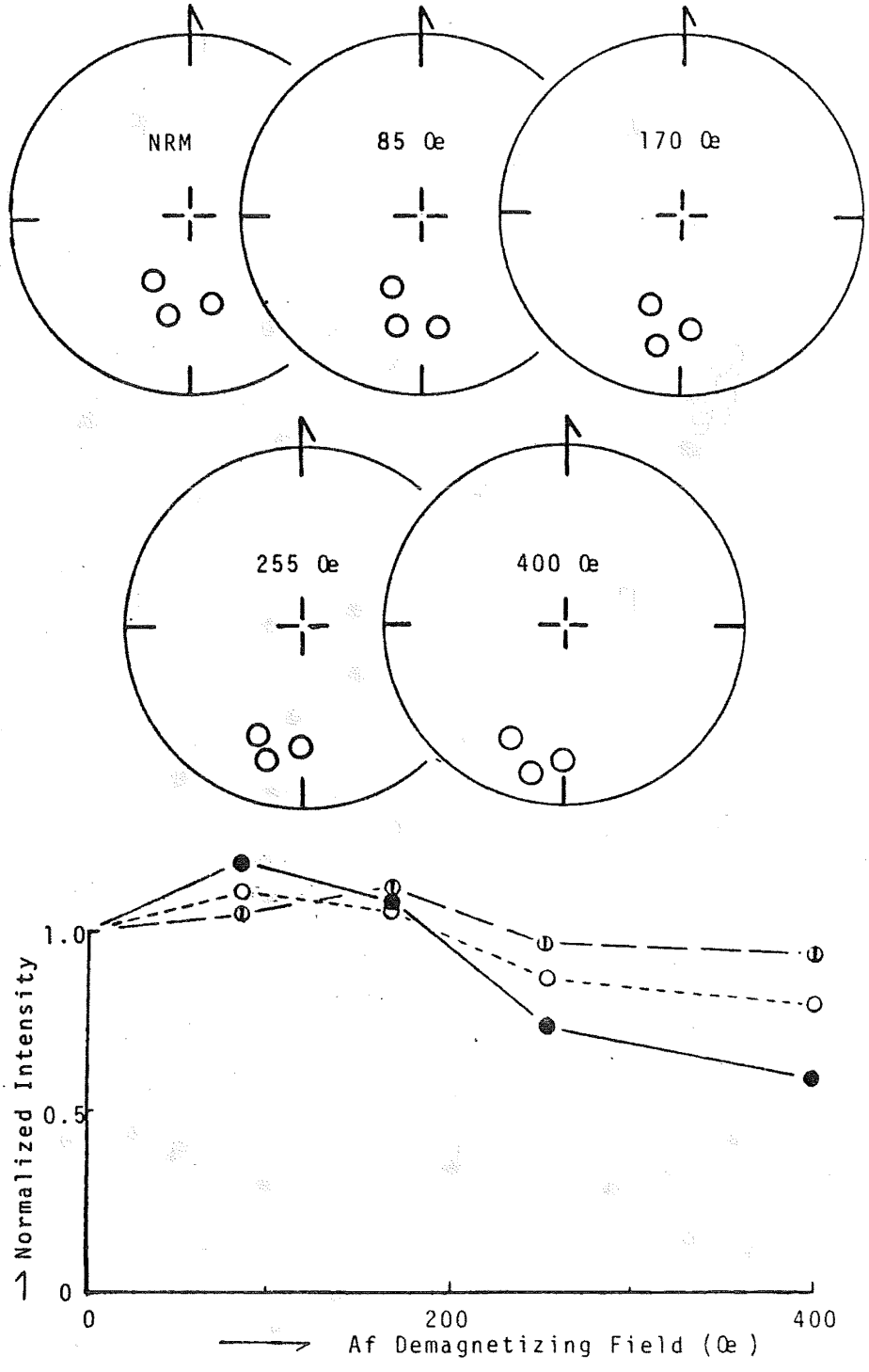

Fig. 2. Af demagnetizing test for NRM of Nagashima rocks (Site A). Top; Directional changes of NRM. Bottom; Intensity changes of NRM.

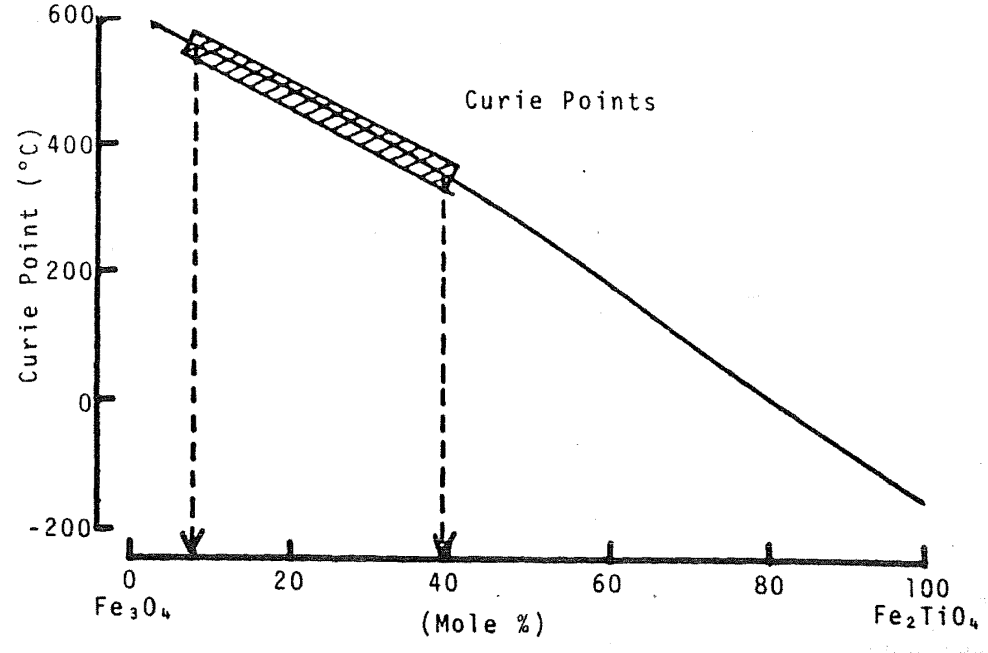

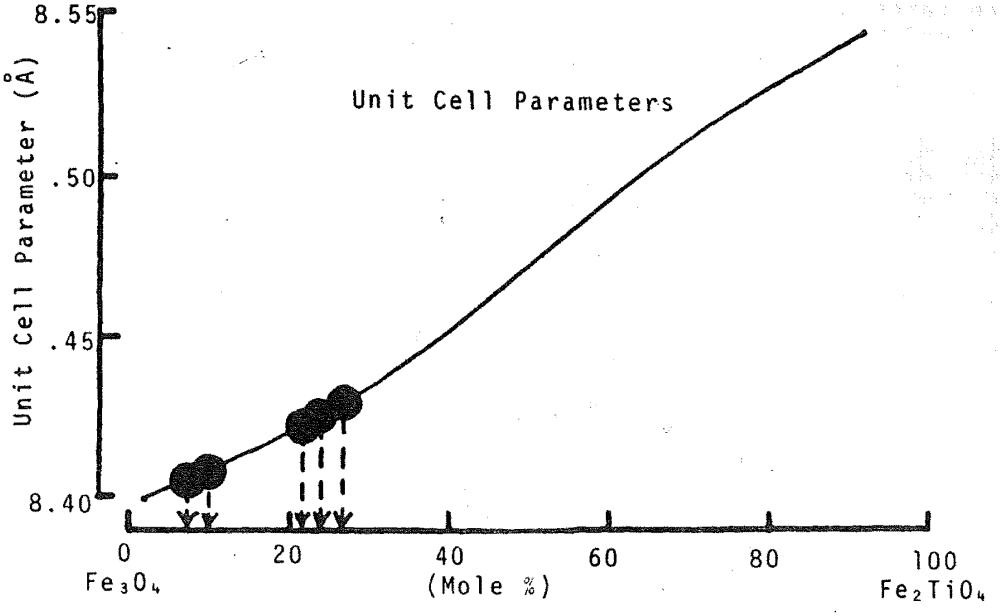

Fig. 3. Top; Curie point obtained by thermo magnetic analysis vs chemical composition for Nagashima rock (site A).
Bottom; Unit cell parameter obtained by X-ray analysis vs chemical composition for Nagashima rock (site A).

A PALEOMAGNETIC RECORD OF POLARITY TRANSITIONS OF THE EARTH'S MAGNETIC FIELD IN PLIOCENE

Haruaki ITO and Katsuyasu TOKIEDA
Physics Department, Shimane University, Matsue, Japan

The granitic complex is exposed in the Tanzawa mountainland, Kanagawa Prefecture, Japan. According to Takita (1974), the complex is composed of many granitic intrusions and the main part of this complex is occupied by tonalite rocks. The four intrusive stages are discerned in the main part of the body. The gabbroic rock is likely to have existed already before intrusions of tonalite rocks. This shows that the gabbroic rock is the oldest in the complex. The Azegamaru type appears to have been formed at the second stage within four intrusive stages.

The apparent size is 20 km in length along the east-west direction and 5 km in width. The age of the body is approximately 4.3 or 5.2 million years according to the K-Ar age determination (Kawano and Ueda, 1966).

Oriented rock samples have been collected from two bodies of the gabbroic rock and the Azegamaru type occupied the main part of the body, as shown in Fig. 1. The gabbroic rock was sampled from three sites along the Sagase creek being a tributary stream of the Doshi river. Samples of the Azegamaru type were taken from 14 sites on successive outcrops along the Inukoe road that crosses the contact zone. Core samples of 1.6 cm in diameter and 2.2 cm long were drilled from the hand samples in the laboratory.

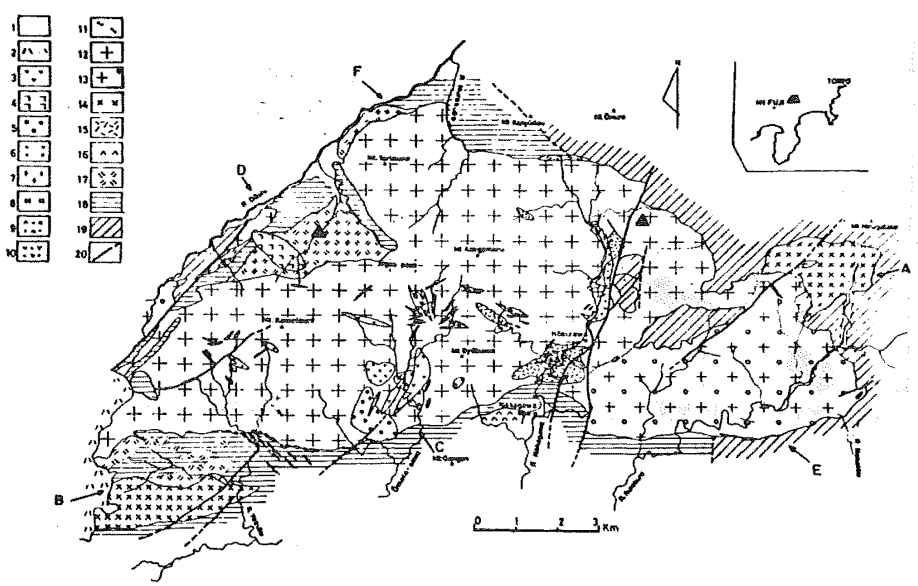

Fig.1 Geological map of the Tanzwa tonalite complex.
12) Azegamaru type (tonalite, quartz diorite).
17) Gabbroic rock.

The NRM of all hand samples was preliminarly measured by an astatic magnetometer and then the NRM of the core samples was measured by the SCT cryogenic magnetometer. Systematic magnetic cleaning by the AF technique was applied to all samples. The optimum peak field of 100 oe was chosen for the samples of this rock body. Curie point determination of the Azegamaru type demonstrated that the dominant magnetic phase was an iron-rich titanomagnetite in all samples investigated as shown in Fig. 2. Results of the measurements are shown in Table 1 and Fig. 3 and 4.

The core samples measured are reversely magnetized, except for a few samples at site 14 within the Azegamaru type. It seems that site 14 is located in the youngest place in our sampling area, because it is situated at the farthest point from the contact zone.

Mean directions of the NRM from two rock bodies appear to demonstrate that the tonalite complex was not subjected to a regional deformation after the intrusion. It is concluded that the reversed NRM which was significantly deviated to the west represents a polarity transion of the geomagnetic field reversal not to be a local deformation of the body.

If the gabbroic rock was the oldest intrusion, the NRM directions of the two rock bodies suggest that the main part in the complex was almost intruded at the time of a field transition from the reversed to the normal. The normally magnetized rocks taken at site 14 support this interpretation because the samples at the site are the youngest considering the cooling history.

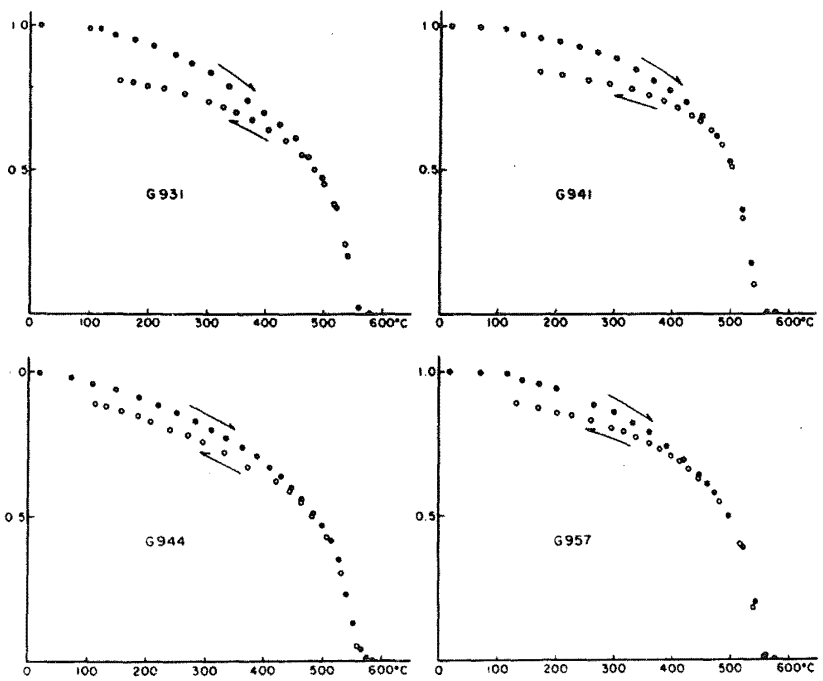

Fig.2 Thermo-magnetic curves.

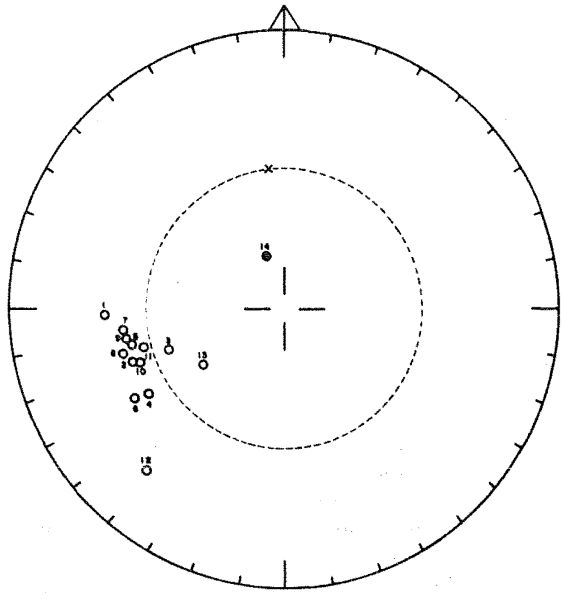

Fig.3 Mean directions of the NRM_{100} of the Azegamaru type. Dots represent normal and open circles represent reversed. Cross mark is the present geomagnetic field direction.

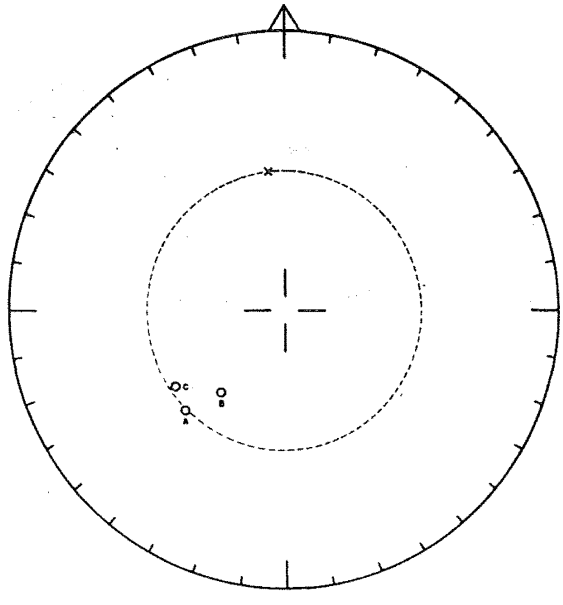

Fig.4 Mean directions of the NRM_{100} of the gabbroic rock. Open circles represent reversed. Cross mark is the present geomagnetic field direction.

Intensities of NRM_{100} (NRM after the demagnetization of 100 oe) among each sampling site in the Azegamaru type has no change significantly. However, the NPM of gabbroic rock has higher intensities than the Azegamaru type. It seems that the intensity of the NRM depends strongly on the bulk of ferromagnetic materials involved.

Virtual geomagnetic poles estimated from the NRM_{100} directions are distributed on the southern part of Africa similar to the distribution of the virtual geomagnetic pole positions obtained from the Japanese rocks of various types and ages (Ito, 1971).

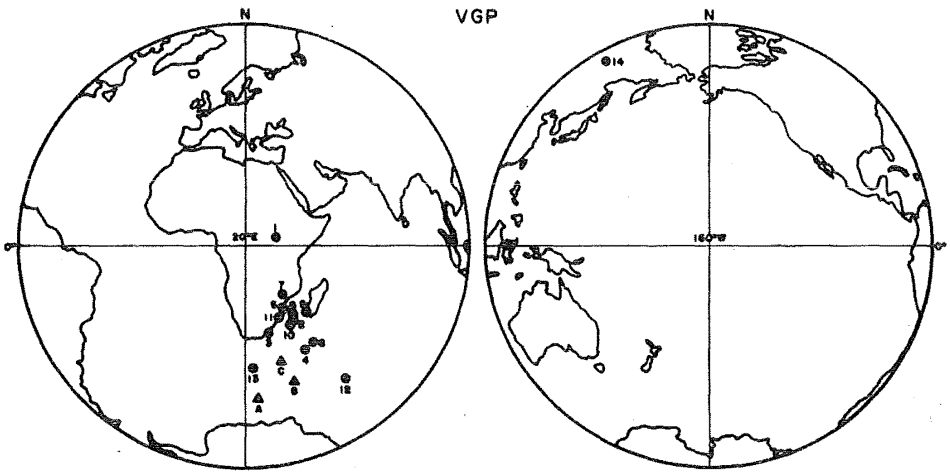

Fig.5 Virtual geomagnetic poles

References

Ito, H. (1971); On the reversal process of the earth's magnetic field in Tertiary, Mem. Fac. Lit. Sci., Shimane Univ., Nat. Sci, 4, 40-45.

Kawano, Y. and Y. Ueda (1966); K-A dating on the igneous rocks in Japan (4) - Granitic rocks in northeastern Japan -, J. Jap. Assoc. Min. Petr. Econ. Geol., 56, 41-55 (in Jspsnese).

Takita, R. (1974); Petrography and the plutonic history of the Tanzawa tonalite complex, Jap. J. Geol. Geogr., 80, 505-523 (in Japanese).

Table 1

	N	D	I	J_r(emu/cc)	k	α_{95}	ϕ	λ
1	5	284°	-24°	2.31×10^{-5}	11.4	23.6°	3.8°N	31.0°E
2	5	251°	-42°	5.26	65.4	9.5°	29.0°S	38.8°E
3	5	250°	-53°	7.28	120.0	7.0°	33.4°S	28.4°E
4	5	238°	-42°	3.56	32.0	13.7°	39.1°S	45.2°E
5	5	257°	-42°	4.20	10.4	24.9°	23.9°S	35.0°E
6	5	239°	-37°	4.85	49.0	11.0°	36.4°S	48.2°E
7	3	262°	-42°	3.91	22.5	26.6°	19.3°S	33.5°E
8	3	255°	-40°	3.25	53.7	17.0°	25.1°S	38.2°E
9	2	252°	-35°	4.13	-	-	25.0°S	42.7°E
10	3	251°	-43°	5.02	32.9	21.9°	29.2°S	38.0°E
11	3	255°	-46°	4.33	64.0	15.5°	27.1°S	33.1°E
12	3	221°	-24°	2.42	16.0	31.9°	46.8°S	70.4°E
13	2	236°	-61°	2.92	-	-	46.8°S	23.0°E
14	2	340°	+75°	3.95	-	-	60.9°N	119.5°E
A	3	226°	-48°	24.70	51.0	17.5°	51.0°S	45.0°E
B	3	218°	-60°	12.63	79.0	13.9°	59.7°S	27.0°E
C	5	235°	-51°	18.57	17.9	18.6°	44.0°S	37.3°E

PALEOINTENSITY DETERMINATION BY A MODIFIED THELLIERS' METHOD

Masaru KONO and Naoko UENO

Geophysical Institute, University of Tokyo, Bunkyo-ku, Tokyo 113
and Natural Science Laboratory, Toyo University, Hakusan
5-28-20, Tokyo 112, Japan

1. Introduction

The magnetic properties of igneous rocks are quite sensitive to heat treatments in a laboratory, and it is commonly observed that the characteristics of thermoremanent magnetization (TRM) are drastically changed by heatings in the course of paleointensity experiments (Coe and Grommé, 1973; Kono, 1974). It is therefore desirable to use the Thelliers' method for paleointensity determination (Thellier and Thellier, 1959), in which the presence of internal consistency in the data is the manifestation of the fact that such changes did not take place in a particular sample. But this method requires a consederable number of heatings and coolings of a sample before one can decide if the experiment is successful and a paleointensity determined, a serious drawback compared to relatively easier methods based on the comparison of coercivity spectra (e.g., van Zijl et al., 1962).

It is noticed in paleomagnetic studies of igneous rocks that the direction of the natural remanent magnetization (NRM) undergoes a similar change in both alternating field (AF) and thermal demagnetizations. Thus if the direction of NRM does not change much in AF demagnetization, it can also be assumed that the direction change is small in thermal demagnetization, such as done in Thelliers' experiment, provided the demagnetization temperature is not too close to the highest Curie point of the sample. Accordingly, it was proposed by Kono (1974) that the Thelliers' method can be performed not only by two heatings as in the conventional technique but also by <u>one</u> heating to each temperature.

In the Thelliers' technique, two heatings are required to separate the NRM component remaining at some temperature T and TRM component acquired between the room temperature and T. However, if the NRM component and TRM component are always in the same directions, we can separate them vectorially using the direction information. An obvious choice of TRM direction is to make it perpendicular to the NRM direction. This can be done by placing a sample in the furnace so as the NRM in it is in the plane perpendicular to the axis of the furnace while a constant magnetic field is applied to the axial direction by a solenoid coil. The entire setup should be placed in a non-magnetic space to avoid the influence of the geomagnetic field.

We have attempted to apply this technique to a historical lava in Hawaii and to Oligocene rhyolite flows and welded tuffs in Colorado. The results are quite encouraging and it appears that the application of the modified method may be fruitful in obtaining paleointensity data of high quality with a smaller amount of experimental time than is needed in the conventional Thelliers' method. It can be seen that most of the superior quality of the Thelliers' method are also attached to the modified method.

2. Experimental

An electric furnace was built of a quartz tube 5 cm inner diameter and 40 cm long, placed in a water jacket. Outside the water jacket, a solenoid coil was wound to produce a uniform, axial magnetic field between 0 and 2 Oe. The furnace with the water jacket was set inside a three-layer permalloy shield in which the residual magnetic field is less than 100 gammas. Samples were placed in the furnace on a quartz sample holder so as the NRM vector lies in a plane perpendicular to the axis of the furnace tube. All the heatings were carried out in air.

In this manner, a controlled magnetic field F_0 was always applied orthogonal to NRM directions. The estimated maximum error in the orientation of the samples is about 5°. To eliminate effects of secondary components of magnetization, samples were first heated to 100°C in a non-magnetic field and the "NRM" direction was determined after this thermal demagnetization. Samples were then heated and cooled under the magnetic field of 0.5 Oe to 100°C and successively higher temperatures.

Fig. 1 shows a typical example of the results by the Modified Thelliers' method. In this case the specimen was taken from a basalt lava erupted from Kilauea on the island of Hawaii in 1750. An adjacent specimen from the same sample was subjected to the ordinary technique and a paleointensity of 0.33 Oe was determined. The NRM of this sample is quite stable and the change of direction was less than 5 degrees both in AF demagnetization to 400 Oe and thermal demagnetization to 500°C. Fig. 1 (a) and (b) show the change of magnetization in magnitude and direction after each step. The direction of remanence moves on a great circle N-T, showing that the sum of NRM and TRM components at intermediate temperatures are confined in a plane formed by total NRM and TRM-producing magnetic field. By taking the O-N-T plane, the change in magnetization vector can be plotted as in Fig. 1 (c), in which the components in ON and OT directions correspond to NRM and TRM components, respectively, so that the end points of the remanence vector lie on a straight line forming an Arai diagram when the experiment was successful.

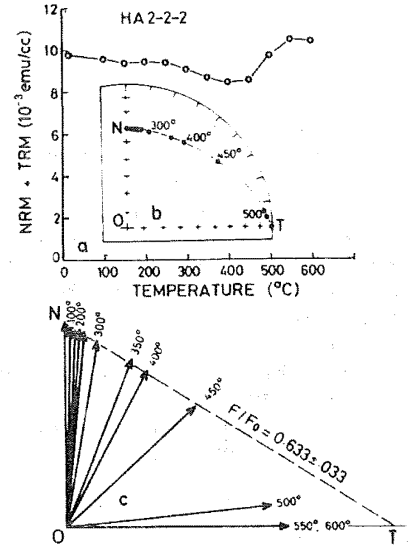

Fig. 1. An example of the modified Thelliers' experiment. Sample is taken from a basalt lava frow erupted in 1750 in Hawaii.

The end points of vectors corresponding to 500°C and higher are not on the straight line, indicating that the TRM capacity of the sample was irreversibly changed by heating, a phenomenon also observed in the adjacent specimen subjected to the ordinary Thelliers' technique. The paleointensity value obtained by the modified method (0.32 ± 0.02 Oe) is in good agreement with the one obtained by the ordinary technique and is a reasonable estimate of the geomagnetic total force in Hawaii in 1750. That the end points of remanence vectors form Arai diagram is one of the favorable points of the modified method, since such a representation may be a great help in understanding the results of paleointensity experiments.

3. Application to Samples from the San Juan Volcanics

The modified Thelliers' method was applied to Oligocene rhyolites of the San Juan volcanic field in Colorado, U.S.A. The San Juan Mountain is a remnant of a volcanic field of about 25,000 km^2 in the southwestern Colorado extending over much of the southern Rocky Mountains and adjacent areas in Oligocene and later times. Many of the cooling units were dated by K-Ar method with exceptionally small experimental errors (Lipman et al., 1970). Paleomagnetism of the San Juan rocks has been reported by Tanaka and Kono (1973). The NRM in these rocks are, on the whole, stable to AF demagnetization up to 400 Oe, and the dispersion of NRM directions are quite small except a few cooling units. Virtual geomagnetic poles are distributed close to the present geographic poles except for the unit SJ15, which apparently corresponds to a time during a geomagnetic reversal or an excursion.

Samples for paleointensity experiments were selected from cooling units with stable NRMs. Two to four specimens from each cooling unit were used in paleointensity studies. Half of the specimens were subjected to the Coe-version of double heating technique (Coe, 1967), in which the first heating is done in a non-magnetic field and the second heating with laboratory magnetic field. The other half was treated by the modified method.

Fig. 2 shows changes in the directions of NRM components

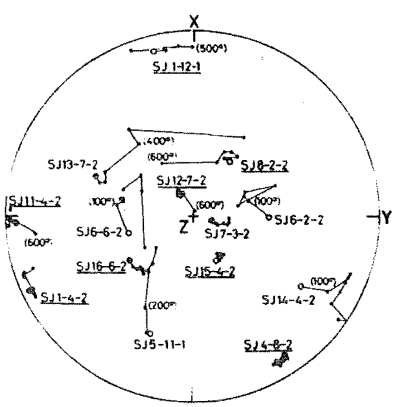

Fig. 2. Change of direction of NRM by thermal demagnetization. Numbers in parentheses indicate temperatures in °C at which deviations of more than 10 degrees from the original 'NRM' directions (Larger circles) were observed. Samples that gave paleointensities are underscored. TRM-inducing field was applied in the Y direction. Solid (open) circles indicate downward (upward) inclinations. Lambert equal area projection.

observed in the ordinary Thelliers' technique. As can be seen from the figure, NRMs of the specimens which gave satisfactory results in paleointensity determination were stable to thermal demagnetization up to about 500°C. On the other hand, most of the unsuccessful samples show a considerable amount of direction change at relatively low temperatures.

NRM-TRM plot (Arai diagram) of successful samples is shown in Fig. 3. The criterion of success of an experiment is similar to the one employed by Kono (1974). In all, 14 specimens out of 30 gave satisfactorily linear NRM-TRM relations. Of these, eight was obtained by the ordinary technique, while six was by the modified, single heating method (Table 1). Among the eight cooling units in Table 1, both methods were good for the four units, while the double heating method gave good results for the other three and only the modified method was good for one. These comparisons show that the two methods are almost interchangeable, except for the cases in which the intensity ratios F/F_0 are considerably different from unity (e.g., SJ 8 and SJ15).

The above suggestion can be substantiated by examining the change of NRM and TRM components in both methods. For almost all units, NRM decay curve and TRM acquisition curve are similar in the two methods. Even the unsuccessful samples show very similar NRM decay and TRM acquisition curves. All in All, the results of the present experiments show that the modified method is almost equally good in paleointensity studies as the original double heating method.

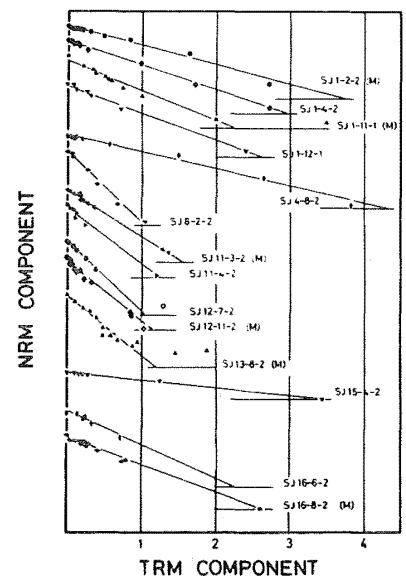

Fig. 3. The NRM-TRM curves of successful samples. Intensities are normalized by those of NRM of individual samples, except SJ15-4-2 which is normalized by 2.5 x NRM. The horizontal lines are the TRM axes for individual samples. Open symbols are the data excluded from linear regression analyses. Samples treated by the modified method are marked by (M).

4. Discussion

The foregoing experiments suggest that the modified method is almost as good as the ordinary method in giving reliable paleointensities. That even unsuccessful samples show quite similar behaviors in these experiments is a positive support for the assumption of constant directions of NRM components.

The essential part in the modifield technique is, as is in

Table 2. Paleointensity Determination: Successful Results

Unit	Sample	T_1 °C	T_2 °C	N	-b	s_b	-r	F Oe	F_{mean} Oe	VDM 10^{25} G cm^3
SJ13	8-2 (M)	20	500	10	0.852	0.096	0.981	0.426	0.426	7.92
SJ12	7-2	20	500	6	.964	.042	.996	.482	.448	8.96
	11-2 (M)	20	600	13	.836	.036	.990	.418		
SJ11	3-2 (M)	20	600	12	.645	.019	.995	.322	.339	5.10
	4-2	20	600	7	.769	.051	.989	.384		
SJ 8	2-2	20	600	7	.956	.057	.991	.478	.478	8.26
SJ15	4-2	20	600	7	.096	.005	.993	.048	.048	1.15
SJ16	6-2	20	500	6	.458	.070	.980	.229	.193	4.46
	8-2 (M)	20	600	12	.371	.015	.992	.186		
SJ 4	8-2	20	600	9	.234	.012	.991	.117	.117	2.58
SJ 1	2-2 (M)	20	600	12	.267	.013	.988	.134	.161	3.90
	4-2	20	600	9	.327	.009	.997	.164		
	11-1 (M)	20	550	10	.404	.039	.983	.202		
	12-1	20	600	7	.364	.022	.991	.182		

(M), data by the modified method; T_1, T_2, N, temperature interval in which NRM-TRM relation is linear and the number of points in this interval; b, slope of NRM-TRM linear regression line; s_b, standard error of the slope b; r, correlation coefficient; F, paleointensity; VDM, virtual dipole moment.

the ordinary method, the selection of suitable samples. We used San Juan rocks with rather a vague criterion of "stability to AF demagnetization". Some of the specimens showed a big change of NRM directions in thermal demagnetization (Fig. 2). However, all of such specimens failed in both kinds of Thelliers' experiments, suggesting that the constancy of NRM directions is a necessary condition for obtaining reliable paleointensity data.

When the intensity ratio F/F_0 is either very small or very large, the modified method gives results with large errors. This is to be expected since an error in the orientation of samples in the furnace will introduce errors not only in TRM, but also in NRM components. For example, an angular error of one degree in the alignment of a sample to the applied field F_0 will cause an error of about 0.02 x TRM component in the NRM component. As it was rather difficult to align samples with errors smaller than 5 degrees, an error of 10 % of TRM should be expected in the modified technique. If the intensity ratio F/F_0 is, say, 0.1, errors in the NRM components are of similar magnitude as NRM when the temperature T is close to Curie point. It may be worthwhile to repeat the experiment on such samples by the Coe-version of the ordinary method or by the modified method with an appropriate laboratory field F_0.

The averaged paleointensity values of individual cooling units (Table 1) are calculated as weighted means of the raw data, using the reciprocals of the standard errors of the regression coefficients s_b as weights. Virtual dipole moments (VDMs) were calculated by the dipole formula

$$VDM = \frac{1}{2} Fr^3 \ (1 + 3\cos^2 I)^{1/2}$$

where r is the radius of the earth and I is the inclination. The mean and the standard deviation of the VDMs for the San Juan volcanics are,

mean	standard deviation
5.29×10^{25} G cm^3	2.84×10^{25} G cm^3 (53.6% of mean)

of which the mean is considerably smaller than the present value (8.0×10^{25}) or the mean of the last 10 m.y. (8.9×10^{25}, Kono, 1971). However, as the number of samples (8) is small and as they contain a definitely non-normal value representing a transition period (SJ15), it can not be decided at present whether the geomagnetic field was significantly weaker in the Oligocene period.

References

Coe, R.S.(1967) J. Geophys. Res. 72, 3247.

Coe, R.S. and C.S. Grommé (1973) J. Geomag. Geoelectr. 25, 415.

Kono, M.(1971) Earth Planet. Sci. Lett. 11, 10.

Kono, M.(1974) J. Geophys. Res. 79, 1135.

Lipman, P.W., T.A. Steven and H.H. Mehnert (1970) Geol. Soc. Am. Bull. 81, 2329.

Tanaka, H. and M. Kono (1973) Rock Mag. Paleogeophys. 1, 71.

Thellier, E. and O. Thellier (1959) Ann. Géophys. 15, 285.

Van Zijl, J.S.W., K.W.T. Graham and A.L. Hales (1962) Geophys. J. Roy. Astron. Soc. 7, 23.

(Presented at IAGA symposium held in XVIth IUGG general meeting in Grenoble; in press in Physics of Earth and Planetary Interiors)

A PALEOMAGNETIC STUDY OF THE IBARAGI GRANITIC COMPLEX

Haruaki ITO and Katsuyasu TOKIEDA
Physics Department, Shimane University, Matsue, Japan

(1) Geological setting and sampling

According to Tainosho (1971), the Ibaragi granitic complex (34°50'N, 135°30'E) consists of two bodies of Nose and Myoken plutons. The Nose pluton is a small intrusive body in elliptical shape differenciated from coarse-grained quartz diorite to fine-grained porphyritic adamellite and it has approximately 5.5 km in width and 10 km in length. This pluton intrudes the Paleozoic formation of Tanba zone. The Nose pluton is, roughly speaking, composed of following three rock types exposed in order from outermost part to innermost part of the pluton.

(a) Coarse and medium-grained quartz diorite
(b) Coarse-grained granodiorite
(c) Fine-grained porphyritic adamellite

The Myoken pluton consists of two rock types of fine-grained pink adamellite and very fine-grained porphyritic pink adamellite.

The Ibaragi granitic complex is extending with the direction of N30°W. Ishizaka (1971) shows that biotites from the representative rock facies give biotite-whole rock ages ranging from 79 to 83 million years for the Nose pluton. The Myoken pluton has younger ages (76 and 77 million years) than those of the Nose pluton. On the other hand, K-Ar ages of the Nose pluton are 74 and 76 million years by Shibata (1971) and the age of the Myoken pluton is 74 million years.

Samples were collected from both of the Nose and Myoken plutons. Although the first plan was to collect samples successively from the outermost part to the innermost part of the body, we could not find continuous outcrops along a few road cuts which intersect at right angles to the isothermal plane yielded within the intrusive body. About ten hand samples were taken at a sampling site and one or two samples were obtained from such a hand sample using core drill machine in the laboratory.

(2) Measurements of NRM and stability tests

The direction of the NRM have been initially measured by an astatic magnetometer at the Shimane University and then by a spinner magnetometer at the rock magnetism laboratory of the University of Pittsburgh. Alternating field demagnetization to 100 oe was done for all samples by tumbling the sample about two axes simultaneously in the three cylindrical μ-metal boxes in which the ambient field was maintained at less than 0.01 % of the Earth's field.

Results of the measurements of the NRM after demagnetization are shown in Table 1. Mean directions of the NRM of all samples after demagnetization of 100 oe are also seen in Table 1. Initial directions of the NRM of some samples were well grouped, and after demagnetization of 100 oe the directions were fixed in situ without great change. The directions of

the NRM of the quartz diorite belonging to the outermost part of the Nose pluton (sites 1 to 19) were easterly deviated in the equal area projection. The samples of granodiorite in the middle part are reversely magnetized, and the direction shows obviously intermediate. Acidic adamellite placed at the innermost part has the normal NRM with directions which are slightly deviated to the east, except for one site (site 13). Samples from the Myoken pluton (sites 20 to 23) are all normally magnetized and the directions are significantly deviated from the present field direction.

According to the geomagnetic reversal time scale (Larson and Pitman, 1972), between 85 and 110 million years is an interval of normal polarity representing the Cretaceous smooth zone as seen in Fig. 1. The existence of the reversely magnetized rocks in the Nose pluton implies that the magnetic age of the pluton is close to the Rb-Sr ages (79-83 million years) by Ishizaka (1971) or the K-Ar ages (74-76 million years) by Shibata (1971).

After thermal demagnetization for some samples, change in direction of the NRM was nothing significantly. Curie temperatures were between 550° to 570°C in all samples investigated. Reflected light microscopy showed that the titanomagnetite is in one generation with large grains of up to several hundred microns. Samples collected from Tarumi have only a little ferromagnetic mineral as long as we observed under the reflected light. This is likely to be a cause that the intensity of the NRM of samples at Tarumi is very weak as compared with that of the other localities. There are no obvious microscopic difference among ferromagnetic minerals in the samples taken from the outermost part, middle part, and innermost part of the complex.

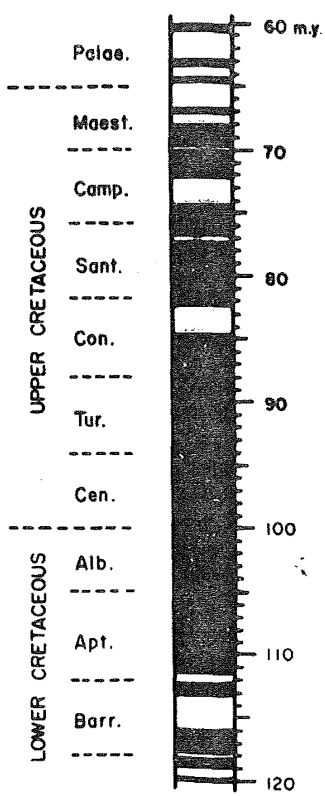

Fig.1 Geomagnetic reversal time scale from 120 to 60 million years after Larson and Pitman (1972).

(3) Analysis of the NRM

Ito (1965) concluded that the intermediate NRM of the Nose pluton was acquired at the time of a transition of the geomagnetic field. However, the age of the intrusion was not known exactly because results of geological observations only suggest that the Nose pluton intruded the upper Paleozoic formations. Therefore, he concluded that the age of this pluton is the Mio-Pliocene age from the fact that the virtual geomagnetic pole positions obtained from this body were close to those from volcanic rocks of the Mio-Pliocene age in southwestern Japan. At present, it is confirmed by the isotopic age determinations that the

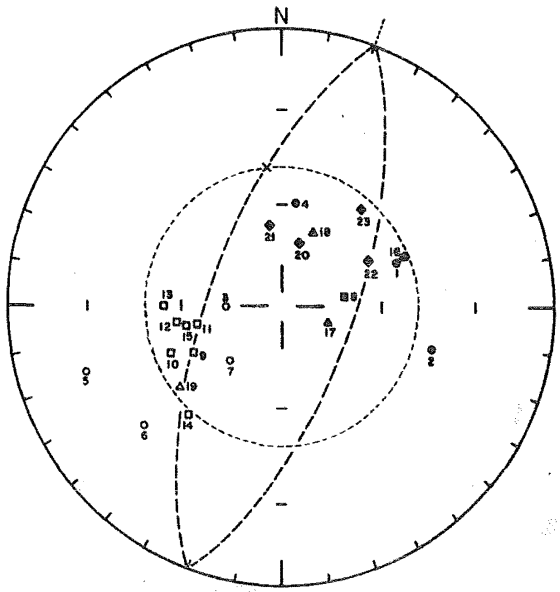

Fig.2 Mean directions of NRM after demagnetization of 100 oe. Dots represent normal and open circles represent reversed. Cross mark represents the present geomagnetic field direction.

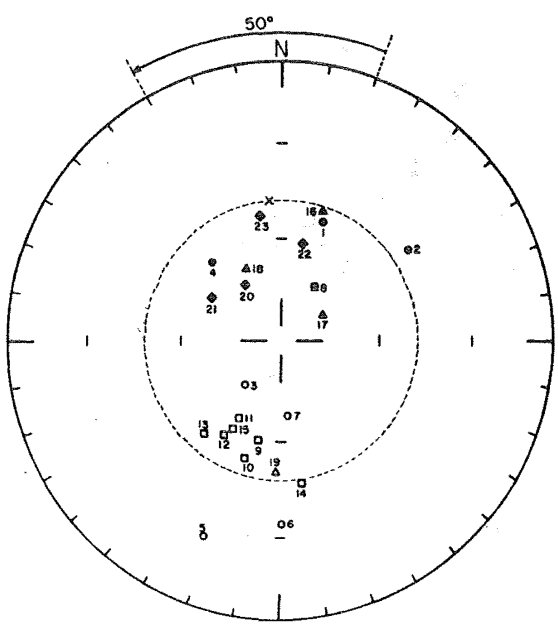

Fig.3 Mean directions of NRM after a rotation of 50° about a vertical axis at the sampling site.

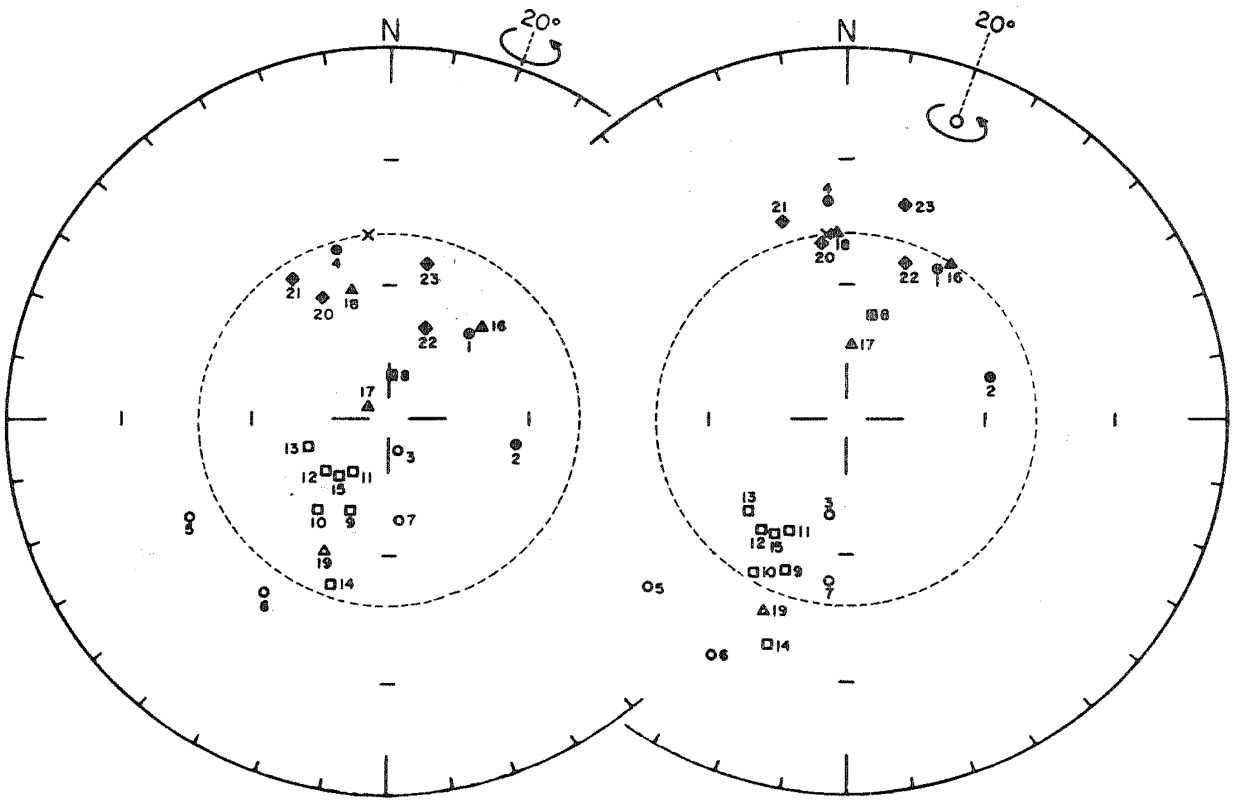

(a) (b)

Fig.4 a) Mean directions of NRM after a rotation of 20° about an axis in the horizontal plane.

b) Mean directions of NRM after a rotation of 20° about an axis a tilted plane from the horizontal plane.

granitic plutons intruded the upper Paleozoic formations in the upper Cretaceous period.

If we accept that the Japanese Islands had bended at least before the Miocene times as pointed out by Kawai et al. (1961, 1962, 1972), it suggests that the Nose and Myoken plutons might be deformed by such crustal movements after the intrusion. The mean directions of the NRM of all sites are shown on the equal net in Fig. 2. As seen in the figure, the intermediate normal directions and the intermediate reversed ones occupy two points about 180° apart from each other on the great circle. Assuming that these intermediate directions of the NRM were acquired at the time of a polarity transition of the geomagnetic field and also that this body was moved by regional tectonic movements such as the bending of the Japanese Islands, traces of the tectonic movements of the granitic bodies should be removed by reasonable methods in order to expose an intrisic reversal record.

The most important question is whether the ancient magnetic field had an axial geocentric dipole in geologic time. Currently available paleomagnetic data indicate that the geomagnetic field was nearly dipolar throughout the upper Cretaceous times (Strangway, 1970; McElhinny, 1973). As a rule, remanent magnetizations which were acquired in a duration of field reversals is roughly opposed to the present field direction except intermediate directions representing a transitional change of the field.

The NRM directions of the Nose pluton are normal by half in the outermost zone (oldest), almost reversed in the middle zone, and normal in the innermost zone (youngest). This shows that the pluton which is a successive intrusion defferentiated from basic quartz diorite to acidic adamellite intruded partly at the time of a polarity transition and partly at the time of a normal field.

The NRM directions of the Myoken pluton are normal and easterly deviated as shown in Fig. 2. From this fact and the intermediate directions of NRM of the Nose pluton, we assumed now that the Ibaragi complex had been subjected to some tectonic movements as a block after the intrusion. Therefore, it is necessary to reveal the traces of such tectonic movements. The following basic procedures were carried out to the NRM directions in order to expose such traces.

(a) A deviation represented by the mean declination was corrected by a rotation about a vertical axis through the sampling site (Clegg et al., 1954; Kawai et al., 1961, 1962, 1972), or by a rotation about an axis in the horizontal plame, which is a bisector of the mean declination and the true north.

(b) A difference between the mean direction of the pluton and the dip of the present field at the site was corrected by a tilting of the pluton or a drift of the pluton along the meridian.

The magnetic vectors after demagnetization of 100 oe are shown in Fig. 2. Most of normal vectors are clustered at about 40° east of the true north as seen in the figure and reversed ones at about 55° west of the south pole. This result shows that the geomagnetic field direction itself has reversed at a time during the formation of the complex. On the other hand,

the NRM directions of Post-Tertiary rocks demonstrate that the mean direction, apart from the reversal, is close to the present field direction (Ito, 1970). Assuming that the geomagnetic field at the given time and place has been the same dipolar field that it is now and has approximately coincided with the present geographical poles, the deviation of the NRM directions in the Nose pluton should imply that the directions have been altered since the formation of the body.

Fig. 3 shows the mean directions of NRM after a rotation of 50° to the west about a vertical axis through the sampling site. This means that the deviation of the NRM has been corrected by the declination only. Fig. 4a shows to have simply rotated the magnetic vectors about an axis in the horizontal plane. The rotation angle in that case is about 20°. It means that the rock body has been subjected to tilting of 20°. In two cases mentioned above, the former implies a drift of the rock body and the latter emphsizes the tilting of the body.

Fig. 4b shows to rotate the magnetic vectors about an axis in a slightly tilted plane from the horizontal plane. In this case, the NRM directions approach the present field direction thoroughly. On the assumption that the principle of minimum movement is applied, we will be able to prefer a rotation about an axis in the horizontal plane or in a tilted plane from the horizontal plane corresponding to tilting of the rock body (Ito, 1975).

Virtual geomagnetic pole positions obtained from the raw NRM directions in Fig. 2 are shown in Fig. 5. It appears that the pole positions from the reversed NRM coincide with those obtained from the Japanese rocks of different places and ages. It seems, however, that the distribution of the virtual poles from the normal NRM is consistent with the pole path obtained from the Miocene intrusive rock in the U.S.A. (Dunn et al., 1971). This apparent break of the pole path is very important to realize traces of tectonic movements after the intrusion or a reversal process of the field.

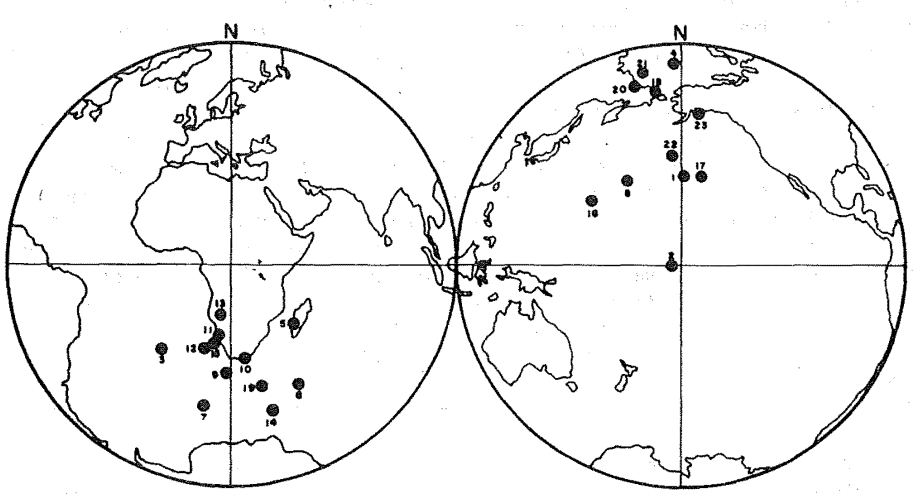

Fig.5 Virtual geomagnetic poles estimated from the mean directions of NRM shown in Fig. 2.

Fig. 6 shows a distribution of pole positions estimated from the NRM directions after a rotation about an axis in a slightly tilted plane from the horizontal plane. It is likely that the virtual pole positions are still situated on a great circle through longitudes 20°E and 160°W.

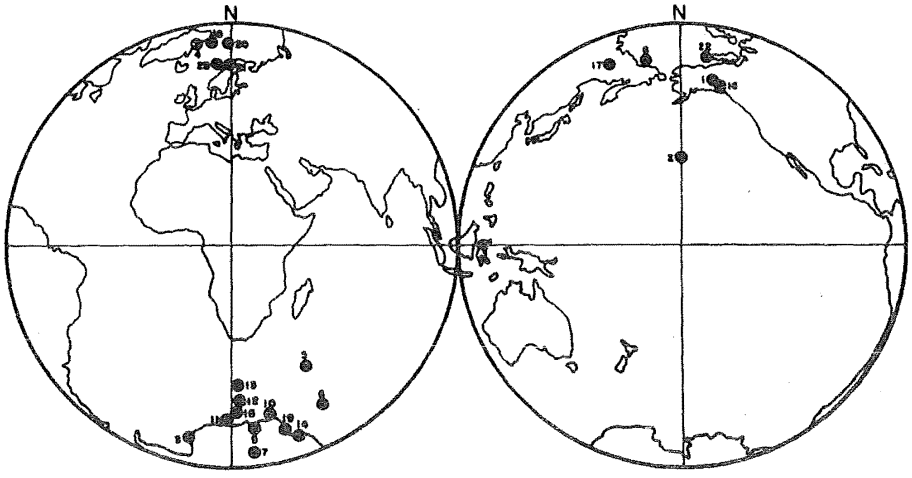

Fig.6 Virtual geomagnetic poles estimated from the mean directions of NRM after a rotation about an axis in a slightly tilted plane from the horizontal plane.

References

Clegg, J.A., M. Almond and P.H.S. Stubbs (1954); The remanent magnetism of some sedimentary rocks in Britain, Phil. Mag., 45, 583-594.

Dunn J.R., M. Fuller, H. Ito and V.A. Schmidt (1971); Paleomagnetic study of a reversal of the earth's magnetic field, Science, 172, 840-845.

Ishizaka, K. (1971); A Rb-Sr isotopic study of the Ibaragi granitic complex, Osaka, Japan, J. Geol. Soc. Jap., 77, 731-740.

Ito, H. (1965); Paleomagnetic study on a granitic rock mass with normal and reversed natural remanent magnetization, J. Geomag. Geoelectr., 17, 113-120.

Ito, H. (1970); Polarity transitions of the geomagnetic field deduced from the natural remanent magnetization of Tertiary and Quaternary rocks in southwest Japan, J. Geomag. Geoelectr., 22, 273-290.

Ito, H. (1975); On an interpretation of the direction of natural remanent magnetization, Mem. Fac. Lit. Sci., Shimane Univ., Nat. Sci., 8, 41-48.

Kawai, N., H.Ito and S. Kume (1961); Deformation of the Japanese Islands as inferred from rock magnetism, Geophys. J. Roy. Astro. Soc., 6, 124-129.

Kawai, N., S. Kume and H. Ito (1962); Study on the magnetization of Japanese rocks, J. Geomag. Geoelectr., 13,150-153.

Kawai, N., T. Nakajima and K. Hirooka (1972); The evolution of the Island Arc of Japan and the formation of granites in the Circum-Pacific belt, J. Geomag. Geoelectr., 23, 263-293.

Larson, R.L. and W.C. Pitman 111 (1972); World-wide correlation of Mesozoic magnetic anomalies, and its implications, Geol. Soc. Am. Bull., 83, 3645-3662.

McElhinny, M.W. (1973); Palaeomagnetism and plate tectonics, Cambridge Univ. Press.

Shibata, K. (1971); K-Ar age of the Ibaragi granitic complex Chikyu-Kagaku, 25, 306-307,(in Japanese).

Strangway, D.W. (1970); History of the earth's magnetic field, McGraw-Hill In., New York.

Tainosho, Y. (1971); Petrology of the Ibaragi granitic complex in the northern part of Osaka Prefecture, Japan, J. Geol. Soc. Jap., 77, 57-70, (in Japanese).

Table 1

	N	D	I	J_r (emu/cc)	α_{95}	K	ϕ	λ
1	5	70°	+53°	18.00 x 10^{-5}	7.1°	118.2	34°N	158°W
2	5	106°	+42°	11.10	7.5°	106.2	0°	163°W
3	5	268°	-74°	9.47	6.0°	165.3	31°S	9°W
4	5	9°	+59°	10.28	6.7°	130.3	81°N	171°W
5	5	253°	-26°	0.31	18.7°	17.7	22°S	44°E
6	10	230°	-34°	o.67	5.7°	71.7	43°S	52°E
7	3	225°	-68°	0.98	9.0°		54°S	5°E
8	10	82°	+71°	4.10	3.9°	154.6	32°N	177°E
9	11	243°	-60°	2.53	5.3°	74.5	41°S	19°E
10	5	249°	-54°	5.52	7.6°	102.7	35°S	25°E
11	5	263°	-58°	9.42	5.8°	178.0	26°S	15°E
12	5	259°	-68°	23.07	12.0°	58.7	31°S	9°E
13	22	270°	-54°	5.37	3.5°	77.8	19°S	16°E
14	5	221°	-48°	1.85	26.4°	9.3	55°S	44°E
15	5	260°	-61°	4.28	31.7°	6.8	29°S	13°E
16	5	107°	+75°	0.43	10.5°	54.2	23°N	165°E
17	5	68°	+50°	0.40	10.3°	56.1	34°N	151°W
18	6	23°	+66°	0.38	7.7°	76.0	68°N	180°E
19	5	233°	-51°	4.12	6.4°	146.0	46°S	34°E
20	4	16°	+70°	2.29	11.0°	71.0	68°N	161°E
21	4	351°	+66°	2.54	26.3°	13.2	75°N	159°E
22	3	63°	+62°	0.71	29.8°	18.2	42°N	164°W
23	5	40°	+53°	0.45	18.3°	18.5	58°N	149°W

1 - 7 : Outermost zone
8 - 15 : Middle zone
16 - 19 : Innermost zone
} Nose pluton
20 - 23 : Myoken pluton

REMANENT MAGNETISM OF KOFFYFONTEIN KIMBERLITE

Kanenori SUWA

Faculty of Science, Nagoya University, Nagoya, 464

Haruaki ITO

Faculty of Arts and Sciences, Shimane University, Matsue, 690

Shoichi KUME

College of General Education, Osaka University, Osaka, 560

Kimberlite is characterized by its diamond bearing nature. The occurrence of this rock, however, is limitted in a certain part of the world and hence it is hard to say that every detail of its magnetism has been examined so far. One of the present authors had an opportunity to visit several diamond mines in South Africa in 1974. The results of brief survey on the remanent magnetization of kimberlite collected are shown here.

Two oriented samples of Mesozoic kimberlite were collected from Koffyfontain mine. The location of the mine is at 25°00'E and 29°24'S. Its altitude is 1095 m above sea level. The mean geomagnetic field at the collecting site is roughly 340° and -65°. Four specimens were drilled from two samples.

Remanent magnetism of specimens was measured by the use of a conventional astatic magnetometer. Soft components of the remanence were demagnetized in A.C. field up to 100 Oe.

The mean direction of n.r.m. was 352° in declination and -71° in inclination, the magnetization being 2.23×10^{-3} emu·cm^{-3} in average. Although this magnetization decreased to about one fifth of the original values after the application of A.C. field, no significant change was observed in the direction.

The mean polarity finally obtained is 349° and -66°. This is close to that of De Beers Mine kimberlite reported by McFadden (1973). Koffyfontein is at 70 km south-south-east of De Beers Mine. The similarity between two n.r.m. indicates that the intrusions of these two pipes were contemporaneous and also that there have been no relative movement between the pipes since their formations.

The virtual position of the South Pole is obtained to be at 50°E and 70°S. Creer (1970) has summarized the palaeomagnetic pole positions and shown that the position for Africa in Cretaceous is at 41°E and 71°S. This coincides extremely well with the present result.

H.L. Allsopp and D.R. Garrett (1975) Physics and Chemistry of the Earth (Pergamon Press, Oxford). Vol. 9, p.605.
K.M. Creer (1970) Proc. 2nd Gondwana Symp. P.55, South Africa.
P.L. McFadden (1973) Extended Abstracts, Intern. Conf. on Kimberlites. p.221, Cape Town.

METAMORPHIC EFFECTS ON THE INTENSITY OF NATURAL REMANENT MAGNETIZATION OF PALEOZOIC GREENSTONES IN CENTRAL JAPAN

Kimio HIROOKA and Isamu HATTORI

Geological Laboratory, Faculty of Education, Fukui University
Bunkyo 3-9-1, Fukui-shi, Fukui 910

Paleomagnetic investigation of Japanese Paleozoic rocks has been scarse because not only of the weakness of remanent magnetization but also of the intensive tectonism and metamorphism which affected the Paleozoic strata during their long geologic history. The effects of metamorphism and alteration of rocks on the nature of magnetization have been suggested qualitatively by several authors (Miyashiro et al., 1970; Miyashiro, 1972; Ozima, 1971; Ozima et al., 1974). For the paleomagnetic studies, the characteristics and the magnitude of the metamorphic effects on the remanence should be understood. In this paper, we attempted to make clear the effects on the natural remanent magnetization (n.r.m.), especially on the intensity and the stability of remanence inherent in the Japanese Paleozoic greenstones.

Late Paleozoic strata in the Fujibashi area, Central Japan are composed of greenstone, chert, sandstone shale and limestone, and form a thick and typical eugeocynclinal succession (mainly middle Permian in age) (Miyamura, 1964; Hattori, in the press). Greenstones occupy more than one third of the succession in volume. Geochemically, some greenstones are tholeiitic in composition, and the others alkali-basaltic (Tanaka, 1970; Sugisaki et al., 1972). They encompass a whole variety of occurrences of basic effusive rocks such as massive and pillow lava and their derivatives. This green stone-rich succession was intruded by a pluton of biotite granite and granodiorite (73 m.y. old, Kawano and Ueda, 1966) about 15 km in diameter. The greenstones are widely distributed from the contact to over 15 km north of the pluton, and show a progressive metamorphic increase from unmetamorphosed or zeolite facies to hornblende hornfels facies (Hattori, 1975).

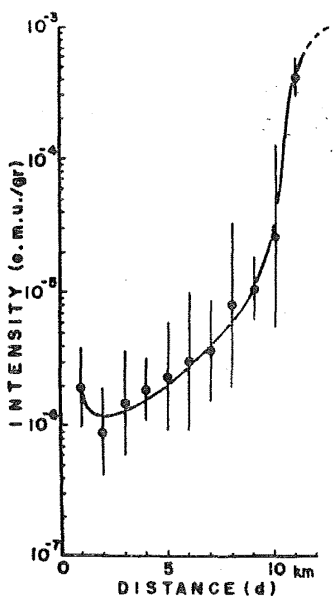

Fig. 1. Relation between the average intensities of n.r.m. of greenstones in the Fujibashi area and the distance from the intruding pluton.

The intensities of n.r.m. were measured for more than two hundred specimens of the greenstones successively collected by the intervals of some tens of meters along a route nearly perpendicular to the contact. The result shows that the average intensities of n.r.m. for every 1 km interval have an apparent relation to the distance (d) from the contact between the granite and the Paleozoics (Fig. 1). This suggests the intensities of n.r.m. dependent upon the metamorphic grade which the rocks have undergone.

In the zone of the lowest metamorphic grade in the Fujibashi area ($d > 12$ km), the greenstones invariably

carry clinopyroxene and plagioclase (generally unaltered) with minor secondary minerals such as chlorite, quartz and calcite, and contain many minute grains of (titano-)magnetite and rarely ilmenite and magnesio-ferrite. The primary magnetite grains are usually fresh under the microscope. Hydrothermal veinlets of epidote, laumontite and pumpellyite occassionally intersect the greenstones. The greenstones of pumpellyite-prehnite facies (d = 5-12 km) is characterized by pumpellyite and a lesser amount of prehnite, most of them occurring in a form of small veinlets. The content of opaque minerals gradually decreases toward the higher grade division, whereas sphene and leucoxene become common, sometimes surrounding magnetite grains. The greenschist facies (d = 4-5 km) is marked with the appearance of epidote and actinolite. Microscopically, the opaque minerals are scarcely interspersed in the mesostasis, and recrystallization of sphene is remarkable. The highest grade of metamorphism in the Fujibashi area corresponds to the hornblende hornfels facies ($d \leqslant 4$ km). The rocks in this facies are invariably composed of green to brown hornblende, epidote (+ clinozoisite), plagioclase and/or biotite. Relic magnetite is hardly found, and skeletal opaque minerals, probably ilmenite in origin, are sometimes observed. Recrystallized and hydrothermally-formed ore minerals including magnetite are sporadically set in the greenstones or in a form of veins.

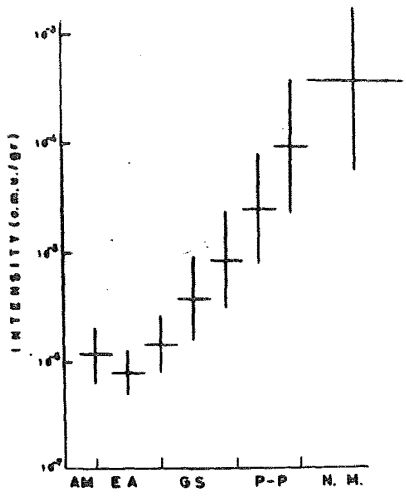

Fig. 2. Relation between metamorphic facies of greenstones and the intensities of n.r.m. AM: amphibolite facies, EA: epidote-amphibolite facies, GS: greenschist facies, P-P: pumpellyite-prehnite facies, N.M.: nonmetamorphic to zeolite facies.

It is evident that the magnetic intensity of rocks bears a reciprocal relation to the development of Fe-bearing silicate minerals such as pumpellyite, epidote, hornblende and sphene. The dependency of magnetic intensity upon the metamorphic mineral associations is examined also in the other Paleozoic greenstones of central Japan (the Wakasa, Nanjo and Mugi-Kamiaso areas). Intensity of n.r.m. of rocks from 34 sites in these area is measured after examining their metamorphic mineral associations. The relation between the average intensity and metamorphic grade is obvious as illustrated in Fig. 2.

Fresh basaltic lavas which poured out recently (for example, from Oshima and Miyakejima in the Izu-Mariana island arc) have been magnetized to the intensity of 10^{-2} to 10^{-1} e.m.u./gr (unpublished data by Hirooka et al.). Submarine basalts retreived from the young ocean floors give the average magnetization of 10^{-2} e.m.u./gr (Watkins et al., 1970; Marshal and Cox, 1971). It is highly probable to expect that ancient geosynclinal basalts such as the greenstones of the Fujibashi area originally possessed this range of magnetization intensity. Obviously, the magnetic intensity rapidly decreases with increase of metamorphic grade, and the original nature of magnetization is remarkably weakened.

The stability of magnetic directions of rocks is also tested by means of the alternating field (a. f.) demagnetization. Based on the stepwise demagnetizations at the peak fields of 100, 150, 200, 250, 300 and 400 oe,

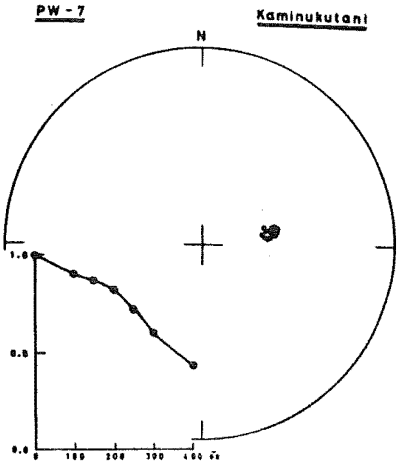

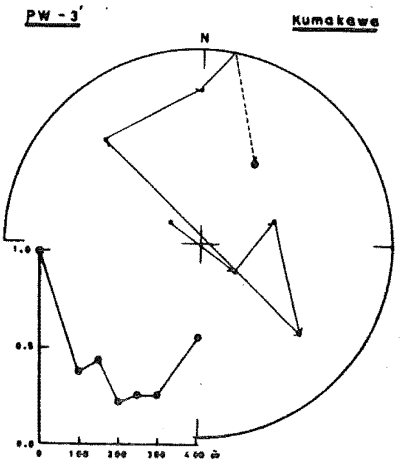

Fig. 3. Effect of cleaning in alternating field for an unmetamorphosed greenstone (Kaminukutani, Nanjo, Fukui Pref.).

Fig. 4. Effect of cleaning in alternating field for a rock of greenschist facies (Kumakawa, Wakasa, Fukui Pref.).

These figures show the change in the direction (plotted on the lower hemisphere of Schmidt projection) and the intensity of n.r.m.

we found that the un- or weakly metamorphosed greenstones bear a stable magnetic direction (Fig. 3). Recently Tokieda (private communication) showed that the stable samples probed by a. f. demagnetization are also very stable to the thermo-demagnetization. The higher metamorphosed rocks are, on the other hand, magnetically unstable as is shown in Fig. 4, and not likely to preserve reliable records of the ancient geomagnetic field. Thus, we probably successful to work with the paleomagnetic data obtained from the rocks of unmetamorphosed to zeolite facies possessing natural remanence comparable in intensity to recent basalts.

We would like to suggest that the weak contrast of the magnetic liniation patterns in the western Pacific might be the resultof low intensity originated by the thermal metamorphism.

References

Hattori, I.(1975)Abst. Program Annual Meeting, Geol. Soc. Japan, 247 (in Japanese).

Hattori, I.(1976) J. Geol. Soc. Japan, 82 (in the press).

Kawano, Y. and Y. Ueda (1966) J. Japan Assoc. Min. Pet. Econ. Geol., 56, 191 (in Japanese).

Marshall, M. and A. Cox (1971) Geol. Soc. Amer. Bull., 82, 537.

Miyamura, M. (1964) J. Geol. Soc. Japan, 71, 5 (in Japanese).

Miyashiro, A. (1972) Tectonophysics, 13, 141.

Miyashiro, A., F. Shido and M. Ewing (1970) Deep-Sea Res., 17, 109.

Ozima, M. (1971) Earth Planet. Sci. Letters, 13, 1.

Ozima, M., M. Joshima and H. Kinoshita (1974) J. Geomag. Geoelectr., 26, 335.

Sugisaki, R., S. Mizutani, H. Hattori, M. Adachi and T. Tanaka (1972) Tectonophysics, 14, 35.

Tanaka, T. (1970) J. Geol. Soc. Japan, 76, 323 (in Japanese).

Watkins, N. D., T. Paster and J. Ade-Hall (1970) Earth Planet. Sci. Letters, 8, 322.

K-Ar AGE OF SHIGA WELDED TUFF , NAGANO PREFECTURE, JAPAN

Osamu MATSUBAYASHI

Geophysical Institute, Faculty of Science, University of Tokyo
Bunkyo-ku, Tokyo 113, Japan

Paleomagnetic studies with K-Ar age determination have revealed that the lava flows of the Kirizumi group, Gumma Prefecture were erupted about 3 m. y. ago with reversed geomagnetic polarity which corresponds to the Mammoth event. Furthermore, a long time interval has been observed between the Kirizumi group and the Hanamagari group which overlies the former (Ozima et al., 1968). Geologically, it is very important to know the ages of the basement rocks of this province, Asama Volcano. For this purpose we collected some rocks from an outcrop which belongs to the Shiga welded tuff associated with the reversed NRM (Aramaki ,1963). In this note we report the result of K-Ar dating for these rocks.

The sampling locality is situated at 36°16' N, 138°30' E, the southern end of the Asama volcanic area. The rock type of the sample is hornblende bearing augite-hypersthene dacite. No alteration products are observed in these rocks and fresh enough for K-Ar dating.

K-content was determined by a flame photometer with internal standard method and Ar analyses were made by the isotope dilution method with Ar-38 tracer. More details of experimental procedures in our laboratory have been reported elsewhere (Ozima et al., 1967).

Table 1

Sample	Weight (gm)	(Ar-40)rad / gm moles	(Ar-40)air / (Ar-40)total (%)	K (%)	Age-* (m.y.)	Age-** (m.y.)
AS04 -52	11.78	8.43×10^{-12}	80.6	1.55, 1.57 } 1.56	3.04	3.12
AS04 -54	12.04	8.25 x10-12	80.4	1.41, 1.42 } 1.42	3.25	3.33

* $\lambda_e = 0.585 \times 10^{-10}\ yr^{-1}$, $\lambda_\beta = 4.72 \times 10^{-10}\ yr^{-1}$, K-40/K=$1.19 \times 10^{-4}$ moles/mole

** $\lambda_e = 0.575 \times 10^{-10}\ yr^{-1}$, $\lambda_\beta = 4.905 \times 10^{-10}\ yr^{-1}$, K-40/K=$1.18 \times 10^{-4}$ moles/mole

The results of the K-Ar dating for whole rocks are given in Table 1. In K-Ar age calculation, if we use the decay constants which have been recommended recently by the committee on geochronology, ISGS, the resultant age increces by about 3% than those calculated after the decay constants used conventionally. For comparison with the previous results, we calculate the ages using both sets of constants. The analytical error in the radiogenic argon measurement is about 6% on account of high air contamination. The reproducibility of potassium analyses is about 1%. Hence, the calculated age includes the error of about 7%for the present work.

Samples AS04-52 and AS04-54 were collected from the same outcrop, but from different part with the distance of about 10 m.. These two samples show nearly the same age within the experimental error. If conventionally

used dacay constants are adopted, the age becomes 3.1± 0.2 m.y. .

According to Aramaki (1963), the Shiga welded tuff probably overlies conformably the Shiga group, whose rocks are the same in lithology with those of the Kirizumi group. These rocks are considered to compose the relatively old basement of the Asama Volcano. Present result indicates that the age of the Shiga welded tuff is nearly the same with those of the upper part of the Kirizumi group, which is older than the Hanamagari group whose K-Ar age is about 1.1 m.y. .

Although the Komoro group may be older stratigraphically than these basement rocks (Aramaki, 1963), it is now established that the basement of the volcano was formed at least more than 3 m.y. ago. If we take into account the result of NRM measurements, we may conclude that the Shiga welded tuff was formed during the Mammoth reversed event in geomagnetic time scale (Cox, 1969).

References

Aramaki, S., (1963) Jour. Fac. Sci. Univ. Tokyo, Sec. II, 14, 229.

Cox, A. (1969) Science, 163, 237.

Ozima, M., M. Kono, I. Kaneoka, H. Kinoshita, K. Kobayashi, T. Nagata. E. E. Larson and D. Strangway (1967) Jour. Geophys. Res., 72, 2615.

Ozima, M., I. Kaneoka, M. Kono, H. Kinoshita, K. Kobayashi, Y. Ohnaka, T. Nagata and S. Aramaki (1968) J. Geomag. Geoelectr. 23, 101.

^{40}Ar-^{39}Ar ISOCHRON AGE OF A MUGEARITE DREDGED FROM SUIKO SEAMOUNT IN THE EMPEROR CHAIN

Kazuo SAITO and Minoru OZIMA

Geophysical Institute, University of Tokyo
Bunkyo-ku, Tokyo, 113, Japan

Introduction

Wilson (1963) first proposed that the linear Hawaiian chain formed as the oceanic crust moved over a magma source fixed in the mantle. Morgan (1972) extended the hot-spot hypothesis to explain the linear alignment of the Emperor seamounts. Clague and Jarrard (1973), on the basis of all the age data available to that time from the Hawaiian-Emperor chain, proposed that the movement of the Pacific plate proceeded in three stages: the plate moved slowly from 70-67 m.y. to 44-42 m.y. about the Emperor pole and even more slowly from 44-42 m.y. to 25-20 m.y. about a pole near the Hawaiian pole and rather fast from 25-20 m.y. to recent times about the Hawaiian pole. Recently, with the addition of two DSDP fossil ages, Lancelot and Larson (1975) suggested a uniform rate of the movement of the Pacific plate from 70 m.y. to the present. Although the general age progression observed along the Hawaiian-Emperor chain appears to support the hot-spot origin of these islands, scancity of age data particularly along the Emperor chain makes it difficult to depict unequivocal movement of the Pacific plate. We present a ^{40}Ar-^{39}Ar isochron age obtained for a mugearite dredged from Suiko seamount in the Emperor chain, hoping that this would help towards better understanding of the above problem.

Sample

During cruise KH68-3, the R/V Hakuhomaru of University of Tokyo dredged a number of rocks at six stations on Suiko seamount. They are basalt, andesite, diorite, granodiorite, hornfels, tufaceous rocks, slate, sandstone and others (Aoki and Hirota, 1971). The sample studies was dredged at station 68-3-9-9, where most of the dredged rocks were olivine basalts. Under a microscope the rock bears phenocrysts of olivine altered to clay minerals, apatites and magnetites. The groundmass consists of subophitic plagioclase-anorthoclase, clinopyroxene, brownish clay minerals (smectite), magnetite, ilmenite and apatite. The rock may be mugearite. Since it is very rare to find mugearite in active island arcs or in continental margins (Miyashiro, private communication), the sample can be considered to have formed in-situ, as opposed to being ice-rafted.

Experiment

^{40}Ar-^{39}Ar stepwise degassing dating was applied to the coarsely crushed samples. The sample (about 1.0 gr) which was sealed in a quartz tube (80 mm x 8ϕ) together with two standard samples (Bern 4M muscovite) were irradiated with

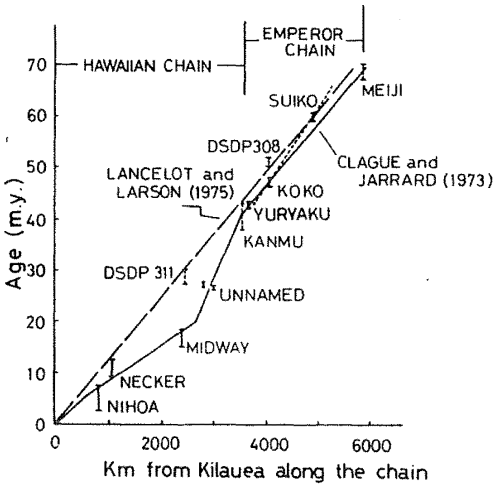

Fig. 1. ^{40}Ar-^{39}Ar apparent age spectrum (Fig. 1-a) and isochron (Fig. 1-b). Asterisk in the isotopes indicates the value corrected for the interfering Ar isotopes. The apparent age spectrum (dotted line in Fig. 1-a) is plotted with $\pm 1\sigma$ (solid line). The y-intercept in the isochron plot is 313.6 $\pm$ 2.9.

JMTR 2 reactir, which gave a total neutron flux of about 5×10^{17} with a thermal to fast neutron ratio of about 10. The following correction factors for interfering Ar isotopes were determined on K_2SO_4 and $CaCO_3$: $(^{36}Ar/^{37}Ar)_{Ca}$ = 0.00026, $(^{39}Ar/^{37}Ar)_{Ca}$ = 0.0017 and $(^{40}Ar/^{39}Ar)_K$ = 0.043. The experimental deteils were given elsewhere (Saito and Ozima, 1976). The results are shown in Figure 1-a and -b. The ^{40}Ar-^{39}Ar age was calculated from the comparison of the slope in Figure 1-b with that obtained for the standard sample. The slope was determined by means of York's method with a correlation coefficient r = 1 (York, 1969). The slope of the isochron gives 58.6 $\pm$ 0.6 m.y., in which the error indicates 1σ. Figure 1-a shows the apparent K-Ar age spectrum, which was calculated by assuming $(^{40}Ar/^{36}Ar)$ = 313.6 (asterisk indicates Ar isotopes corrected for the interfering Ar isotopes) determined as the y-intercept of the isochron in Figure 1-b. From the well defined isochron and the flat apparent age spectrum, we conclude that the age is reliable.

The conventional K-Ar age of 40.4 m.y. which was previously reported for andesite dredged from the same dredging station (Ozima et al., 1970) may reflect Ar-loss of this sample, since the sample is considerably altered. Otherwise, since andesite is very common in active island arcs, one may possibly think that the rock was rafted by ice from Kuril islands or Kamchatka. The existence of granodiorite and hornfels on Suiko seamount suggests this possibility.

Discussion

Figure 2 shows a plot of the island or seamount age (m.y.) as a function of distance (km) along the Hawaiian-Emperor chain, which was redrawn from Figure 5 in Clague and Jarrard (1973). The DSDP fossil ages (DSDP 311 and 308, Scientific Staff, 1973) and the ^{40}Ar-^{39}Ar isochron age of Suiko seamount is also included in the Figure. The solid line indicates the age progression proposed by Clague and Jarrard (1973). In drawing the age progression line, Clague and Jarrard used all the age data available to them at that time. The only criterion they used to choose the data was experimental quality. Lancelot and Larson (1975),

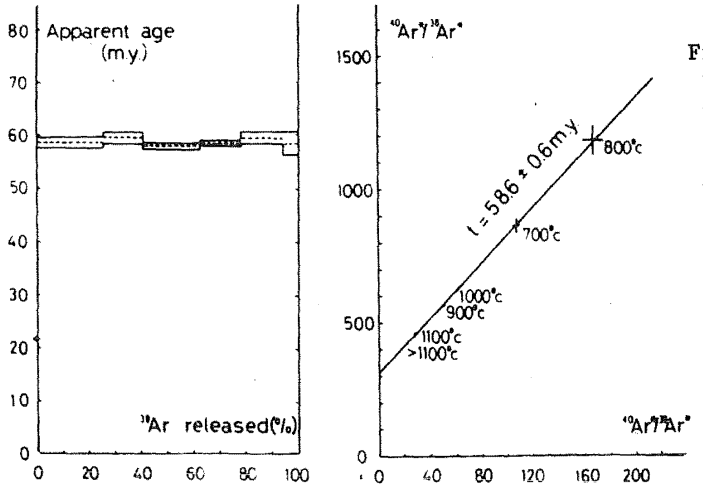

Fig. 2. Ages of volcanism from Kilauea volcano, Hawaiian-Emperor chain as a function of distance from Kilauea volcano, Hawaii. Figure is redrawn from Fig. 5 in Clague and Jarrard (1973) with additional data (DSDP 308, 311, Suiko seamount) and the two age progression lines (Lancelot and Larson, 1975, and the present work).

however, chose older ages if there were more than two ages from the same seamount or island, since recurrent volcanism may occur along seamount chains. Hence, with the use of the DSDP age data rather than the radiometric ages from Midway atoll and Koko seamount, they proposed a uniform rate for the Pacific plate movement (chain line in Figure 2). The newly obtained ^{40}Ar-^{39}Ar isochron age for Suiko seamount does not contradict either the Clague and Jarrards' (1973) or the Lancelot and Larsons' (1975) age progression lines. However, in order to obtain the age progression, the following point must be carefully considered.

If there is considerable time span for the growth of a seamount or an island, meaningful age progression can be obtained only by comparing the age of the commencement of volcanic activity in each island. Comparison of ages representing different stages in volcanic activity would not be very meaningful. It is, however, very difficult to obtain samples which are representative of the earliest volcanic activity. Hence, as a practical approach to this problem, we may compare the ages of the final stage in the volcanic activities which may be represented by the rocks dredged from the top of a seamount or from the top flow in an island. Undoubtedly such samples are of easier access. Also, fossil age data should be treated with caution, since it is in general difficult to estimate the age gap between the fossil and the underlying basement rock ages. If we take these criteria to choose age data, this leaves us with only two radiometric ages from the Emperor chain, that is, the ^{40}Ar-^{39}Ar isochron age from Suiko seamount and the concordant K-Ar ages from Koko seamount. Also the K-Ar age from Midway core may be preferable to the age given by DSDP 311, since the latter may represent the earlier stage of the volcanic activity in this part of the Hawaiian archipelago (Lancelot and Larson, 1975). This choice of age data would then suggest an even slower rate of the

Pacific plate motion for the Emperor chain, i.e., about 6 cm/y (shown by dotted line). Because of scantiness of age data, however, it is obvious that more radiometric data, preferably from the top flow in seamounts, are needed to draw a definite conclusion about the age progression of the Emperor chain.

Although in the above discussion we assumed the existence of a significant time gap between the earlier and the later stages in volcanic activity. Little is known about the time span for the growth of a seamount. It is difficult to judge whether the difference between DSDP 311 and the Midway atoll ages, and also between DSDP 308 and the Koko seamount ages do represent the age gap between the earlier and the later stage in their volcanic activities, or whether it results from uncertainties in the K-Ar ages or in the fossil ages or others.

If the age gap between DSDP 311 and Midway which is at least 10 m.y., does reflect the time span for the growth of the island, we should expect a more than 10 m.y. life time for the magma source which has formed Midway atoll and its adjacent archipelago. Such a long life of a magma source would certainly impose crucial constraint on any hot-spot model. For example, the magma source may have to be assumed to have existed in the moving plate, since it is otherwise difficult to suppose that magma has been supplied to an island or a seamount horizontally over a distance of more than 1,000 km from a source fixed in the mantle. This implies that a 'hot spot' was responsible only for supplying heat to produce a magma source in the moving plate. At any rate, the problem is still very much open to further investigation. Here, it may suffice to emphasize that the time span for the growth of a seamount has such important bearings in the understanding of the oceanic crustal structure.

References

Aoki, H. and H. Hirota (1971) Marine Science, 3, 852.

Clague, D.A. and R.D. Jarrard (1973) Geol. Soc. Amer. Bull., 84, 1135.

Lancelot, Y. and R.L. Larson (1975) (in preparation)

Morgan, W.J. (1972) Amer. Asso. Petrol. Geol. Bull., 56, 203.

Ozima, M., I. Kaneoka and S. Aramaki (1970) Earth Planet. Sci. Letters, 8, 237.

Saito, K. and M. Ozima (1976) (to be published in Amer. Geophys. Union Monograph)

Scientific Staff, Leg 32 (1973) Geotimes, Dec.,14.

Wilson, J.T. (1963) Can. J. Phys., 41, 863.

York, D. (1969) Earth Planet. Sci. Letters, 5, 359.

Rb, Sr AND $^{40}Ar/^{39}Ar$ ANALYSES OF XENOLITHIC ULTRAMAFIC ROCKS FROM THE OKI-DOGO ISLAND, JAPAN

Ichiro KANEOKA*, Shigeo ZASHU* and Eiichi TAKAHASHI**

Geophysical Institute* and Geological Institute**,
University of Tokyo, Bunkyo-ku, Tokyo 113, Japan

1. Intoduction

Some of xenolithic ultramafic rocks are considered to have been brought from the upper mantle and it is very important to study them for understanding the properties of the deep interior of the earth. In Japan, such ultramafic rocks have been rarely found and those from Itinomegata, northeastern Japan, are most famous (e.g. Aoki, 1971). Recently many ultramafic rocks, including spinel lherzolites, have been found as inclusions in alkali-olivine basalts from the Oki-Dogo Island, southwestern Japan (Takahashi, 1975). These rocks will give many important informations for understanding the properties of the upper mantle (and/or lower crust) under the Japanese Islands. In this note, we report some results on Rb, Sr contents and Ar-40/Ar-39 age studies of these rocks.

2. Samples

Samples were collected by one of us (E.T.) from Kuroshima (KRB) and Oku (OKD), eastern parts of the Oki-Dogo Island. Various types of ultramafic and mafic rocks are included as xenoliths in alkali-olivine basalts such as spinel lherzolites, dunites, wehrlites, harzburgites, etc. Samples used in this study are tabulated in Table 1.

Table 1. Xenolithic ultramafic rocks from the Oki-Dogo Island

Sample No.	Host Rock	Rock Type	Mineral Assemblage*
ET 7405 10B-10	OKD	Clino-pyroxenite	cpx≫mt> opx
ET 7405 10B-13	OKD	Lherzolite	oliv > opx≫ chromian spinel >cpx
ET 7405 10B-27	OKD	Plagioclase bearing wehrlite	oliv > cpx≫ plagio >oxide apt
ET 7405 13A-2	KRB	Lherzolite	oliv > cpx > opx> chromite ~ picotite
ET 7405 13A-18	KRB	Lherzolite	oliv > opx > cpx> chromian-spinel

* cpx: clino-pyroxene, opx: ortho-pyroxene, mt: magnetite, oliv: olivine, plagio: plagioclase, apt: apatite.

From their textures, samples 10B-13 and 10B-27 are considered to be cumulates. Samples 10B-10 and 13A-2 may also be cumulates. Sample 13A-18, however, is considered to be a block of upper mantle material from its texture and mineral assemblage.

Host rocks are alkali-olivine basalts and their formation ages were determined to be about 6 m y. and 2.5 m.y. for OKD and KRB samples respectively by K-Ar method.

Chemical analyses of major elements are given in Table 2. More details on samples and sampling localities are reported elsewhere (Takahashi, 1975).

Table 2. Analytical results of major elements in xenolithic ultramafic rocks from the Oki-Dogo Island

SAMPLE	10B-10	10B-13	10B-27	13A-2	13A-18
ROCK TYPE	CPX-NITE	LHERZOLITE	WEHRLITE	LHERZOLITE	LHERZOLITE
HOST ROCK	OKD	OKD	OKD	KRB	KRB
SiO_2	48.12	42.90		41.75	44.49
TiO_2	1.25	0.09		0.08	0.07
Al_2O_3	5.89	1.82		1.65	1.52
Fe_2O_3	3.95	1.57		2.22	1.02
FeO	6.41	8.62		11.56	7.14
MnO	0.17	0.13		0.16	0.13
MgO	16.83	41.99		40.40	42.66
CaO	15.57	2.18		1.26	2.12
Na_2O	0.55	0.17		0.13	0.10
K_2O	< 0.03	< 0.03		< 0.03	< 0.02
H_2O (-)	0.20	0.10		0.26	0.20
H_2O (+)	0.75	0.30		0.34	0.32
P_2O_5	0.09	TRACE		TRACE	TRACE
Cr_2O_3	0.27	0.37		0.37	0.34
TOTAL	100.08	100.27		100.21	100.13

(ANALYST : H. HARAMURA)

3. Rb and Sr analyses

Rb and Sr contents were measured by isotope dilution method for both xenolithic ultramafic and host basaltic rocks. K content of basalt was measured with a flame photometer with internal standard method. Analytical results are given in Table 3.

Basaltic rocks belong to alkaline-rock series and their K and Rb contents are relatively high. Sr contents are also high of the order of 800-900 ppm. These results are in good agreement with those for some basaltic rocks from the same area by H. Kurasawa (personal communication, 1975).

Xenolithic ultramafic rocks contain less Rb and Sr than ultramafic inclusions from other areas, but more than the so-called alpine-type peridotites (Fig. 1). Although their Sr contents change with the factor of about 8, their Rb contents change with the factor of only 3. Higher Sr content of sample 10B-27 probably

Table 3. K, Rb and Sr contents in xenolithic ultramafic rocks from the Oki-Dogo Island

Sample No.	K (%)	Rb (ppm)	Sr (ppm)	K/Rb	Rb/Sr
OKD	1.49±0.01	67.2±3.4	907±27	222	0.0741
KRB	1.83±0.01	48.9±0.1	798±18	374	0.0613
ET 7405 10B-10	<0.03*	0.167±0.022	14.1±2.9	<1800	0.0118
ET 7405 10B-13	<0.03*	0.288±0.011	10.0±1.9	<1040	0.0288
ET 7405 10B-27	----	0.431±0.005	44.5±3.0	---	0.00969
ET 7405 13A-2	<0.03*	0.283±0.059	5.86±0.22	<1060	0.0386
ET 7405 13A-18	<0.02*	0.382±0.024	7.77±0.95	<524	0.0491

* These values are taken from Table 2.
N.B. Each value in content is given as an averaged one for at least replicate analyses.

reflects the existence of plagioclase in this rock. From its texture and mineral assemblage, sample 13 A-18 is considered to be of upper mantle origin. However its Rb and Sr contents are not so different from those of other rocks which might be cumulates.

The relation between these rocks and host rocks may be more clarified with their Sr-87/Sr-86 ratios, which is now being studied.

Fig. 1. Rb and Sr contents in some ultramafic rocks.

+ Alpine-type peridotites
○ Ultramafic inclusions
△ Ultramafic zones in stratiform sheets
} Stueber & Murthy (1966)
● This study

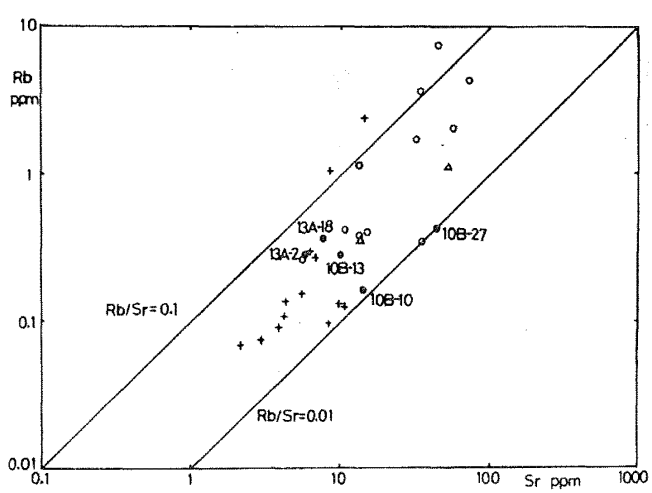

4. $^{40}Ar/^{39}Ar$ age studies

Ultramafic rocks generally contain excess Ar and conventional K-Ar method is invalid for evaluating the formation age of these rocks. As shown in the previous section, their Rb and Sr contents and Rb/Sr ratios are low and it is very difficult to apply Rb-Sr method for dating such rocks except for very old rocks. Although even Ar-40/Ar-39 method cannot always determine the definite formation age of these rocks, it can give the reasonable upper limit or proper estimate of its formation age in favourable cases (Kaneoka, 1974).

Samples were wrapped in Al foil and irradiated with fast neutrons of the order of 10^{18} nvt in the JMTR reactor. Ar was degassed for one hour at each temperature, which was measured with an optical pyrometer. After necessary corrections are made, Ar-40/Ar-39 ages are calculated, assuming that all Ar-36 observed is the component of present-day atmospheric Ar, whose Ar-40/Ar-36 ratio is 295.5 (Nier, 1950). Although this assumption may not always be valid (Kaneoka, 1975), its effect will be not so serious to get general age patterns.

An example for sample 10B-27 is given in Fig 2. Since Ar-40/Ar-36-Ar-39/Ar-36 plot also gives good informations, this representation is adopted with a conventional age-fraction of Ar-39 released plot.

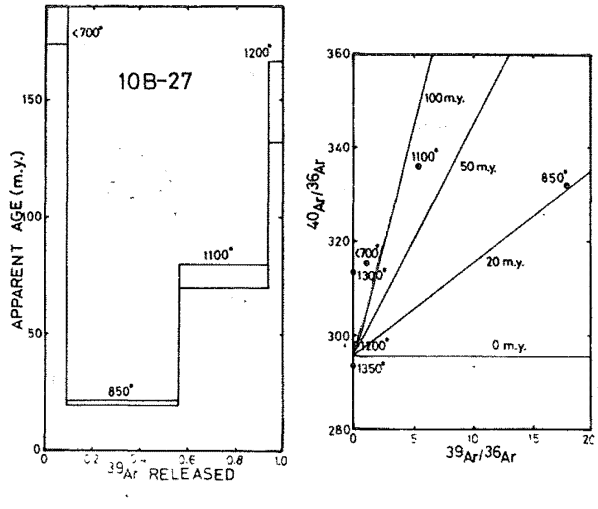

Fig.2. $^{40}Ar/^{39}Ages$ of sample 10B-27.
In the left figure, the height of each rectangle corresponds to 2 σ error range. The number in the figure indicates the temperature in degrees C.

As shown in Fig 2, the apparent Ar-40/Ar-39 ages are high at low and high temperatures and the minimum age is observed at intermediate temperature, which typically represents the existence of excess Ar-40 in both retentive and unretentive trapping sites (Kaneoka, 1974). The minimum age is about 21 m y.. Since only 850°C fraction gives this age, it should be regarded to represent the upper limit of its formation age. As shown in the Ar-40/Ar-36-Ar-39/Ar-36 plot, 1300°C fraction still shows a little high Ar-40/Ar-36 ratio of about 309, indicating the existence of excess Ar-40 in this fraction.

This is more clearly shown in Fig 3. Ar-40* (radiogenic component) has two peaks at 1100°C and 1300°C fractions, which is different from the release pattern of Ar-40 (total). Fig. 3 also indicates the clear difference of the degassing temperature between K-derived Ar-39 and Ca-derived Ar-37, the former is degassed at lower temperatures, while the latter at higher temperatures. The release patterns of Ar-39 and Ar-40* are much different, which also indicates that most Ar-40* is not in-situ originated.

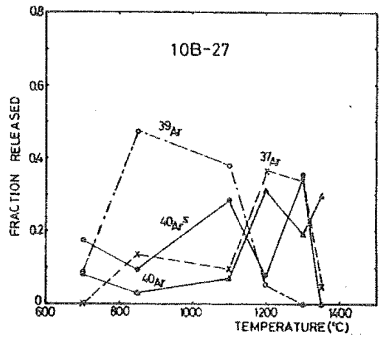

Fig 3. Release patterns of Ar for sample 10B-27.

$^{40}Ar^*$: radiogenic component.

^{40}Ar : total Ar-40.

Since the release pattern of Ar-36 is similar to that of Ar-40, it is not included in the figure.

From the amount of Ar-39, K content can be estimated to be about 370 ppm for sample 10B-27. This is more abundant than those of other samples (10B-10, 67 ppm; 10B-13, more than 90 ppm; 13A-2, 220 ppm), which may also reflect the existence of plagioclase in this sample.

As for the release patterns of ages, similar results are obtained for the other samples, though the minimum ages are different (10B-10, 56 m.y.; 10B-13, 330 m.y.; 13A-2, 39 m y.). However, 850°C fraction was accidentally lost from the line during the purification procedure of gases for sample 10B-13. This is probably the main reason for its relatively high minimum age. Unfortunately, no result was obtained for sample 13A-18 due to insufficient degassing procedures.

From these results, it is concluded that radiogenic Ar-40 observed in xenolithic ultramafic rocks with the amount of about $(1-4)\times10^{-7}$ ccSTP/g is mostly excess Ar. Their formation ages would be less than 20-30 m.y., which is not incompatible with the geological environments in this area.

5. Summary

Rb and Sr contents in xenolithic ultramafic rocks from the Oki-Dogo Island are less abundant than those of ultramafic inclusions from other areas studied by Stueber & Murthy (1966), but more than those of alpine-type peridotites. These rocks might be formed less than 20-30 m.y. ago, but contain some amount of excess Ar-40.

References

Aoki, K (1971) Cont. Min. Petrol., 30, 314.

Kaneoka, I. (1974) Earth Planet. Sci. Lett., 22, 145.

Kaneoka, I. (1975) Geochem. J., 9, 113.

Nier, A. O. (1950) Phys. Rev., 77, 789.

Stueber, A. M. and V. R. Murthy (1966) Geochim. Cosmochim. Acta, 30, 1243.

Takahashi, E. (1975) J. Geol. Soc. Japan, 81, 81.

RARE GAS FRACTIONATION PATTERNS IN TERRESTRIAL SAMPLES AND THE EARTH-ATMOSPHERE EVOLUTION MODEL

Minoru OZIMA* and E. Calvin ALEXANDER, Jr.

Department of Geology and Geophysics, University of Minnesota
Minneapolis, Minnesota 55455, U. S. A.

Introduction

Studies of the elemental and isotopic ratios of the rare gases in the earth have proven to be a significant source of information about the earth-atmosphere evolution process. A pioneering example is Brown's (1952) work which called attention to the enormous depletion, relative to the solar abundances, of the rare gases in the terrestrial atmosphere. Brown argued that the depletion suggested that the earth's atmosphere was formed by the degassing of the solid earth, i.e. that the earth's atmosphere is secondary. A secondary origin of the atmosphere is also suggested by the ^{40}Ar inventory in the earth (Schillibeer and Russell, 1954; Damon and Kulp, 1958; Turekian, 1959; Wasserburg, 1964), since ^{40}Ar from the decay of ^{40}K in the earth is more than sufficient to account for ^{40}Ar in the present atmosphere.

Isotopic evidence of radiogenic rare gases imposes important time constraints on the evolution of the earth-atmosphere system. For example, Boulos and Manuel (1971) have found radiogenic ^{129}Xe in a natural gas which, they conclude, indicates that the earth was degassed within a few half lives of ^{129}I ($t_{1/2}$ = 17 m.y.). Using the $^{40}Ar/^{36}Ar$ regime in the earth, Ozima (1975) reached the same conclusion that the degassing of the earth occurred within a few hundred million years after the formation of the earth.

Additional information about the earth-atmosphere evolution process can be obtained by examining the elemental ratios of the rare gases in various terrestrial materials. Two distinct patterns of primordial rare gases have been found in the solar system (Signer and Suess, 1963): A solar component, which is associated with the direct implantation of the solar wind into grain surfaces; and a planetary component, which was apparently trapped in solid grains during the condensation of the solar nebula. The abundance pattern in the atmosphere is very close to the planetary pattern except that Xe appears to be depleted by about a factor of 10 in the atmosphere by adsorption onto sediments (Canalas et al., 1968; Fanale and Cannon, 1971).

Dymond and Hogan (1973) have reported elemental abundances of rare gases extracted from the glassy rims of submarine basalts which are markedly different from the atmospheric abundances. They argue that these gases represent samples of rare gases in the mantle and resemble the solar abundance pattern rather than the atmospheric pattern. They, therefore, conclude that the evolution of the mantle and atmosphere have been "decoupled". In a series of papers Fisher (1970, 1973, 1974) has also reported the existence of primordial rare gases in glassy rims of submarine basalts, but argues that the gases resemble the planetary pattern rather than the solar pattern. Fisher's last paper includes Dymond and Hogan's data.

If the glassy rims of submarine basalts do contain samples of mantle derived rare gases, then these samples may be fractionated since the basalts themselves are a fractionated sample of the mantle. While Dymond

and Hogan and Fisher explicitly recognized the possibility that the gases they report represent fractionated samples of the mantle and/or atmospheric reservoirs, they discuss the fractionation in terms of Henry's law solubility (Blander et al., 1959) (which is clearly inadequate to explain a portion of the data, see Ozima and Alexander, 1975, in this volume). Both groups then proceed to discuss their data in terms of mixtures of various hypothetical reservoirs in a manner which partially ignores fractionation effects. Until the fractionation is understood and corrected for, any inference concerning the composition of the original reservoir is suspect.

The purpose of the present paper is to examine all of the available data on the rare gas abundances in terrestrial material in an attempt to define empirically the types of fractionations which occur. Using the fractionations so defined, we can then draw inferences concerning the composition of the mantle rare gases. We also discuss a misconception of the behavior of Henry's law solubility which has been widely quoted in the literature.

Observed Abundance Patterns

The shaded regions in Fig. 1 show the abundance patterns of rare gases for all of the analyses of terrestrial materials currently available in the literature (Mazor and Wasserburg, 1965; Bogard et al., 1965; Canalas et al., 1968; Bennett and Manuel, 1970; Mazor, 1972; Mazor and Fournier, 1973; Dymond and Hogan, 1973; Hennecke and Manuel, 1975a, 1975b; Sherrill, 1975). Since He can easily escape from the earth's gravitational field, He data is not included in the compilation. The only selection criterion we used was that sufficient data be available to allow the calculation of the ^{22}Ne, ^{36}Ar, ^{84}Kr and ^{130}Xe contents of each sample. This criterion, however, eliminates all of Fisher's (1970, 1973, 1974) data and Phinney's (1972) data and part of Canalas et al.'s (1968) data due to the absence of Ne data. The rare gas abundance data are plotted using a fractionation factor F^m:

$$F^m = \frac{(^mX/^{36}Ar)_{sample}}{(^mX/^{36}Ar)_{air}} \quad . \qquad 1.$$

Equation 1 is similar to the fractionation factor proposed by Canalas et al. except that we have chosen to normalize to

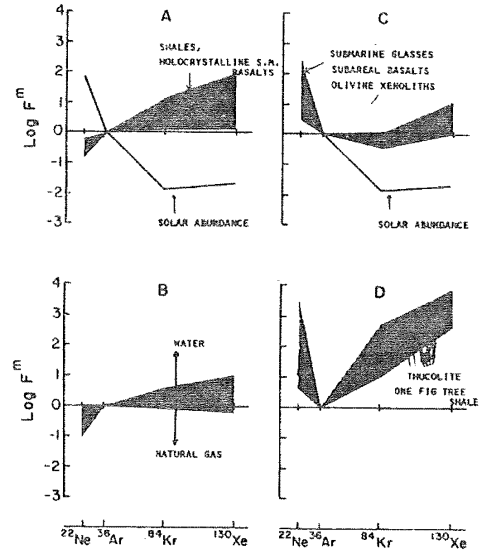

Fig. 1. Terrestrial rare gas fractionation patterns. All availabe terrestrial rare gas data yield fractionation patterns which plot in the shaded regions. A sample containing gas of atmospheric composition will plot as a horizontal line at log $F^m = 0$. The solar abundance pattern is shown by the solid lines in Figs. 1A and 1C. Figs. 1A and 1B define the Type 1 pattern which is dominated by the pattern established by the absorption of atmospheric rare gases into water. The pattern formed by absorption of atmospheric gases into water at 20°C is shown by the line in Fig. 1B. Fig. 1C defines the Type 2 pattern. Fig. 1D defines the Type 3 pattern.

^{36}Ar in the atmosphere instead of ^{130}Xe in the solar abundance. The reason for this change will become clear below.

As can be seen in Fig. 1 rare gas abundance patterns in terrestrial materials can be divided into three types:

Type 1. Figs. 1A and 1B demonstrate the first type of fractionation pattern. This Type 1 pattern is characterized by a depletion of Ne and an enrichment of Kr and Xe relative to ^{36}Ar when compared to atmospheric abundances. The Type 1 pattern is similar to, and includes the pattern produced by the solubility of atmospheric rare gases in water (Mazor and Fournier, 1973). The water solubility pattern is shown as the line in Fig. 1B. The shaded region of Fig. 1A contains four of the five analyses of Fig Tree shale (Canalas et al., 1968) and three analyses of holocrystalline submarine basalts (Dymond and Hogan, 1973). The shaded region of Fig. 1B includes all of the available data on rare gases in natural gases and waters (Mazor and Wasserburg, 1965; Bennett and Manuel, 1970; Mazor, 1972; Mazor and Fournier, 1973) with the exception of datum #10 in Mazor and Fournier.

Type 2. Fig. 1C demonstrates the second type of fractionation pattern. This Type 2 pattern is characterized by an enrichment of Ne and Xe and a slight depletion of Kr relative to ^{36}Ar when compared to atmospheric abundances. The shaded region in Fig. 1C contains Dymond and Hogan's (1973) analyses of the quenched rims of submarine basalts and Hennecke and Manuel's (1975a, 1975b) analyses of a subareal basalt and a Hawaiian olivine xenolith which contained liquid CO_2 inclusions. The Type 2 pattern is shown in greater detail in Fig. 2. In Fig. 2 the shaded region is defined by Dymond and Hogan's analyses. Henneke and Manuel's analyses are shown as the stars and triangles. The filled circles show Kirsten's (1968) data for the solubilities of rare gases in molten enstatite at 1500°C. It should be emphasized that Kirsten only measured the solubilities of He, Ne, and Ar and the data he lists for Kr and Xe are theoretical extrapolations.

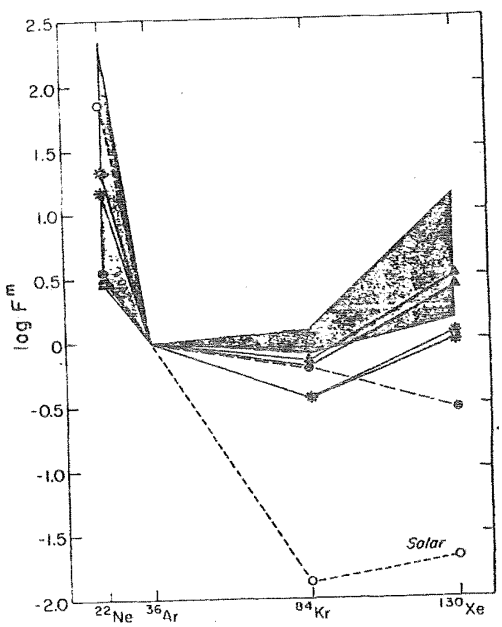

Fig. 2. An expanded view of the Type 2 pattern. The shaded region contains Dymond and Hogan's (1973) analyses of the quenched rims of submarine basalts. The data shown as stars are from Hennecke and Manuel's (1975a) analyses of a subareal basalt. The data shown as triangles are from Hennecke and Manuel's (1975b) analyses of an olivine xenolith which contained liquid CO_2 filled inclusions. The filled circles show the pattern which is obtained by combining Kirsten's (1968) data on the solubility of rare gases in molten enstatite at 1500°C with the partial pressure of each rare gas present in the atmosphere. The open circles show the solar pattern.

There is clear isotopic evidence that the Type 2 pattern does not represent fractionated gases of atmospheric isotopic composition. All of these samples yield $^{40}Ar/^{36}Ar$ ratios higher than the atmospheric value. The Hawaiian olivine xenolith contains excess radiogenic ^{129}Xe and Lupton and Craig (1975) have recently shown that the quenched rims of submarine basalts contain He with a $^{3}He/^{4}He$ ratio higher than the atmospheric value. These rocks therefore, contain samples of non-atmospheric rare gases, probably fractionated, presumably from the source regions of the rocks, i.e. the mantle.

Type 3. Fig. 1D demonstrates the third type of fractionation pattern. This Type 3 pattern is characterized by large enrichments of Ne, Kr and Xe relative to ^{36}Ar when compared to atmospheric abundances. The shaded region of Fig. 1D contains rare gas data from thucolite (Bogard et al., 1965; Sherrill, 1975) and from Fig Tree sample #4 (Canalas et al., 1968). Sherrill's recent work gives the results of a step-wise heating analysis of thucolite. The temperature release patterns Sherrill obtained for Ne and ^{36}Ar are very different from those he obtained for Kr and Xe. 83.7% of the total Xe and 77% of the total Kr are released at 250°C and an additional 15.5% of the Xe and 4% of the Kr are released at 400°C. In comparison only 22% of the Ne and 14% of the ^{36}Ar are released by 400°C and the maximum fractional releases occur at 1800°C.

None of the three types of patterns are very close to the solar abundance pattern (Cameron, 1973) which is shown as the lines in Figs. 1A and 1C.

Type 1. It is clear that the Type 1 pattern is dominated by rare gas fractionations established by the low temperature absorption of rare gases from the atmosphere into water. The rare gas abundances in shales and natural gases should be similar to those observed in water since shales must have occuluded considerable amounts of (sea) water during formation and natural gases seem to contain mainly recycled ground water (Bodversson and Lawall, 1972). The D/H and $^{18}O/^{16}O$ isotopic ratios in geothermal steam (Craig, 1963) suggest a similar origin. The shales tend to be even more enriched in the heavier gases than water which probably indicates a preferential retention of the heavier gases in the shales.

Dymond and Hogan's (1972) holocrystalline basalt data display a Type 1 pattern which is consistent with equilibration with the rare gases dissolved in sea water - as they point out. This is in agreement with the mass of experimental evidence (C.F. Irving, 1970; Corliss, 1971) that holocrystalline submarine basalts interact extensively with sea water. The Type 1 pattern is not consistent, however, with Henry's law solubilities (see below) which is the context in which Dymond and Hogan and Fisher have discussed their data.

Type 2. The samples containing gases displaying the Type 2 pattern are potentially the most valuable since there is clear isotopic evidence that these samples contain non-atmospheric rare gases. The gases in these rocks, however, have been subjected to many, at least potentially fractionating situations during: (1) the formation of the parent magmas in the mantle, (2) the transportation of that magma to the near surface, and (3) the eruption or emplacement of the magmas in the near surface environment.

It is clear as a first order observation, that gases with the Type 2 abundance pattern cannot have been a quantitatively important input into the atmosphere if the atmosphere is conservative of Ne as is normally assumed. The Ne abundance in the atmosphere would be much higher if the Type 2 pattern had contributed significantly.

Dymond and Hogan (1973) argue that the Type 2 pattern as displayed in their analyses of the quenched rims of submarine basalts indicates the presence of solar primordial gases in the mantle. Their argument is based

mainly on the $^{20}Ne/^{36}Ar$ ratios observed in the quenched rims which are similar to the solar values and higher than the atmospheric or planeatry values. Fisher (1974) argues that these same data indicate the presence of "planetary" primordial gases in the mantle. Fisher's argument is based on the Kr/Xe and $^{36}Ar/Kr$ ratios but ignores the Ne data.

We feel that the Type 2 pattern represents a fractionated samples of "planatary" primordial gas from the mantle. Hennecke and Manuel's (1975b) analyses of a Hawaiian olivine xenolith present the simplest case since the rare gases in the analyses were presumably contained in liquid CO_2 filled inclusions within the xenolith. These inclusions should have avoided fractionations during eruptions and may have avoided fractionations during transport from the mantle. As Hennecke and Manuel point out, and as is shown in Fig. 2, the rare gas pattern in the xenolith agrees well with the pattern obtained by combining Kirsten's (1968) enstatite solubility data with the atmospheric abundances except that Xe is enriched by about a factor of ten in the xenolith. Hennecke and Manuel conclude that the elemental ratios of nonradiogenic Ne, Ar and Kr in the mantle are very near to the atmospheric values but that the Xe/Kr ratio is $\sim$10 times higher than the atmospheric value — i.e. that the mantle contains "planetary" gas. The upturn in the Type 2 pattern at Xe is, therefore, an artifact of our normalization to the atmosphere which is depleted in xenon.

While qualitatively similar to the xenolith patterns, the Type 2 patterns from the basalts show much higher enrichments in Ne than do the xenolith patterns. We offer the following model as a possible explanation of the large Ne (and He) enrichments relative to Ar and the heavier rare gases. We assume that the rare gas patterns recorded in the basalts are representative of the patterns present in their parent magmas and that the fractionations occurred during the generation of the magmas in the mantle. This assumption seems justified since the gases trapped in these rapidly cooled eruptive rocks, particularly the glassy rims of the submarine basalts, would not have had time to undergo significant fractionationd during eruption. Although the generation of magma is still poorly understood, we follow the general assumption that basaltic magmas represent partial melts of the upper mantle and form when a decrease in pressure causes the solidus to fall below the existing thermal gradient. Since the rare gases should be more soluble in the liquid than the residual solids there should be an inflow of gases from the residual solids to the magma. The atomic abundance ratio of Ne/Ar in the diffusing inflow would be proportional to the ratio of their diffusivities, D_{Ne}/D_{Ar}. The ratio of the diffusivities is not proportional to the square root of the ratio of the masses as is normally assumed.

The diffusivities of rare gases through mantle materials at the relevant temperatures and pressures are not known. However, Perkins and Begeal (1971) and Perkins (1973) have reported data for rare gas diffusivities through SiO_2 glass at 1000°C. While the mantle clearly is not made of SiO_2 glass at 1000°C, in the absence of more relevant data, the SiO_2 glass data will perhaps serve to illustrate the phenomenology of our model.

The rare gases in the magma should be a composite of the inflowing rare gases and those originally contained in the material melted to form the magma. Perkins and Begeal (1971) report that the diffusivity, and permeability of Ne through SiO_2 glass is about three orders of magnitude greater than Ar at 1000°C. We should expect therefore that the rare gases in the magma should show a progressive and large enrichment of the lighter gases relative to the bulk composition of the mantle gases. Such a trend is demonstrated in the Ne/Ar ratio in the Type 2 pattern.

The Ar/Kr and Kr/Xe ratios are not progressively enriched in the Type 2 pattern, however. This is because the absolute value of the diffusivity is as important as its relative value. As stated above, the relative value of D_{Ne} is about three orders of magnitude greater than D_{Ar} at 1000°C. The value of D_{Kr} and D_{Xe} are presumably progressively smaller but no data exists. (The permeability of Kr through silicate glass at 1000°C is ∿100 times smaller than the Ar permeability (Perkins and Begeal, 1971).) The mean diffusing length, $\sqrt{2Dt}$, is about 100 meters for Ne in silicate glass at 1000°C in a million years. The mean diffusing length is only 3 meters for Ar in a similar situation and is presumably shorter for Kr and Xe. Ne (and He) diffusion into the magma will be significant and result in enormous enrichments, whereas diffusion of the heavier rare gases are insignificant. The abundance pattern of the heavy rare gases should be dominated by bulk melting and will be similar to the abundance pattern in the original mantle rocks. The apparent Xe enrichment in the Type 2 pattern is, therefore, again an artifact of normalization which indicates that the mantle Xe/Kr ratio is ∿10 times the atmospheric value.

The recent report by Fisher (1975) of high radiogenic $^{4}He/^{40}Ar$ ratios in the quenched rims of submarine basalts follows naturally from our model and does not require the anomalous K/U ratios postulated by Fisher. Mass balance requires that the solid residue from the partial melting be depleted in light gases relative to the heavier gases. Gramlich and Naughton (1972) have shown that lherzolite nodules, which they conclude represent unfused residue from the partial melting process, contain $^{4}He/^{40}Ar$ ratios which are lower than reasonable.

Fig. 2. demonstrates that in order to explain the abundance pattern in the quenched rims of the submarine basalts as fractionated gas of solar composition one must postulate a two order of magnitude enrichment of Kr and Xe relative to Ar and Ne or a two order of magnitude depletion of Ar and Ne relative to Kr and Xe.

Type 3. The origin of the Type 3 pattern is not clear. Sherrill's (1975) data indicates that the Type 3 pattern may be a hybrid pattern with the Kr and Xe dominated by low temperature adsorption while the Ne and Ar are dominated by a high temperature component. The Type 3 pattern is only represented by a rare mineral and one analysis of shale, and it may not be very important quantitatively. Phinney's (1972) shale data lie in the heavy gas portion of the Type 3 pattern, however, and the Type 3 pattern may prove to be significant as more data accumulate.

Discussion

Ideally one would take the observed rare gas abundance patterns and correct for fractionation effects to calculate the abundance pattern in the mantle. The almost complete absence of the relevant distribution coefficients, solubilities, diffusion parameters, adsorption parameters, etc., however, prevent such a direct approach. The works of Fanale and Cannon (1971) and Kirsten (1968) represent the preliminary attempts to obtain the relevant parameters. We are therefore restricted to semi-quantitative "consistency" arguments. We have shown that the rare gas abundance patterns observed in terrestrial materials are consistent with a simple earth-atmosphere evolutionary model. The essential assumptions in this model are: (A) the present terrestrial atmospheric rare gases closely approximate the total rare gas inventory in the earth with the notable exception of Xe and (B) the rare gases in the mantle, which represent only a small fraction of the earth's total inventory, have an abundance pattern roughly similar to that present in the atmosphere, again with the exception of Xe. There seems to be growing evidence to support the first assumption (Fanale, 1971) particularly those based on the ^{40}Ar inventory (Turekian, 1959) and the $^{40}Ar/^{36}Ar$ regime in the earth (Ozima,

1975). There are however, contradictory views about the second assumption (Dymond and Hogan, 1973; Fisher, 1974). Part of this apparent contradiction stems from an incomplete understanding of how the various fractionations influence the data.

Fig. 3A shows a Kr/Xe versus $^{36}Ar/Kr$ diagram which has been used extensively (Fisher, 1970, 1973, 1974; Phinney, 1972; Dymond and Hogan, 1973; Hennecke and Manuel, 1975) to interpret rare gas data from terrestrial samples. The solid line has a slope of 0.83 and is the empirical line which Fisher and Phinney maintain describes the locus of samples fractionated from an atmospheric reservoir. The dashed line has a slope of 1.20 and is the line which Dymond and Hogan draw to represent the same fractionation process. All of these workers discuss their lines in terms of Blander et al.'s (1959) thermodynamic model for the solubility of rare gases in molten fluorides even though Blander et al.'s data and model indicate that the light gases are more soluble than the heavy gases. Only the upper right hand portions of the lines are even potentially explainable using Blander et al.'s model (see Ozima and Alexander, 1975, in this volume). In addition, estimates of the slope of that line segment vary from 0.5 to 2.4 depending on which value for the atomic radii of the rare gases one chooses.

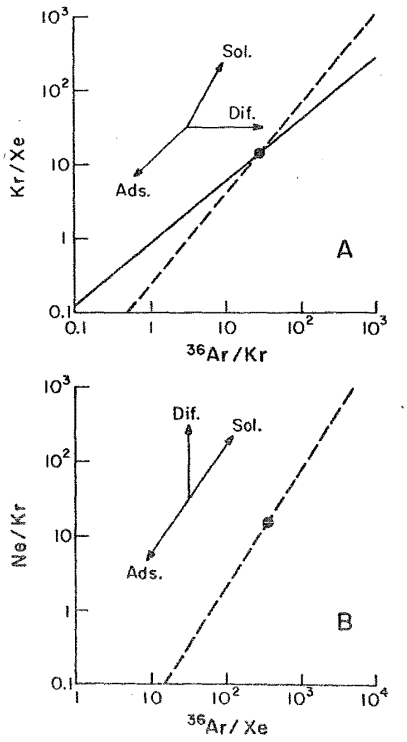

Fig. 3. The general directions that fractionation process move rare gas ratios on Kr/Xe versus $^{36}Ar/Kr$ and Ne/Kr versus $^{36}Ar/Kr$ plots. The solid point is the atmospheric composition. The solid line in Fig. 3A has the slope used by Fisher (1970, 1973, 1974) and Phinney (1972) and the dashed line in Figs. 3A and 3B have the slopes adopted by Dymond and Hogan (1973). The unit vectors vectors show the general directions that high temperature solubility (Sol.), low temperature adsorption (Ads.) and diffusion (Dif.) will move data on the diagrams. The Dif. vector shows the direction that the fractionation of gases diffusing into a sample will move data on the diagrams. Diffusion of gases out of the sample will move points in the opposite direction.

At least three fundamentally different process fractionate gases and therefore move the locus of points on diagrams such as Fig. 3A. These processes are : 1) high temperature solubility, 2) low temperature adsorption and 3) diffusion. The general directions which these processes move points are shown by unit vectors in the upper left hand portion of Fig. 3A. The direction shown for the diffusion vectors are for gases diffusing into a sample. Diffusion out of a sample will move a point the opposite direction. We emphasize that these are general directions only. The locus of data produced by each process is probably a broad triangular sector whose apex is the atmosphere point. At this stage, however, we have no good of estimating how broad the sectors are.

Fig. 3B shows a Ne/Kr versus $^{36}Ar/Xe$ diagram which Dymond and Hogan have used in a manner analogous to Fig. 3A. The comments and objections that apply to the line in Fig. 3A are equally valied to Fig. 3B except that diffusion moves the data in a different direction in Fig. 3B.

While diagrams similar to Figs. 3A and 3B are perhaps useful formats to display data, it simply is wrong to maintain that any line drawn through the atmosphere point on the diagrams described the locus of all samples produced by known fractionation processes from a reservoir of atmospheric composition. We recommend that the use of such lines be abandoned or at least that their meanings (if any) be defined much more carefully.

All three of the fractionation processes discussed above are capable of producing large effects and it is likely that many individual samples contain gas modified by more than one of the processes. We wish to emphasize that none of the fractionation processes depend on $(M_1/M_2)^{1/2}$ as is normally assumed in the theoretical discussions of rare gas fractionations. The fractionations are complicated and largely unknown functions of the atoms' radius, polarizability, etc. and very large differential fractionations are the rule rather than the exception. Attempts to estimate the rare gas abundances in the earth on the basis of the trapped rare gases in rocks should proceed with extreme caution therefore. These fractionation effects, however, should not produce large isotopic effects since the effective radius of the isotopes should be very similar (with the possible exception of $^3He/^4He$). The isotopic composition of rare gases in the solid earth is therefore, much more amenable to experimental attack.

Summary

A. Rare gas abundance data currently available for terrestrial samples define three distinct types of fractionation patterns: Type 1, characterized by a progressive enrichment of the heavier gases; Type 2, characterized by a large enrichment of Ne and a slight apparent enrichment of Xe and Type 3, characterized by large enrichments of Ne, Kr and Xe relative to Ar.

B. The Type 1 pattern, which is represented by the rare gases contained in shales, natural gases, holocrystalline submarine basalts, and natural waters, is produced by the low temperature adsorption of rare gases from the atmosphere - usually via sea water.

C. The Type 2 pattern, which is defined by the rare gases contained in the quenched rims of submarine basalts, a subareal basalt, and an olivine xenolith from Hawaii, is produced by a combination of high temperature solubility and diffusion and bulk melting in the mantle.

D. The Type 3 pattern, which is defined by a single shale analysis and by the rare gases in thucolite, is not completely understood but may represent a hybrid pattern.

E. All of the data are consistent with fractionations from reservoirs of atmospheric elemental composition except that Xe is about a factor of 10 more abundant (relative to the other gases) in the mantle than in the atmosphere.

If future rare gas data substantiate the proposed classification of rare gas fractionation patterns in terrestrial materials, the earth-atmosphere evolution model assumed above will be on a firmer basis. The continued study of rare gas abundance patterns in terrestrial materials, therefore, can yield important constraints on the theories of the origin of the atmosphere. Data on all four of the heavy rare gases, however, is necessary to distinguish the various fractionation patterns.

References

Bennett, G.A., and O.K. Manuel (1970) Geochim. Cosmochim. Acta., 34, 593.
Blander, M., W.R. Grimes, N.V. Smith, and G.M. Watson (1959) J. Phys. Chem., 63, 1164.
Bodvarsson, G., and R.P. Lawall (1972) J. Geophys. Res., 77, 4472.
Bogard, D.D., M.W. Rowe, O.K. Manuel, and P.K. Kuroda (1965) J. Geophys. Res., 70, 1965.
Boulos, M.S., and O.K. Manuel (1971) Science, 174, 1334.
Brown, H. (1952) The Atmosphere and the Earth and the Planets (Univ. of Chicago Press, Chicago).
Cameron, A.G.W. (1973) Space Sci. Rev., 15, 121.
Canalas, R.A., E.C. Alexander, Jr. and O.K. Manuel (1968) J. Geophys. Res., 73, 3331.
Corliss, J.B. (1971) J. Geophys. Res., 76, 8128.
Craig, H. (1963) Nuclear Geology in Geothermal Area (Spolato Italy), 17.
Damon, P.E., and J.L. Kulp (1958) Geochim. Cosmochim. Acta, 13, 280.
Dymond, J., and L. Hogan (1973) Earth Planet. Sci. Lett., 20, 131.
Fanale, F.P. (1971) Chem. Geol., 8, 79.
Fanale, F.P., and W.A. Cannon (1971) Earth Planet. Sci. Lett., 11, 362.
Fisher, D.E. (1970) Earth Planet. Sci, Lett., 9, 331.
Fisher, D.E. (1973) Nature, 244, 344.
Fisher, D.E. (1974) Geophys. Res. Lett., 1, 161.
Fisher, D.E. (1975) Nature, 256, 113.
Gramlich, J.W., and J.J. Naughton (1972) J. Geophys. Res., 77, 3032.
Hennecke, E.W., and O.K. Manuel (1975a) Nature (in press).
Hennecke, E.W., and O.K. Manuel (1975b) preprint.
Irving, E. (1970) Can. J. Earth Sci., 7, 1528.
Kirsten, T. (1968) J. Geophys. Res., 73, 2807.
Lupton, J.E., and H. Craig (1975) Earth Planet. Sci. Lett., 26, 133.
Mazor, E. (1972) Geochim. Cosmochim. Acta, 36, 1321.
Mazor, E., and R.O. Fournier (1973) Geochim. Cosmochim. Acta, 37, 515.
Mazor, E., and G.J. Wasserburg (1965) Geochim. Cosmochim. Acta, 29, 443.
Ozima, M. (1975) Geochim. Cosmochim. Acta, 39, 1127.
Perkins, W.G. (1973) J. Vac. Sci. Tech., 10, 543.
Perkins, W.G., and D.R. Begeal (1971) J. Chem. Phys., 54, 1683.
Phinney, D. (1972) Earth Planet. Sci. Lett., 16, 413.
Schillibeer, H.A., and R.D. Ruseell (1954) Ceochim. Cosmochim. Acta, 8, 16.
Signer, P., and H.E. Suess (1963) Earth Science and Meteoritics (New York), 241.
Sherrill, R.D. (1975) J. Geophys. Res. (preprint submitted to)
Turekian, K.K. (1959) Geochim. Cosmochim. Acta, 17, 37.
Wasserburg, G.J. (1964) The Origin and Evolution of Atmospheres and Oceans (New York) 83.

(Submitted to Rev. Geophys. Space Phys.)

* On leave of absence from the Geophysical Institute, University of Tokyo, Tokyo, 113, Japan.

SOME COMMENTS ON RARE GAS SOLUBILITY IN LIQUID

Minoru OZIMA* and E. Calvin ALEXANDER,Jr.

Department of Geology and Geophysics, University of Minnesota
Minneapolis, Minnesota 55455, U. S. A.

The sorption of rare gas atoms (i) into a melt can be expressed as:

$$C_i = P_i \cdot K_i \quad (1)$$

where C_i is the concentration of the rare gas sorbed, P_i is the partial pressure of a gas present during sorption. From thermodynamic considerations, Blander et al. (1959) showed that K_i, the Henry constant, can be expressed as:

$$K_i = a \exp(-br_i^2) \quad (2)$$

where a and b are the functions of the melt and r_i are the effective radii of rare gas atoms. From Eq. (1) and (2) the following relation for the set of i and j rare gas atoms can be derived:

$$\ln(C_i/C_j) = \ln(P_i/P_j) - b(r_i^2 - r_j^2) \quad (3)$$

Similarly for the set of k and i rare gas atoms,

$$\ln(C_k/C_i) = \ln(P_k/P_i) - b(r_k^2 - r_i^2) \quad (4)$$

From Eq. (3) and (4) we have:

$$\frac{\ln(C_i/C_j) - \ln(P_i/P_j)}{\ln(C_k/C_i) - \ln(P_k/P_i)} = \frac{r_i^2 - r_j^2}{r_k^2 - r_i^2} \quad (5)$$

Substituting Kr, Xe, ^{36}Ar for i, j, k atoms and letting P_i, P_j, P_k be the partial pressures of the rare gases in the atmosphere, we have the following expression from Eq. (3) and (4):

$$\ln(C_{Kr}/C_{Xe}) - \ln(P_{Kr}/P_{Xe}) = -b(r_{Kr}^2 - r_{Xe}^2) \quad (6)$$

$$\ln(C_{36Ar}/C_{Kr}) - \ln(P_{36Ar}/P_{Kr}) = -b(r_{36Ar}^2 - r_{Kr}^2) \quad (7)$$

From Eq. (5) we have:

$$\frac{\ln(C_{Kr}/C_{Xe}) - \ln(P_{Kr}/P_{Xe})}{\ln(C_{36Ar}/C_{Kr}) - \ln(P_{36Ar}/P_{Kr})} = \frac{r_{Kr}^2 - r_{Xe}^2}{r_{36Ar}^2 - r_{Kr}^2} \quad (8)$$

Eq. (8) was first derived by Fisher (1970). From Eq. (8) it follows that the data for rare gases sorbed in a melt which is equilibrated with the atmosphere must lie on a straight correlation line on a $\ln(C_{Kr}/C_{Xe}) - \ln(C_{36Ar}/C_{Kr})$ diagram, the correlation line being called a melt line (Phinney, 1972) or an air equilibration line (Dymond and Hogan, 1973). The distribution of the data for the samples upon the melt line is determined by Eq. (3) and (4).

---

* On leave of absence from the Geophysical Institute, University of Tokyo, Tokyo, 113, Japan.

From thermodynamic considerations, Blander et al. showed that the coefficient b can be expressed as:

$$b = \frac{18.08}{RT} \cdot \gamma \qquad (9)$$

where R and T denote the gas constant, and the absolute temperature. Though γ should be understood to represent the microscopic surface tension, Blander et al. suggested that it can be approximated by a macroscopic surface tension. Since b is always a positive quantity as seen in Eq. (9) and $r_{36Ar} < r_{Kr} < r_{Xe}$, the right hand side of Eq. (6) and (7) are always positive. Consequently, if we plot the data for the rare gas compositions in the melt equilibrated with the atmosphere in the ln (C_{Kr}/C_{Xe}) - ln (C_{36Ar}/C_{Kr}) diagram, the data must lie on the upper right part of the melt line. In fact the rare gas sorbed in the molten submarine basalts (Fisher, 1970) and the molten enstatite (Kirsten, 1968) in the atmospheric rare gas composition do lie on the upper right part of the melt line with respect to the atmospheric rare gas composition. Conversely, any data which lie on the lower left extension of the melt line (e.g., several submarine basalts studied by Fisher (1970)) cannot be explained by the above melt theory as assumed by Fisher (1970, 1973, 1974) and by other authors (Phinney, 1972; Dymond and Hogan, 1973).

References

Blander, M., W.R. Grimes, N.V. Smith, and G.M. Watson (1959) J. Phys. Chem, 63, 1164.

Dymond, J., and L. Hogan (1973) Earth Planet. Sci. Lett., 20, 131.

Fisher, D.E. (1970) Earth Planet. Sci. Lett., 9, 331.

Fisher, D.E. (1973) Nature, 244, 344.

Fisher, D.E. (1974) Geophys. Res. Lett., 1, 161.

Kirsten, T. (1968) J. Geophys. Res., 73, 2807.

Phinney, D. (1972) Earth Planet. Sci. Lett., 16, 413.

UNIQUENESS PROBLEM IN THE SPHERICAL HARMONIC ANALYSIS OF THE GEOMAGNETIC INCLINATION DATA

Masaru KONO

Geophysical Institute, University of Tokyo, Bunkyo-ku, Tokyo 113

In a previous report (Kono, 1974), it was proved that the geomagnetic direction data (inclination and declination) are sufficient for uniquely determining the geomagnetic potential within a multiplicative constant. That the complete knowledge of a single angle (such as declination) may not be enough and different solutions satisfy the same boundary condition was also shown (Kono, 1973).

Of special geophysical interest is the case where input data are given by inclination. Abundant information of inclination change in the past is now available from paleomagnetic studies of ocean and lake sediment cores. As it is nowadays relatively easy to obtain vertical sections of such sediments without declination information, the use of inclination data will continue to be a major source of geomagnetic information. Some attempts have already been reported to use such data to infer the gross structure of the paleomagnetic field (Opdyke and Henry, 1969; Georgi, 1974).

For inclination data sets, it does not seem possible to produce analytical examples of non-uniqueness such as given for the case of declination data sets (Kono, 1973). The expression to be equated for the two potential fields $Z/(X^2+Y^2)^{1/2}$ is irrational and cannot be made linear with respect to the Gauss coefficients by simple manipulation.

However, it can be shown that if two mutually independent potentials W and W' produce fields with equal inclination on the sphere, at least one of the two potentials contains infinite number of spherical harmonics. This property of inclination datasets prevent the construction of simple examples of non-uniqueness. Since no clear-cut examples can be found, numerical approach was taken to investigate the possible non-uniqueness of harmonic analyses based on inclination data. The method of searching non-unique example is as follows. Sets of 100 to 140 randomly distributed points were chosen on the sphere and the "observed" inclinations at these points were calculated from the potentials of either an axial dipole field or the International Geomagnetic Reference Field for 1965.0 (IGRF, IAGA Working Group, 1969).

Potentials with K harmonics can be represented, for the sake of brevity, by a K-dimensional vector $\underline{G}$ $(G_1, G_2, \ldots, G_K)$ where the components are the Gauss coefficients corresponding to completely normalized spherical harmonics, i.e.,

$$G_1=g_1^0/\sqrt{3},\ G_2=g_1^1/\sqrt{3},\ G_3=h_1^1/\sqrt{3},\ G_4=g_2^0/\sqrt{5},\ \ldots\ldots \qquad (1)$$

Since we are dealing with only the directions of the field, the magnitude of $\underline{G}$ is indeterminate and we can make $\underline{G}$ a unit length vector.

$$|\underline{G}| = \sum_{k=1}^{K} G_k^2 = 1 \qquad (2)$$

To search for a potential W which produces the same inclinations on the sphere as another potential W', we consider the sum

$$E(\underline{G}) = \sum_{i=1}^{N} (1 - \cos\Delta I_i) = \text{minimum} \tag{3}$$

where $\Delta I_i = I_i - I_i'$ is the difference of two inclinations calculated from the two potentials W and W' (corresponding to the vectors $\underline{G}$ and $\underline{G}'$) for the i-th data point. When W is coincident with W', $\bar{E}$ takes the minimum value of zero

$$E(\underline{G}') = 0 \tag{4}$$

Our problem is to find $\underline{G}$ ($\neq G'$) which also makes the value of E a minimum. We have shown however, that more than one absolute minima (non-unique solutions) cannot be found if the vector $\underline{G}$ is finite dimensional. Therefore, local minima were searched instead, and the stability of these minima were studied by successively increasing the number of Gauss coefficients.

The search was initiated with trial vectors $\underline{G} = \underline{e}_k$, where $\underline{e}_k$ is a unit vector in the direction of the k-th coordinate axis. Since the problem is non-linear, the method of steepest descent was utilized to locate the local minimum. If $E(\underline{G})$ is not a local minimum, we can expand E near $\underline{G}$ in a Taylor series

$$E(\underline{G} + b\underline{r}) = E(\underline{G}) + \sum_{k=1}^{K} br_k \frac{\partial E}{\partial G_k} + \sum_{k=1}^{K} \sum_{j=1}^{K} \frac{b^2 r_j r_k}{2} \frac{\partial^2 E}{\partial G_j \partial G_k} \tag{5}$$

where $\underline{r}$ is taken in the direction of maximum change, i.e., the gradient of E,

$$\underline{r} = \text{grad } E(\underline{G}) = \sum_{k=1}^{K} \underline{e}_k \frac{\partial E}{\partial G_k} \tag{6}$$

Neglecting the terms of third or higher orders in b, the minimum value of E can be found if

$$b = \left(-\sum_{k=1}^{K} r_k \frac{\partial E}{\partial G_k}\right) \Big/ \left(\sum_{j=1}^{K} \sum_{k=1}^{K} r_j r_k \frac{\partial^2 E}{\partial G_j \partial G_k}\right) \tag{7}$$

This procedure was repeated with the value of $\underline{G}$ in (5) replaced by the new value (which is equal to $(\underline{G} + b\underline{r})/|\underline{G} + b\underline{r}|$), until a satisfactory convergence was observed.

When the procedure was applied to 8-dimensional $\underline{G}$ corresponding to dipole and quadrupole terms, all the calculations started from $\underline{G} = \underline{e}_k$ (k = 1,....,8) located the absolute minimum both for the axial dipole field and the IGRF. When calculations were done for dipole, quadrupole, and octapole (K = 15), a few local minimum were found but they turned out to be unstable; when the dimension K of the vector $\underline{G}$ was increased they were no longer minima and the absolute minima was located by the search procedure.

When K was increased to 24, it was found that about a quarter of the searches started with $\underline{G} = \underline{e}_k$ (k = 1, ..., 24) located local minima, which, in this case, were stable even if K was increased successively up to 80. Fig. 1 shows the changes of various parameters in one example with the increase of the dimension of $\underline{G}$. The potential W' is an axial dipole field.

The parameters plotted in this figure are the mean inclination difference $\langle\Delta I\rangle$, the mean angular difference $\langle\Delta A\rangle$ for the N data points, and the potential difference ΔW defined as

$$\langle\Delta I\rangle = \sum_{i=1}^{N} |\Delta I_i| /N \tag{8}$$

$$\langle\Delta A\rangle = \sum_{i=1}^{N} \cos^{-1}[\sin I_i \sin I_i' + \cos I_i \cos I_i' \cos(D_i - D_i')]/N \tag{9}$$

$$\Delta W = 1 - \sum_{k=1}^{K} G_k G_k' \tag{10}$$

Also shown in the figure are the values of $E(\underline{G})$ (small open circles) and inclination and angular differences averaged over the whole sphere (large circles). Obviously, the fit of inclination data becomes more and more convincing as the number of Gauss coefficients increased, while the two potentials are essentially different. The fact that ΔW is nearly constant for K larger than 35 shows that this minimum is really stable. Fig. 2 shows histograms of ΔI and ΔA over the surface of the sphere. Although inclination values were evaluated only at finite data points in order to obtain the potential W, approximation in inclination

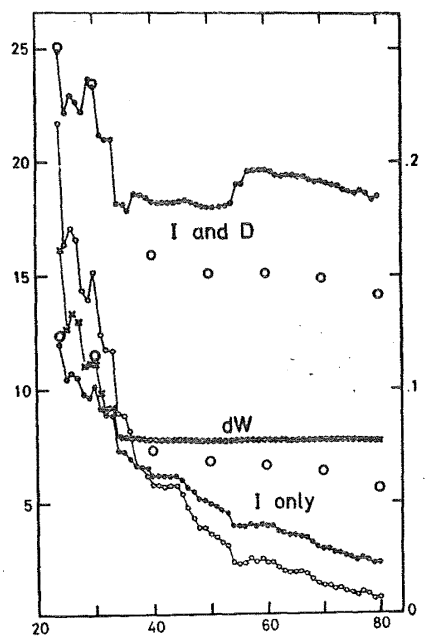

Fig. 1. Change in parameters of fit to an axial dipole field when the dimension K is increased. Small circles indicate error angles averaged over the 140 data points. Large open circles indicate error angles averaged over the sphere. Note the almost constant difference between the two potentials W and W'.

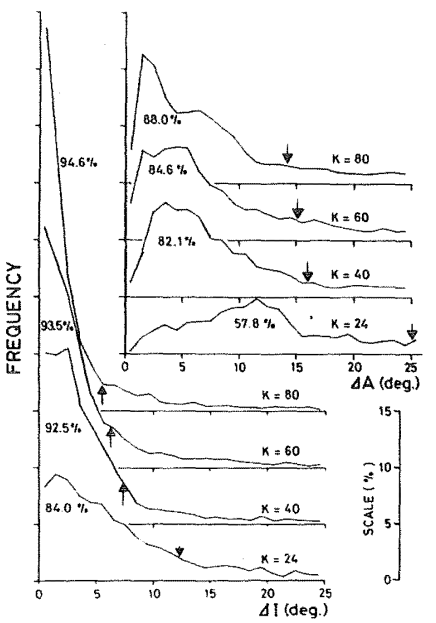

Fig. 2. Histograms of ΔI and ΔA over the whole sphere for the fit of Fig. 1. Percentages indicate the fraction of differences less than 25°. Arrows show the mean values.

for the whole sphere becomes more and more good with the inclusion of more Gauss coefficients while that in both declination and inclination is not prominent.

Fig. 3 is an example of local minimum search with IGRF as the potential W'. The essential feature of the change of parameters of fit is the same as in Fig. 1; <ΔI> being steadily decreasing with the increase of K while <ΔA> and ΔW are nearly constant for K larger than 50. The lower half of Fig. 3 shows that after about K = 40, the first eight components of vector $\underline{G}$ stay almost constant even if the number of components are increased to 80, showing the stability of the solution and the corresponding minimum.

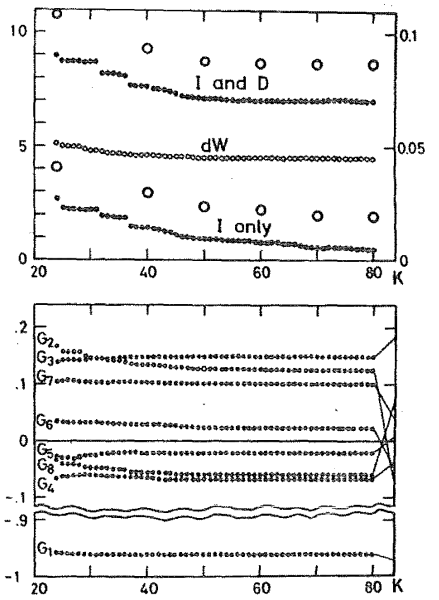

Fig. 3. Change in parameters of fit to IGRF with the increase of the dimension of $\underline{G}$. For the upper figure, see the legend of Fig. 1. The lower figure shows the change of the first eight components of $\underline{G}$ with K. The values of IGRF is indicated in the extreme right.

Before concluding, it must be pointed out that for $K \geq 24$ many solutions of equation (3) were found which were different from each other; the search started with different trial vector $\underline{G}$ always ended in finding a different local minimum if the absolute minimum was not located. It can therefore be said that there are many local minima of $E(\underline{G})$ which are potential candidates for the non-unique solutions of the boundary value problem.

The foregoing examples do not prove but are suggestive of the existence of non-unique solutions for such boundary conditions. In actual analyses, the number of data are finite and they contain errors, which in the case of paleomagnetic data are typically about 10°. It is quite probable that for such data set there are many local minima in $E(\underline{G})$ with comparable magnitudes. In such cases it would become virtually impossible to distinguish the real and pseudo solutions by any numerical procedure. So, although the mathematical problems remain, it may be concluded that inclination data sets may, in practice, be not sufficient for obtaining unique potentials.

References

Georgi, D.T. (1974) Geophys. J. Roy. Astron. Soc. 39, 71.
IAGA Working Group (1969) J. Geomag. Geoelectr. 21, 569.
Kono, M. (1973) Rock Mag. Paleogeophys. 1, 118.
Kono, M. (1974) Rock Mag. Paleogeophys. 2, 91.
Opdyke, N.D. and K.W. Henry (1969) Earth Planet. Sci. Lett. 6,139.

(Submitted to J. Geomag. Geoelectr.)

ORGANIC ELEMENTS IN LAKE BIWA AND THE CLIMATE

Naoto KAWAI

Department of Physics, Faculty of Engineering Science,
Osaka University, Toyonaka, Japan

A geomagnetic record with almost no gap of interruption since the Brunhes epoch was compiled when fossil magnetism preserved in Lake Biwa was measured, and carefully arranged in the chronological order by Kawai et al. (1972).

Beside the secular variation disclosed in details as shown on a long time span of the Quaternary epoch, they found that the Brunhes' field was frequently interrupted more than four times by a recurrence of short geomagnetic weakening. The normal field continued steadily for about 100,000 years and encountered the weakening. The weak field, being 10,000 years or less in the length of life time, recovered to the former field at each time. The time required for one weakening is so short as 1,000 years or less.

Prior to the report on the lake sediments, Wollin et al. (1971) found out similar geomagnetic fluctuation existing in an ocean core collected from the north Pacific. The same fluctuation can partly be seen in the report (Kawai et al. 1973 a, b) who dealt in detail with another core obtained in the same ocean, at a point 170°W in longitude and 38°N in latitude. The frequent field weakenings are now being almost accepted by the specialists as a global phenomenon happening in the Quaternary period.

Wollin et al. (1971) tried to observe change of oxgen isotope o^{18} contained in the core sediments. Based upon the analysis they came to a conclusion that a climatic change has taken place in such a way that the atmospheric temperature rose up at each time when the field was reversed.

In contrast Kawai (1972) estimated that it dropped during the particular moment of the geomagnetic weakening. He summarized it on the basis of geochemical and paleontrogical investigations, using the same lake sediments (Fuji and Horie 1972, Handa 1972, Koyama 1972, Nakai 1972). Of the various physicochemical informations gathered so far, anomalies in the concentration of organic, carbohydrate and protein carbon relative to the total carbon found by Handa (1972) and Koyama et al. (1973) deserve to be reviewed in connection with the geomagnetic change. They are shown in Fig. 1 for comparison. The uppermost curve shows the geomagnetic fluctuations while the second, third, and fourth were the fluctuations in organic, carbohydrate and protein carbon, respectively. Four dotted lines were drawn vertically showing each depth at which the weakened field had appeared.

General tendency to decrease gradually with depth is evident in the curves showing each ratio. This is due to the effect of decomposition of organic substances buried in the sediments into natural gas and remaining carbon. Besides this general trend in each curve, there exist a number of abrupt decreases of the ratio which take place one after another in a rythmic

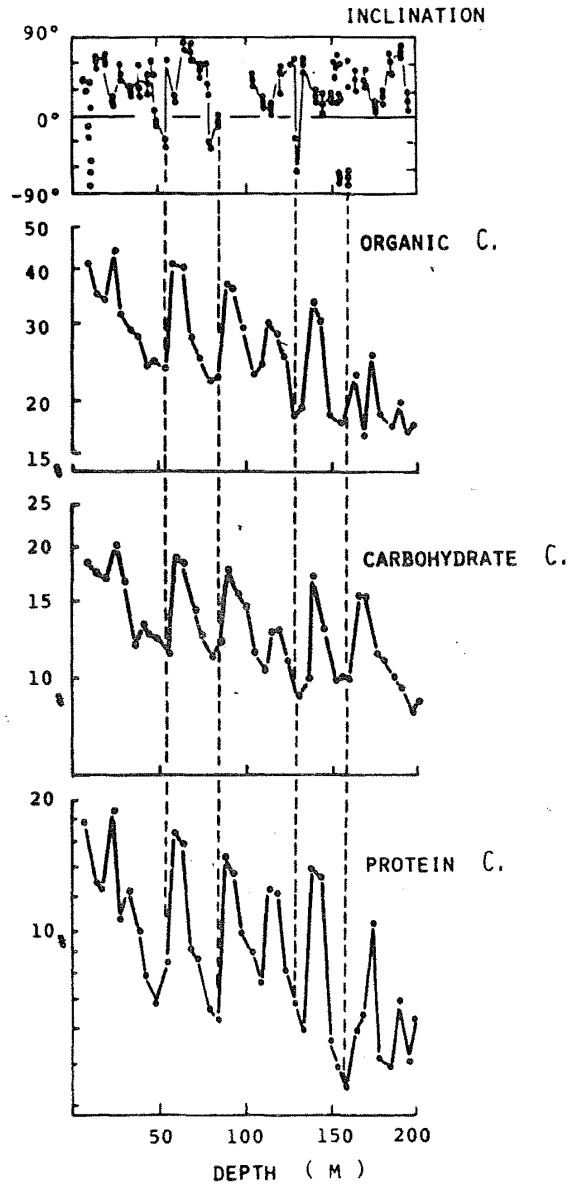

Fig. 1 Geomagnetism vs organic substance.

succession. As clearly indicated by the four vertical lines, swift geomagnetic transition and the drop of the ratio occurred almost simultaneously. These carbonic elements were derived mainly from botanical and zoological remains brought into the lake bottom. Organic materials had been produced presumably in and around the lake, and transfered by water till they were finally stored in the lake basin. The total carbon is made up mostly of the organic stuffs, while inorganic carbon is very scarce.

Photosynthesis plays a dominant role in the formation of such organic substances in a lake located in the middle latitude. Sudden decrease of these ratios, therefore, strongly indicates a suppressed state of the photosynthesis which recurred in the past.

Each drop of the production rate took place within a very limitted interval of time. The fact could hardly be understandable indeed, if each were assumed as having occurred accidentarily and independently of the geomagnetic events.

The field weakening is missing, however, at the depth of about 110 m. Specimen in the vicinity of the depth carry too weak remanent magnetism to be measured, leaving on the diagram a gap that masked unfortunately the geomagnetic event in question.

Photosynthesis should drop when the radiation of sun-beams become scarce. Production of organic stuffs is directly reduced.

Low intensity of the radiation of sun-beams, when prolonged, easily makes a low temperature atmosphere in which the biological activity is depressed. The cooler atmosphere accompanies a dry predominant climate in which the botanical activity is depressed, too. The cool and dry climate is indirectly but effectively related to the scarcity of organic stuffs accumulated in the lake sediments. The direct and indirect effects can cooperate to bring the production of the carbonic elements down abruptly as Handa (1972) and Koyama et al. (1973) have observed.

One needs, therefore, a mechanism with which the beams reaching the earth were reduced on the one hand and a short period geomagnetic weakening took place simultaneously on the other.

Uffen (1963) once supposed that proton and electrons trapped in the Van Allen band would reach the earth at the time of the geomagnetic polarity transition, and disturb directly the living matters on the earth. The effect was soon reviewed and discovered by Black (1967) to be an over-estimation but still large enough to affects the atmosphere. Study by Kigoshi and Hasegawa (1966) evidently shows that the production rate of the radioactive carbon C^{14} from atmospheric nitrogen can be expressed by a rapidly increasing function of decreasing geomagnetic field intensity, implying that falling high energy particles into the atmosphere increase in number in the declining magnetosphere. The abnormal state may have been given rise to in the atmosphere.

In order that these sharp drops of carbonic staffs may be explained most easily, sun-beams that irradiated the earth in the past was hypothesized by Kawai (1972) to have been scattered around the earth.

An explanation alternative is that the magnetosphere is

playing an important role of the green house effect for the earth. The sphere is made up of magnetic lines of force deformed by solar wind, high energy protons, plasma, electrons, and more than four ionospheres.

Besides, the outer atmosphere contains of H_2O, OH^-, O^3 layer etc. They all absorb light energy with respective and characteristic wave length to prevent the outward heat flow from the earth.

At the time of the geomagnetic weakening, the above layers become thinner together with the magnetosphere to increase the outward flow. While at the time of the geomagnetic strengthening, the layers become thicker to decrease it. The integrated effect of the flow with time is the cause of the climatic change.

REFERENCES

Black, D.J. (1967) Earth Planet. Sci. Letters 3, 225.

Fuji, N. and S. Horie (1972) Proc. Japan Acad. 48, 500.

Handa, N. (1972) Proc. Japan Acad. 48, 510.

Kawai, N. (1972) Proc. Japan Acad. 48, 687.

Kawai, N., K. Yaskawa, T.Nakajima, M. Torii and S. Horie (1972) Proc. Japan Acad. 48, 186.

Kawai, N., T. Nakajima, K. Hirooka and K. Kobayashi (1973 a) Proc. Japan Acad. 49, 820.

Kawai, N., T. Nakajima, K. Yaskawa, K. Hirooka and K. Kobayashi (1973 b) Proc. Japan Acad. 49, 619.

Kigoshi, K. and H. Hasegawa (1966) J. Geophys. Res. 71, 1065.

Koyama, T. (1972) Proc. Japan Acad. 48, 505.

Koyama, T., N. Handa, R. Ishiwatari, K. Ogura, A. Mizuno, M. Terashima, M. Koyama, T. Hori, J. Okuda, T. Fujinaga, T. Takeuchi, and S. Horie (1973) Jap. J. Limnol., 34, 75.

Nakai, N. (1972) Proc. Japan Acad. 48, 516.

Uffen, R.J. (1963) Nature 198,143.

Wollin, G., D.B. Ericson, W.F. Ryan, and J.H. Foster (1971) Earth Planet. Sci. Letters 12, 175.

PALAEOMAGNETISM AND PALAEOCLIMATE

Naoto KAWAI, Tadashi NAKAJIMA

Department of Physics, Faculty of Engineering Science, Osaka University, Toyonaka, Japan

Katsuyasu TOKIEDA

Physics Department, Shimane University, Matsue, Japan

Kimio HIROOKA

Geological Laboratory, Faculty of Education, Fukui University, Fukui, Japan

1) Relation between the geomagnetic intenstiy and direction

Since Thellier's pioneer work (1959), there has been an increasing interest on the geomagnetic secular variation since the prehistoric time or even more remote past. Within any baked earth there remain the direction and intensity of the past geomagnetism at the time when it was fired. The secular field can be trace back when we can collected many datable specimens and measure. From the various data already obtained on the several spots on the earth (Kawai et al. 1965 and 1967, Kawai and Hirooka 1967, Weaver 1967), one can extract at least such a common movement of the magnetic axis as shown in Fig. 1. In the past since AD 0 the magneitc axis has inclined from that of the earth's rotation by 1/6 rad. and continuously moved anti-clockwise with a period of approximately 1,500 years. Besides, the same axis has been moving clockwise simultaneously with the radius about 1/12 rad. and the period equal to 500 years. The two motions are so combined that the magnetic pole draws a figure of the clover leaves on the earth's surface. The rate at which the magnetic axis moves along the periphery of the leaves becomes speedy when the axis comes closer to the rotational axis. In contrast, it becomes sluggish when the magnetic axis appart from the latter and reaches the respective centres of the three leaves.

Next, the intensity data summarized by Smith (1967 and 1968) and Kitazawa (1970) render us to suppose that the field goes greatly up and down even within half a millenium and repeats rather regularly, despite that the latter author has smoothed away the fluctuation to make out a period of 8,000 years for the geomagnetic oscillation.

When, however, the recent data by Tokieda (1975) are taken into account to be combined, the above-mentioned regular fluctuation becomes almost prooved. At least four times the existence of the leaf has been confirmed since AD 0. Before Christ, however, only two maxima and minima can be perceptible with relatively different intervals at 4,500, 8,000, 3,500 and 6,000 BP, respectively (see the upper curve in Fig. 2).

When the variation of intensity and that of direction since AD 0 are carefully put together, it becomes clear that field itself strengthens at each time when the magnetic axis and the rotational axis are going to coincide. Whereas, it weakens when the magnetic axis aparts from the latter. This relation is completely hold in the entire Brunhes Epoch. As clearly marked out at each time of the geomagnetic excursions and events of weakening, the declination has been fliped up even above the horizontal plane (Kawai et al. 1972, Nakajima at al. 1973, Yaskawa et al. 1973).

The archaeomagnetic data older than 9,000 BP are unfortunately lacking. For the secular field of the antiquity, however, the record obtained from Lake Biwa (Kawai et al. 1975 a) is sufficiently available. It is possible to join the secular field from the baked earths and that from the sediments

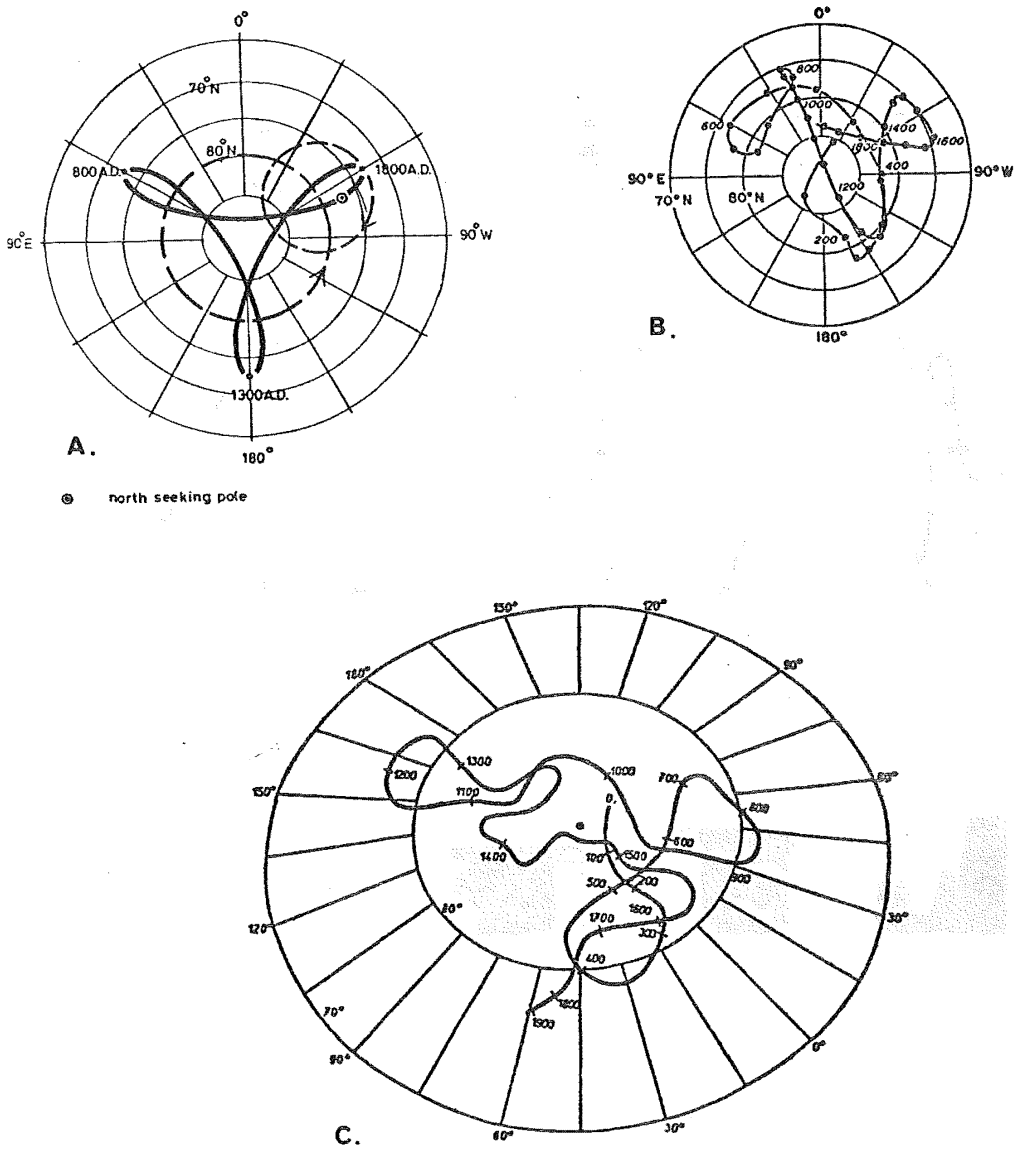

Fig. 1 A. Locus of the pole (after Kawai et al. 1967).
B. Locus from Japan (after Hirooka 1971).
C. Locus from North America (after Weaver 1967).

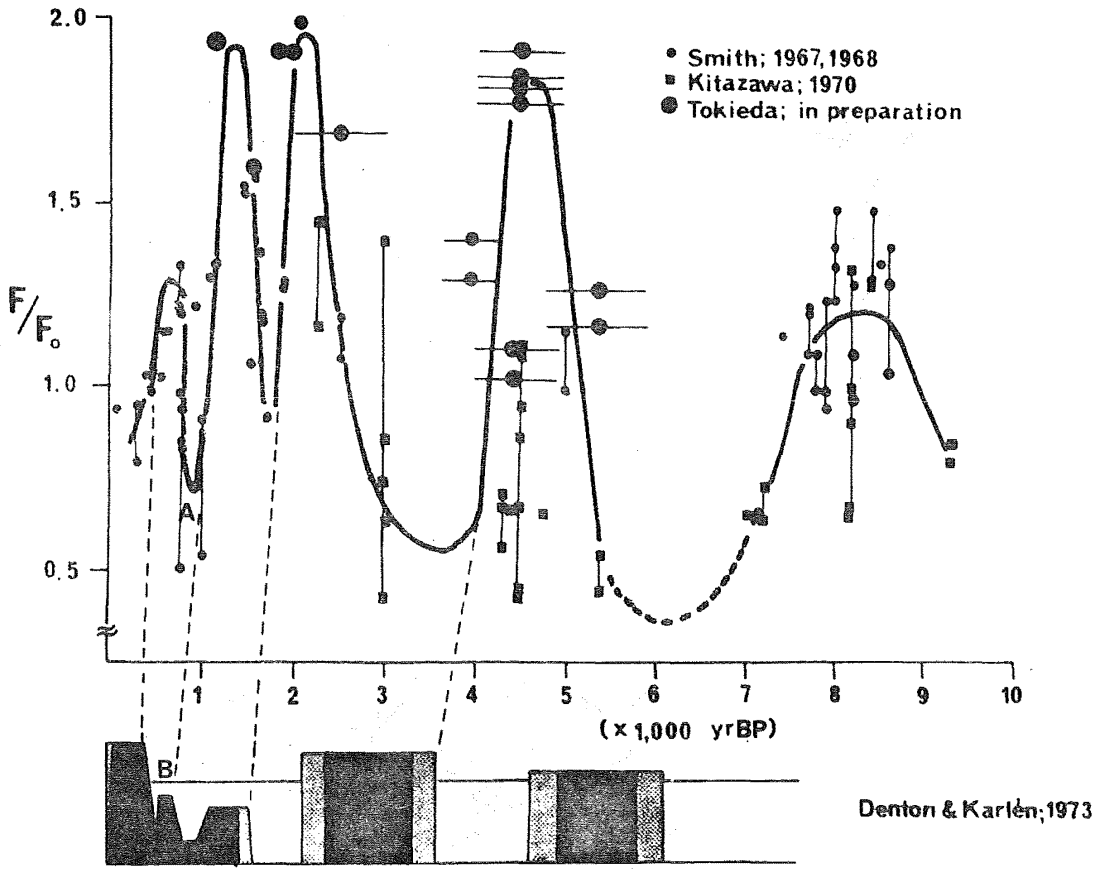

Fig. 2 Upper Figure
Intensity variation in the historic time.

Lower Figure
Glacier expansion(black) and retreat (white).
Pre-glacial and post-glacial climate is shown by the dotted belt.

without any time gap (Fig. 3).

A great drop of the intensity is evidently seen around 9,000 BP. A low geomagnetic field had persisted since 18,000 BP to 10,000 BP. This interval is accepted by many geologists as the latest Würm ice age. This interval represented by the low geomagnetic field, however, involves several minor field rises of which that around 12,000 BP is rather conspicuous. Although the geomagnetic oscillation with period of 8,000 years is envisaged by both Bucha (1970) and Kitazawa (1970) from their data, it is rather hard for us to recognizes it in the joint geomagnetic record over the prehistoric time (Fig. 3).

2) Relation between the geomagnetic intensity and the climate

In both the archaeomagnetic and palaeomagnetic record there exist a clear relation between the geomagnetic field strength and the past climate as will be described here in the next.

The historical climatic change worldwide is very well demonstrated by the well-dated glacial developments and the retreats studied by Denton and Kåren (1973) from Yukon, Lapland and Alps as shown in the lower curve in Fig. 2. It is quite clear that each geomagnetic weakening calls forth a climatic depression, the weakening forerunning the latter definitely. On the other hand each geomagnetic strengthening also accompanies a climatic recovery.

Recent study of the archaeology in Arizona by Karlstrom et al.(1974) shows that the relic of the vegetation has been found from the desert at the time when the glacier has been developing in the high latitude regions of the northern-hemisphere. Each vegetation was occurring almost simultaneously with the corresponding geomagnetic weakening.

As Keimatsu (private communication) has confirmed, in 1126 a red swaying aurora has been seen at Hangchow of which the latitude is so low as 30°14'. In 1138 the similar one is observed and recorded in the Chinese astronomical report (Keimatsu et al. 1968). As Fritz (1873) has reported, the same aurora has been observed at Prague, too. The particular time of the astronomical event corresponds to the recent geomagnetic weakening as shown by A in Fig. 2. It is more reasonable to assume that the area from which the aurora was visible became widened significantly whilst the geomagnetic field was being weakened. A small glacier develop is clearly marked in the curve by Denton and Karlén (1973) as shown by B in Fig. 2.

The obtained geomagnetic field variation is indeed a worldwide phenomenon together with the climatic change.

In many studies of the secular change the westward drift of the non-dipole fields has been considered to play a dominant rôle. Even if we accept it as real clue, the drifting fields are too small to explaine the actual intensity change clarified from the past. The maximum field is more than four times greater than the minimum one. In explaining the secular change the weakening and strengthening of the main dipole field are better be admitted frankly, rather than we depend only on the small drifting fields.

To be mentioned next is the Quaternary secular variation which came out of Lake Biwa sediments. As has been reported in this annual report (Kawai et al.), the palaeomagnetic measurements with continuous cubic specimens went on slowly but surely in Osaka University down to the depth of 60 m measured from the boring core head. The length of time for the measured part of the core is approximately 110,000 years. Although the old measurement (Kawai et al. 1972, Yaskawa et al. 1973) successfully manifested the four Biwa events and two excursions, the new informations concerned eleven extra excursions out of the Brunhes normal field. It is now assumed that the event and excursion are the phenomena similar to the geomagnetic extreme weakening (or vanished geomagnetism) in the stage transitional from the Matuyama to Brunhes Epoch discovered recently from an ocean core taken from the equatorial Pacific (Kawai et al. 1975 b, Kawai and Nakajima 1975). They differ from

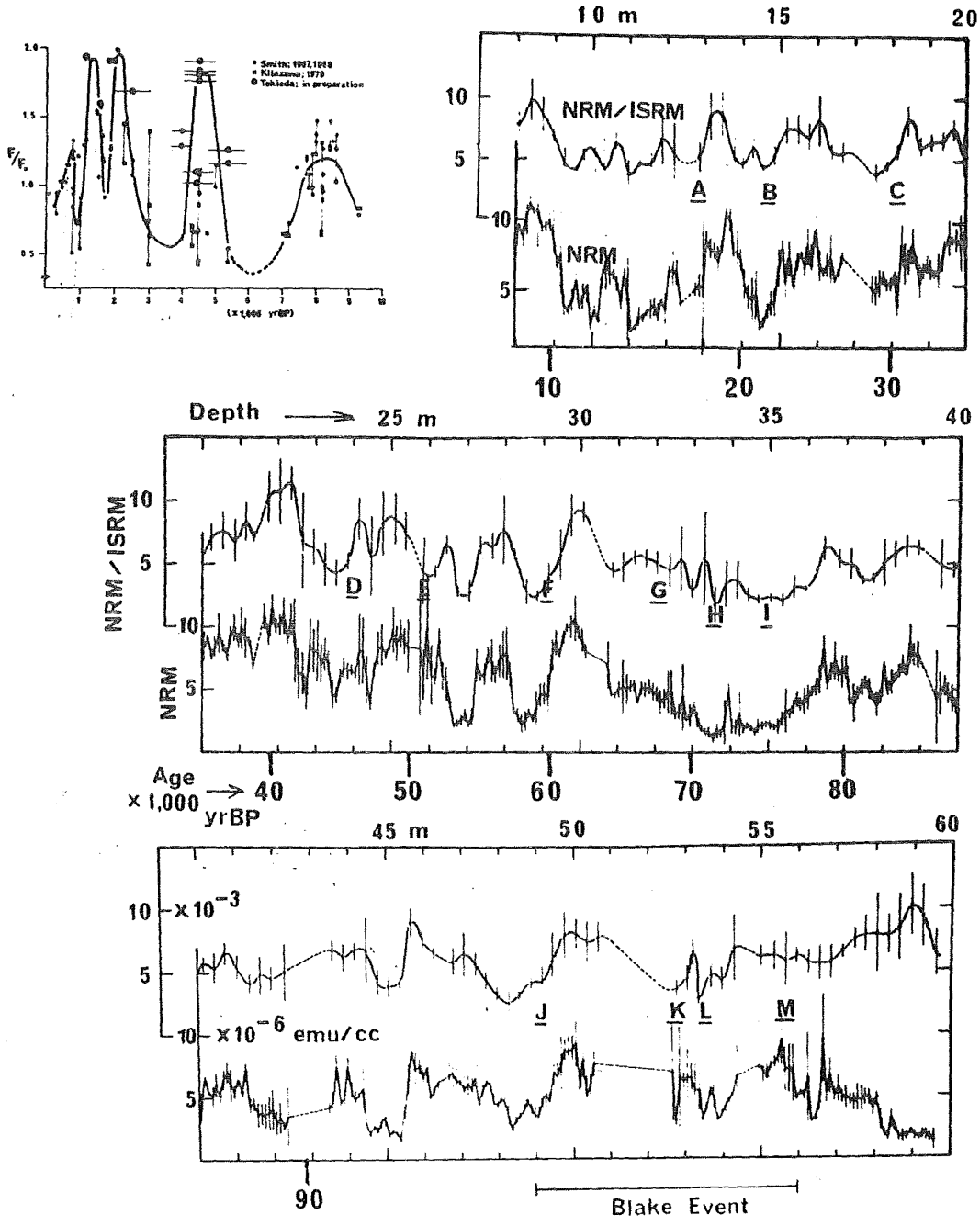

(AGE: Kanari and Takenoya 1975)

Fig. 3 Joint geomagnetic intensity curve from present back to 110,000 years.
A,B, ...,L and M: geomagnetic excurtion

it, in that the field decline for only a short duration, and being undone with no change of polarization.

It becomes more important further to expand the study backwards in the time span. For this purpose the present authors proposed to make a co-oprative research with the Ocean Reserch Institute of University of Tokyo, in which the counter partners were responsible for the sampling of the ocean cores from various places in the Pacific and its coarse survey. We were responsible for the preparation of continuous samples and the measurements.

A core was so sliced successively that a series of thin sections with thickness about 4.3 mm are obtained. As already reported (Kawai et al. 1975) one of the core No. KH 73-4-7 contains the Matuyama-Brunhes boundary, Jaramillo and Olduvai event. From the uppermost part of the core, one geomagnetic event was discovered. From the rate of deposition determined with respect to the ocean core, it is assumable that it coresponds with the Biwa III event.

In the phase transitional from the Matuyama to the Brunhes Epoch, a great drop of the geomagnetic intensity was observed. The ratio NRM/ISRM decreased down to 1/40 compared with maximum value. It seems as if neither the dipole nor the non-dipole field had existed in the phase which was at least more than 10,000 years longer. The new field (the Brunhes field) was born in the direction opposite to the Matuyama field long after the death.

When the geomagnetic record from Lake Biwa and that from the Pacific are compiled in one diagram Fig. 4, one can see that the two records overlap in the middle part for about 150,000 years. The white vertical belts shows the geomagnetic weakening, thickness being the duration of it. The black part corresponds to the high geomagnetic field.

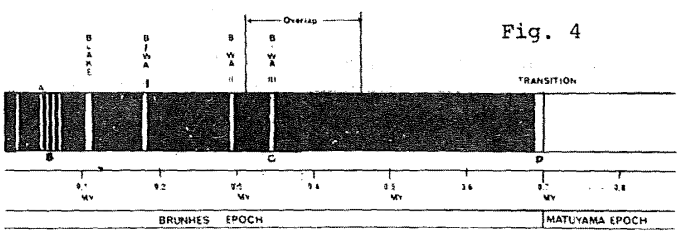

Fig. 4

It is interesting to suppose that the Mindel ice age is the consequence of the vanished geomagnetism in the stage transitional from Matuyama to Brunhes Epoch. While Riss ice age is the consequence of both the Biwa III and Biwa II weakening, since the glaciation has a tendency to have culminated twice.

The start of the Würm ice age lies on the Blake event and it occurred intermittently on the earth for a prolonged duration after the Blake event. Since then the excursions increased in number, too. Under this condition the Würm glaciation fluctuated frequently till 10,000 BP from which the great recovery of the climate took place tending to prehistoric.
The geomagnetic recovery was also the forerunning phenomenon of the climatic rise.

The human history and culture development are not independent of the worldwide climatic change. The relation has been found by one of the authors (N.K) and reported in his book (1976). It seems interesting to make the abstract of the theory in order to emphasize the geomagnetism vs climate relation. In the past before BC 6 millenium high intensity and warmer climate coexisted. The relic of the ancient culture remaines in the very high latitude regions along the great rivers. The Pyramids were constructed along the Nile in the end of the first ice age around 6 millenium BP when the human activity culmiated with the help of the expansion of irrigation along the river.

The Aryan could survive in the steppe belts of the northern hemisphere and enjoyed their normadic life. Some trives could succeeded in farming near the Black Sea (at Tolipolie). In the begining of the second ice age

at 3,600 BP, the water become scarce in the steppe due to the ice condensation in the surrounding mountaine chains. The shrinking steppe turned the Aryan away from the belts. One of them came down to Iran looking for the shortest way through the Caspian coast. Other trives selected a south-west route to reach the Mediteranean. The trives came later to Iran must have gone farther south till they reach India. In the middle of the same ice age the Buddism was born in India along the Ganges of which the latitude is so low as 25°N that no reasonable culture could survive in the hot severe climatic environment subsequently followed. The same climate render the ancient Maya culture represented by the Palenque's stone coffin to develop in the Yucatan peninsula at which the jungle had retreated and soil met dry wind, making there the agriculture to be initiated.

In the begining of the little ice age of 500 AD when the earth began to be enclosed by the third cold weather, the northern part of China was attacked by Hsiung-nu and occupied by one country and others, as the results 16 countries being built successively. Together with this movement Huns pushed the East Gautae which pushed the west gautae. Finally the Roman empire had to recieve the forces from the northern neighbours. Whilst the West Roman went to ruin, the great migration of the races occurred in Europe. In the middle of ice age after 1,200 AD the climate become suddenly cold as shown by the glacier development in Fig. 2. The Mongolian empire rose up with Chinggis Khan as the king. His invincible cavalry migrated more than 15 degrees south in latitude during the battles. Then it invaded the eastern Europe through the silk road. Then the main China except Vietnam was almost completely occupied by the descendants of Chinggis Khan.

It is interesting to assume that the cold climate after the weak geomagnetism makes the human lives in the high latitude belt harder in one hand, and those in the equatorial belt easier on the other.

References

Bucha, V., R.E. Taylor, R. Berger, E.W. Haury (1970) Science 168, 111.

Denton, G.H. and W. Karlén (1973) Quaternary Res. 3, 155.

Fritz, H. (1873) Verzeichniss Beobachteter Polarichter, Wein.

Hirooka, K. (1971) Mem. Fac. Sci. Kyoto Univ., Sel. Geol. Mineral. 38, 167.

Kanari, S. and Y. Takenoya (1975) Paleolimnology of Lake Biwa and the Japanese Pleistocene.(Third Issue) (in print).

Karlstrom, N.V., G.H. Gumerman and R.C. Euler (1974) Geological Society of America Rocky Mountain Section Meeting, Flagstaff, Arizona, 768-792.

Kawai, N., K.Hirooka and S. Sasajima (1965) Proc. Japan Acad. 41, 398.

Kawai, N. and K. Hirooka (1967) J. Geomag. Geoelectr. 19, 217.

Kawai, N., K. Hirooka and K. Tokieda (1967) Earth. Planet. Sci. Letters 3, 48.

Kawai, N., K. Yaskawa, T. Nakajima, M. Torii and S.Horie (1972) Proc. Japan Acad. 48, 186.

Kawai, N. (1972) Proc. Japan Acad. 48, 687.

Kawai, N., T. Nakajima, K. Yaskawa, M. Torii, N. Natsuhara (1975 a) Rock Magnetism and Paleogeophysics 3.

Kawai, N., Y. Otofuji, T. Nakajima and K. Kobayashi(1975 a) Proc. Japan Acad. 51, 634.

Kawai, N. and T. Nakajima (1975) Proc. Japan Acad. 51, 640.

Kawai, N. (1976) Mystery of the Geomagnetism.(Kodansha, Tokyo) (in Japanese) (in print).

Keimatsu, M., N. Fukushima and T. Nagata (1968) J. Geomag. Geoelectr. 20, 45.

Kitazawa, K. (1970) J. Geophys. Res. 75, 7403.

Nakajima, T., K. Yaskawa, N. Natsuhara, N. Kawai and S. Horie (1973) Natura Pphys. Sci. 244, 8.
Smith, P.J. (1967) Geophys. J. Roy. astr. Soc. 13, 483.
Smith, P.J. (1968) Geophys. J. Roy. astr. Soc. 16, 457.
Thellier, E. and O. Thellier (1959) Ann. Géophys. 15, 285.
Yaskawa, K., T. Nakajima, N. Kawai, M. Torii, N. Natsuhara and S. Horie (1973) J. Geomag. Geoelectr. 25, 447.
Weaver, K.F. (1967) National Geographic Magazine 131, 696.

Reprinted from National Report of the
Geodynamics Project of Japan (August 1975)

(2) PALEOMAGNETISM AND ROCK MAGNETISM

Investigations with various objectives have been carried out by using the methods of rock magnetism and paleomagnetism as a part of Geodynamics Project. Purposes of these investigations are to clarify the geomagnetic field variations, mechanisms of magnetizations in rocks, movements of Japanese islands in geological periods.

Some of the results of these studies have been published in scientific journals, but many others are still in the stages of preparation or preprints. For the latter, extended English abstracts are available in the form of the annual progress reports of the Rock Magnetism and Paleogeophysics Research Group in Japan (Rock Magnetism and Paleogeophysics, vol. 1, 1973; vol. 2, 1974). These reports summarize rock magnetic and paleomagnetic studies carried out in Japan. Therefore, if a full paper has not been published yet, reference is made here to these extended abstracts.

A. ARCHEOMAGNETISM

Hirooka (1973) collected over two hundred oriented samples from old kilns located in Hokuriku district (see Fig. II-7 for the location). Ages of the samples were estimated by fission track dating, by old documents, or by the type of potteries found in these kilns, and they span from the 2nd to 19th centuries. Changes in inclination and declination obtained from these samples are in good accord with the data obtained from southwestern Japan (Hirooka, Mem. Fac. Sci. Kyoto Univ., Ser. Geol. Mineral., 38, 167, 1971). Domen (1974 a) and Domen and Muneoka (1973, 1974 a) performed archeomagnetic researches on old tiles and alluvial deposits in Yamaguchi Prefecture. They also obtained estimates of paleo intensities by a method slightly modified from the Thelliers' original technique.

A kiln was constructed after the style of 7th century kiln called "Noborigama," and pine logs were burned in it just as was done in the older times. Nakajima et al. (1974) recorded the temperatures in various parts of the kiln and found that after about twelve hours' firing the kiln floor attained a temperature of more than 700°C, well above the Curie points of the ferromagnetic minerals contained in baked earths. Oriented samples collected from the kiln after firing were measured. Their natural remanent magnetization (NRM) was quite stable to alternating field (af) demagnetization and the mean direction of NRM was about 3 degrees apart from the direction of ambient field measured before the firing of the kiln. This result shows that archeomagnetic results obtained from such old kilns may have a very high reliability.

Nakajima and Kawai (1973) compared their inclination and declination data of top 6 m of the Lake Biwa sediment core with archeomagnetic results from southwestern Japan. When some averaging was done with the sediment data, there seems to be fairly good correspondence of maxima and minima in sedimentary and archeomagnetic data. It seems that inclination error is absent in the remanent magnetization (RM) of Lake Biwa sediment, just as in the case of deep-sea sediments. It is therefore concluded that the use of lake sediments may be a good way to expand the archeomagnetic researches.

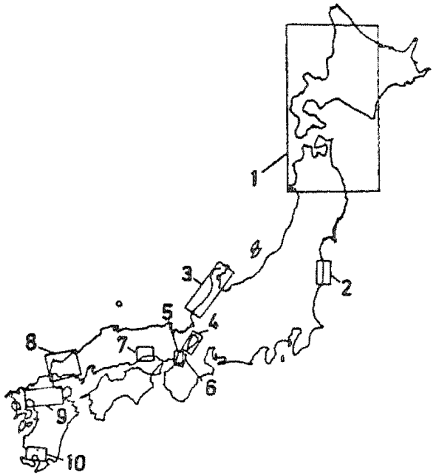

Fig. II-7.
Index map showing the location of sampling areas for paleomagnetism in Japan. 1: Hokkaido and Northernmost Honshu (Ito and Tokieda, 1972 a); 2: Pacific coast of Fukushima Prefecture (Manabe, 1973); 3: Hokuriku (Hirooka, 1973); 4: Lake Biwa (Kawai et al., 1972; Nakajima and Kawai, 1973; Yasukawa, 1973 b; Yasukawa et al., 1973); 5: Ibaragi granite complex (Kanaya and Noritomi, 1974); 6: Osaka Group (Torii, 1973; Torii et al., 1974); 7: Himeji volcanics (Kono et al., 1974); 8: Yamaguchi Prefecture (Domen, 1974 a; Domen and Muneoka, 1973, 1974 a); 9: Cenozoic rocks of Kyushu (Domen and Muneoka, 1974 b);

B. REVERSALS AND FLUCTUATIONS IN THE BRUNHES POLARITY EPOCH

Several reports have been published in recent years concerning existence of short-period polarity reversals or excursions of the geomagnetic field in the Brunhes epoch (0 to 0.69 m.y.). The most detailed reports are based on the magnetization of Lake Biwa sediment core in which several reversals or excursions were found (Kawai et al., 1972; Yasukawa et al., 1973; Yasukawa, 1973 a, b; 1974). An example of such changes at about 26 m in depth corresponding to 49,000 y BP is shown in Fig. II-8. Apart from the excursions, they suggest short duration reversals at about 110,000 y BP, 180,000 y BP, and 295,000 y BP (yasukawa, 1973 b).

Other evidences of reversals were found in a sediment layer of Fukushima Prefecture (Manabe, 1973), in a pyroclastic flow in the southern Kyushu (Sasajima, 1973), and in the "Kasuri" tuff of Osaka Group (Torii, 1973; Torii et al., 1974). The latter two formations are dated by fission track method as 72,000-110,000 y BP Inuzako pyroclastic flow in Kyushu) and 0.38 m.y. ("Kasuri" tuff), respectively. The reversal found in Kyushu and the youngest one in the Lake Biwa sample may correspond to the Blake event, so far found only in deep-sea cores. It is quite uncertain at this stage whether these and other reversals found in the Japanese samples represent truely world-wide reversals or only excursions of the geomagnetic field. However, it should be emphasized that these studies reveal the hitherto poorly understood phenomena of short period fluctuations of the geomagnetic field.

C. CENOZOIC PALEOMAGNETISM

Kawai et al. (1973 a, b) studied the NRM of a deep-sea core, measuring at 1 mm interval by a specially designed astatic magnetometer, and found that the

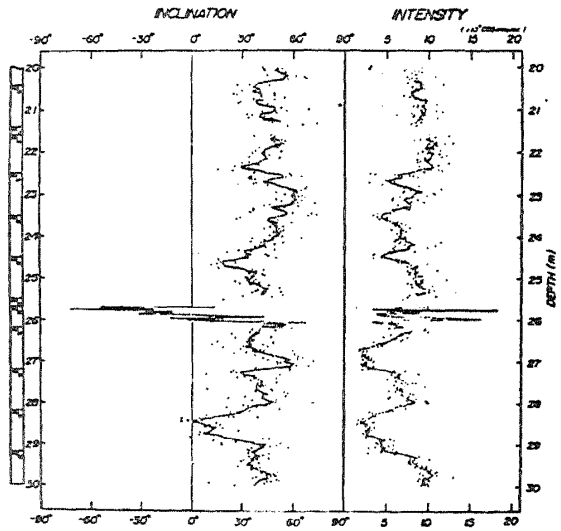

Fig. II-8. An example of anomalous changes of direction and intensity of magnetization in the sediment core of Lake Biwa. Smooth curves show the seven-point moving averages. After Yasukawa et al. (1973).

reversals at Jaramillo-Matuyama and Matuyama-Brunhes boundaries took place quite suddenly, say, within 1,000 years, although the overturns of inclination and declinationand the minimum of NRM intensity did not take place simultaneously. Kobayashi and Mizutani (1973) also studied the NRMs in deep-sea cores and found that the pattern of NRM fluctuations in intensity is quite similar in cores taken a few thousand kilometers apart. They suggest that such fluctuations may in part be caused by the change of the strength of the geomagnetic field.

Paleomagnetism of Cenozoic rocks on land was studied in the northern Kyushu (Domen and Muneoka, 1974 b), in Osaka Group (Torii et al., 1974), and in San Juan Mountains, Colorado, U.S.A. (Tanaka and Kono, 1973, 1974 a).

D. CRETACEOUS AND OLDER ROCKS

Ito and Tokieda (1974 a) collected granodiorite and quartz diorite

samples from twelve sites in Hokkaido and the northernmost part of the Honshu Island. Ages of most of these rocks are given by K-Ar method as late Cretaceous between 90 and 120 m.y. The results show that declination of the Hokkaido rocks is easterly (30° to 80°) in accordance with the earlier interpretation of the tectonic movements of the Japan arc put forward by Kawai et al. (1971, J. Geomag. Geoelectr., 23, 243-248 and 267-293) that the Hokkaido Island was subjected to a clockwise rotation in Cenozoic relative to the Honshu Island.

Kono et al. (1974) investigated rhyolites and dacites of Himeji volcanics of Cretaceous age both by paleomagnetic methods and by K-Ar dating. The ages are found to be around 70 M.y., although some rocks gave younger ages because of argon loss due to the heating by later intrusions of granitic rocks. After af demagnetization, all of the 33 cooling units showed reversed RM. Scatter in the mean directions of individual cooling units was quite large. It seems very difficult to explain this scatter by instability of NRM or by secular variation in that period. It may represent a period of abnormally high fluctuations such as reversals or excursions. Kanaya and Noritomi (1974) measured a granite pluton of 76 and 79 m.y. and obtained well-grouped normal and reversed directions which trend in NE-SW directions.

Ito and Tokieda (1974 b) also studied granites in South Korea with ages between 70 and 160 m.y. The NRM directions in these rocks are not much different from the axial dipole field directions at the sampling sites. Therefore, it can be assumed that Korea (and the continent beyond) stayed essentiallly at the same place since Cretaceous without appreciable rotation, while the Japanese arc was bending and the Japan Sea was opening. Yasukawa (1973 c) tried to reconstruct paleogeographic map of Japan in Cretaceous period from paleomagnetic data of Japan and Korea. His result shows that the Northwestern Honshu should be placed south of the Southwestern part, instead of north as was presumed previously. What this means is not clear at the present stage.

E. PALEOINTENSITIES

Kono (1974) applied the Thelliers' method to the 65 m.y.-old basalts from Decçan Traps, India. Samples were selected from lavas with ferromagnetic minerals with high Curie temperatures, which showed stability against af demagnetization. The samples with reversed NRM gave paleointensities which are quite similar to the present value (dipole moment: 8.0x10 G cm), while those corresponding a R-N transition gave dipole moments about a third of the ordinary value. Kono (1973 b) summarized the paleointensity data obtained by the Thellier's method from volcanic rocks of Cenozoic and upper Cretaceous ages (Fig. II-9) and concluded that the geomagnetic field intensity was essentially of the same magnitude in this period with the mean around 9 x 10 G cm and a variable standard deviation, except Brunhes normal epoch when the field was about 50% stronger. The field intensity is considerabley reduced when it was reversing its polarity (Fig. II-9), and the fluctuation of the dipole moment seems to be well represented by a normal distribution. Kono and Pavoni (1973) also used the Thellier's method on Permian porphyllite from Lugano area, Switzerland and obtained a paleointensity of 0.70 Oe.

F. ROCK MAGNETISM

It is well known that basalts dredged from the deep ocean floor show, quite commonly, very peculiar properties compared with volcanic rocks on land. Ozima dn his co-workers have been trying to explain such magnetic properties of dredged basalts by maghemitization (low temperature oxidation) of titanomagnetite under the influence of sea water. They measured Curie points, lattice constants,

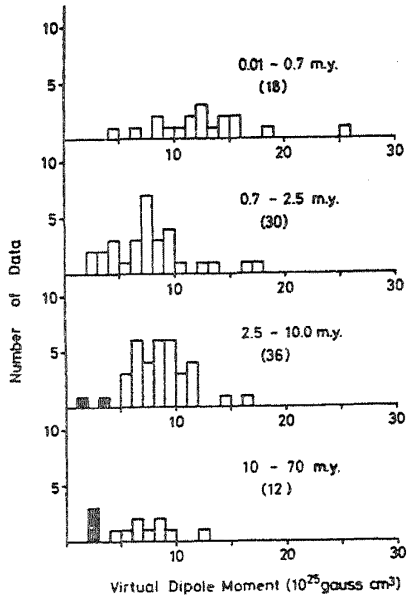

Fig. II-9.
Histograms of paleointensity data (expressed as the magnitudes of virtual dipole moments) obtained by the Thelliers' method. White portion is for normal or reversed polarity, black for intermediate or transition period. Numbers in the brackets indicate the total number of data. After Kono (1973 b).

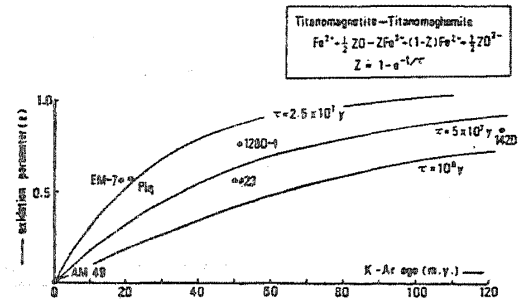

Fig. II-10. Relation between oxidation parameters (z) of ferromagnetic minerals and K-Ar ages of submarine basalts. Curves indicate the changes calculated assuming first order rate processes with various time constants. After Ozima et al. (1974 b).

and chemical composition of ferromagnetic minerals contained in natural oceanic basaltic rocks dredged or drilled from the sea floor. All of these rocks show that they were more or less affected by low temperature oxidation process (Joshima, 1973). They also measured K-Ar and Ar-Ar ages of the same rocks (Ozima et al., 1974 a) and compared them with the rock magnetic results. There is a strong evidence that the older the ages of the rocks, the more oxidized are the ferromagnetic minerals in them (Fig. II-10). They conclude that oxidation takes place as a rate process of the first order and that thickness of the oxidized layer increases as the oceanic crust spreads from the mid-oceanic ridges (Ozima and Joshima, 1973; Ozima et al., 1974 b).

It has also been noted that highly maghemitized minerals may show total/partial self-reversal phenomena. Using a dredged basalt sample, Sasajima and Nishida (1974) demonstrated a case in which the ferromagnetic separates, after certain heat treatments, show an N-type thermomagnetic curve and hence the self-reversal of thermoremanent magnetization (TRM). They interpreted this self-reversal as caused by the redistribution of cations in a thermally activated system.

Methods to distinguish titanomaghemites or substituted titanomagnetites by magnetic measurements were proposed by Momose and Inagaki (1973) and by Domen (1974 b), respectively.

Kono and Akimoto (1974) measured the ferromagnetic minerals contained in Kimberlite from South Africa by thermomagnetic and X-ray diffraction methods and concluded that titanomaghemite may be the carrier of NRM in this Kimberlite. Kobayashi and Nomura (1974) studied ferromagnetic constituents in deep-sea sediments taken from the bottom of the Pacific Ocean. It was found that they are mainly titanomagnetite (not altered to titanomaghemite) and that they are stable in the deep-sea environment.

Sugiura and Nagata (1973) applied magnetic methods to estimate the nickel concentration in metallic phases of meteoritic and lunar rocks.

A striking discovery of native iron in a terrestrial volcanic rock was reported by Momose (1974) from thermomagnetic analyses of andesitic rock erupted in 1973 on the newly formed island of Nishinoshima-Shinto, in Bonin Islands, south of Honshu. It was necessary to magnetically separate the sample so as to "enrich" the native iron in the separation process, as by far the most abundant ferromagnetic mineral in this rock was titanomagnetite with about 35 mol % ulvospinel. It is believed that this is the first discovery of genuine native iron in volcanic rocks, as the previous findings were concerned with such objects as trees burning under the heat of a lava or very complex system such as ophiolites.

Tanaka and Kono (1974 b) constructed an electric furnace with oxygen fugacity control by H_2-CO_2 gas mixtures. The aim of their study is to clarify the mechanism of "chemical changes" which so often hinders the determination of paleointensities by comparison of NRMs and TRMs produced in the same samples. It is often observed that TRMs produced in laboratory by heating samples in air are stronger than NRM and also they are magnetically harder. Preliminary results

of Tanaka and Kono indicate that when samples containing titanomagnetites are heated to more than 600°C in oxidizing atmospheres, a larger and magnetically harder TRM is produced than when they are heated under reducing conditions. Such differences in the nature of TRM seem inevitable in practical experiments. Paleointensity data obtained by the Thelliers' method are therefore superior to the data by other methods, since occurrence of such chemical changes can be detected by the Thelliers' experimental technique.

G. MISCELLANEOUS

Kono (1973 a) proposed a method to estimate the duration of volcanism of a volcanic complex by measuring the polarity changes of NRM recorded in the successive lava flows of such a complex. This method is based on the assumptions that both the geomagnetic reversals and the eruption of lava flows from a volcano can be described by Poisson processes with independent time constants. Both of these assumptions seem to be satisfied as good approximations. Then, mathematical treatments based on the probability theory leads the estimates of duration of volcanism when the number of successive lavas and the number of reversals observed in them are given. Application to the cases where true duration is known shows that this method gives indeed good estimate of the periods of volcanism. Kono applied this method to the lavas of Western Ghats of Deccan Traps, India, and obtained a maximum time span of about 3 m.y. This estimate is also consistent with the results of K-Ar dating and the geological evidence concerning with the mode of emplacement of these lavas.

It is proved that even without the paleointensity values, paleomagnetic data of inclination and declination are, when amply well known over the surface of the earth, sufficient to uniquely determine the geomagnetic potential up to a multiplicative constant (Kono, 1973 c, 1973 d). Inclination and declination data with a single value of paleointensity at some points over the surface of the earth will, then, be taken to contain the complete information about the magnetic field. When declination only or inclination only is known, however, there are many essentially different fields which equally well satisfy these boundary conditions (Kono, 1973 c, also in preparation, 1975).

121

PUBLICATIONS

Domen, H., An example of estimation of archeomagnetic field intensity by old roof tiles, Bull. Fac. Sci. Yamaguchi Univ., 24 (2), 7-11, 1974 a.

Domen, H., An estimation of the concentration of lattice substituted elements in rocks using rock magnetic data, Bull. Fac. Sci. Yamaguchi Univ., 24 (2), 13-19, 1974 b.

Domen, H. and H. Muneoka, Archeomagnetic study on some remains of the ancient times in Yamaguchi Prefecture, Bull. Fac. Sci. Yamaguchi Univ., 23 (2), 27-32, 1973.

Domen, H. and H. Muneoka, A brief note on the remanent magnetic measurement of the diluvial deposits in Yamaguchi Prefecture, West Japan, Rock Mag. Paleogeophys., 2, 32-33, 1974 a.

Domen, H. and H. Muneoka, A progress report on paleomagnetic study on Cenozoic rocks from Northern Kyushu Island, West Japan, Rock Mag. Paleogeophys., 2, 38-39, 1974 b.

Hirooka, K., Archeomagnetic study in Hokuriku district, Rock Mag. Paleogeophys., 1, 29-33, 1973.

Ito, H. and K. Tokieda, Tilting of Hokkaido Island and Kitakami Mountains deduced from the NRM of Cretaceous granitic rocks, Rock Mag. Paleogeophys., 2, 54-58, 1974 a.

Ito, H. and K. Tokieda, Paleomagnetism of Cretaceous granites in South Korea, Rock Mag. Paleogeophys., 2, 59-61, 1974 b.

Joshima, M., Magnetization of oceanic basalt, Rock Mag. Paleogeophys., 1, 9-12, 1973.

Kanaya, H. and K. Noritomi, Remanent magnetization of Ibaragi granitic complex, Rock Mag. Paleogeophys., 2, 50-53, 1974.

Kawai, N., K. Yasukawa, T. Nakajima, M. Torii and S. Horie, Oscillating geomagnetic field with a recurring reversal discovered from Lake Biwa, Proc. Japan Acad., 48, 186-190, 1972.

Kawai, N., T. Nakajima, K. Yaskawa, K. Hirooka and K. Kobayashi, The oscillation of field in the Matuyama geomagnetic epoch, Proc. Japan Acad., 49, 619-622, 1973 a.

Kawai, N., T. Nakajima, K. Hirooka and K. Kobayashi, The transition of field at the Brunhes and Jaramillo boundaries in the Matuyama geomagnetic epoch, Proc. Japan Acad., 49, 820-824, 1973 b.

Kobayashi, K. and S. Mizutani, Expression of fluctuations of the geomagnetic field intensity in deep-sea cores.Rock Mag. Paleogeophys., 1, 59-64, 1973.

Kobayashi, K. and M. Nomura, Ferromagnetic minerals in the sediment cores collected from the Pacific basin, J. Geophys., 40, 501-512, 1974.

Kono, M., Geomagnetic polarity changes and the duration of volcanism in successive lave flows, J. Geophys. Res., 78, 5972-5982, 1973 a.

Kono, M., Geomagnetic paleointensities in the Cenozoic, Rock Mag. Paleogeophys., 1, 83-87, 1973 b.

Kono, M., Uniqueness of the spherical harmonic analysis of the geomagnetic field based on the inclination and declination data, Rock Mag. Paleogeophys., 1, 118-123, 1973 c (Correction, ibid., 2, 91-93, 1974).

Kono, M., Spherical harmonic analysis of the geomagnetic field from inclination data, Rock Mag. Paleogeophys., 124-129, 1973 d.

Kono, M., Intensities of the earth's magnetic field about 60 m.y. ago determined from the Deccan Trap basalts, India, J. Geophys. Res., 1135-1141, 1974.

Kono, M. and S. Akimoto, Magnetic properties of Kimberlite, Rock Mag. Paleogeophys., 2, 2-4, 1974.

Kono, M. and N. Pavoni, An attempt of paleointensity determination of Permian porphyllites and Tertiary granodiorites, Rock Mag. Paleogeophys., 1, 88-91, 1973.

Kono, M., M Ozima and K. Wadatsumi, Paleomagnetism and K-Ar ages of Himeji volcanics, Rock Mag. Paleogeophys., 2, 45-49, 1974.

Manabe, K., Geomagnetic reversal recorded in the late Pleistocene sediments, Rock Mag. Paleogeophys., 1, 51-52, 1973.

Momose, K., Thermomagnetic curves of ferromagnetic minerals extracted from the lava flows of Nishinoshima-Shinto, Japan, Rock Mag. Paleogeophys., 2, 1, 1974.

Momose, K. and S. Inagaki, On discrimination of respective remanent magnetisms of titanomagnetite and titanomaghemite, Rock Mag. Paleogeophys., 1, 7-8, 1973.

Nakajima, T. and N. Kawai, Secular geomagnetic variation in the recent 60,000 years found from the Lake Biwa sediments, Rock Mag. Paleogeophys., 1, 34-38, 1973.

Nakajima, T., M. Torii, N. Natsuhara, K. Yaskawa, M. Takagi, K. Ikeguchi and N. Kawai, Remanent magnetism of the reconstructed ancient kiln, Rock Mag. Paleogeophys., 2, 28-31, 1974.

Nishida, J. and S. Sasajima, On the possibility of self-reversal caused by redistribution of cations between two sub-lattices, Rock Mag. Paleogeophys., 2, 10-14, 1974.

Ozima, M. and M. Joshima, Rock magnetic structures of oceanic crust, Rock Mag. Paleogeophys., 1, 1-6, 1973.
Ozima, M., K. Saito and M. Joshima, K-Ar, Ar- Ar dating and magnetic studies of Leg 7 and Leg 17 basalt samples, EOS, Trans. AGU, 54, 989, 1974 a.
Ozima, M., M. Joshima and H. Kinoshita, Magnetic properties of submarine basalts and the implications on the structure of the oceanic basalt, J. Geomag. Geoelectr., 26, 335-354, 1974 b.
Sasajima, S., Possible Blake event as revealed in a pyroclastic flow occurring in southern Kyushu, Japan, Rock Mag. Paleogeophys., 2, 45-50, 1974.
Sasajima, S. and J. Nishida, On the self-reversal of TRM in a highly oxidized submarine basalt, Rock Mag. Paleogeophys., 2, 5-9, 1974.
Sugiura, N. and T. Nagata, The volumetric histogram of nickel concentration in metal particles of lunar and meteorite samples, Rock Mag. Paleogeophys., 1, 21-25, 1973.
Tanaka, H. and M. Kono, Paleomagnetism of the San Juan volcanic field, Colorado, U.S.A., Rock Mag. Paleogeophys., 1, 71-76, 1973.
Tanaka, H. and M. Kono, Origin of NRM of San Juan volcanic rocks from Colorado, U.S.A., Rock Mag. Paleogeophys., 2, 20-23, 1974 a.
Tanaka, H. and M. Kono, A furnace for thermal demagnetization using oxigen partial pressure control technique, Rock Mag. Paleogeophys., 2, 24-27, 1974 b.
Torii, M., Paleomagnetic investigation of a water-laid volcanic ash layer in the Osaka Group, Rock Mag. Paleogeophys., 1, 65-70, 1973.
Torii, M., S. Yoshikawa and M. Itihara, Paleomagnetism on the water-laid volcanic ash layers in the Osaka Group, Sennan and Senpoku Hills, southwestern Japan, Rock Mag. Paleogeophys., 2, 34-37, 1974.
Yaskawa, K., Rate of sedimentation for young loose sediment, Rock Mag. Paleogeophys., 1, 1973 b.
Yaskawa, K., Drift of southwest Japan relative to South Korea since late Mesozoic--a paleomagnetic approach to the origin of the Japan Sea--, Rock Mag. Paleogeophys., 1, 77-82, 1973 c.
Yaskawa, K., When did magnetization fix in loose sediments?, Rock Mag. Paleogeophys., 2, 15-19, 1974.
Yaskawa, K., T. Nakajima, N. Kawai, M. Torii, N. Natsuhara and S. Horie, Paleomagnetism of a core from Lake Biwa (I), J. Geomag. Geoelectr., 25, 447-474, 1973.

AUTHOR INDEX